JPRS L/9745

20 May 1981

USSR Report

PHYSICS AND MATHEMATICS

(FOUO 4/81)

FBIS FOREIGN BROADCAST INFORMATION SERVICE

APPROVED FOR RELEASE: 2007/02/08: CIA-RDP82-00850R000400010041-1

NOTE

JPRS publications contain information primarily from foreign newspapers, periodicals and books, but also from news agency transmissions and broadcasts. Materials from foreign-language sources are translated; those from English-language sources are transcribed or reprinted, with the original phrasing and other characteristics retained.

Headlines, editorial reports, and material enclosed in brackets [] are supplied by JPRS. Processing indicators such as [Text] or [Excerpt] in the first line of each item, or following the last line of a brief, indicate how the original information was processed. Where no processing indicator is given, the information was summarized or extracted.

Unfamiliar names rendered phonetically or transliterated are enclosed in parentheses. Words or names preceded by a question mark and enclosed in parentheses were not clear in the original but have been supplied as appropriate in context. Other unattributed parenthetical notes within the body of an item originate with the source. Times within items are as given by source.

The contents of this publication in no way represent the policies, views or attitudes of the U.S. Government.

APPROVED FOR RELEASE: 2007/02/08: CIA-RDP82-00850R000400010041-1

JPRS L/9745

20 May 1981

USSR REPORT

PHYSICS AND MATHEMATICS

(FOUO 4/81)

CONTENTS

FLUID DYNAMICS

UDC 533.6.011.72+535.33

POPULATION INVERSION BEHIND A DETONATION WAVE PROPAGATING IN A MEDIUM WITH VARIABLE DENSITY

Moscow IZVESTIYA AKADEMII NAUK SSSR: MEKHANIKA ZHIDKOSTI I GAZA in Russian No 1, Jan-Feb 80 pp 65-71

[Article by M. I. Podduyev, Moscow]

[Text] The use of detonation to produce an active medium has been studied in many papers. It has been suggested that use be made of dispersal of the products of detonation of an acetylene-air mixture into a vacuum [Ref. 1], and also cooling of the products of detonation of a mixture of hydrocarbons with air through a nozzle [Ref. 2, 3]. In Ref. 4, detonation of a solid explosive was used to set up population inversion in a CO_2-N_2-He(H_2O) gas mixture. Lasing on HF molecules has been experimentally observed behind an overdriven detonation wave front propagating in a mixture of F_2O-H_2-Ar in a shock tube [Ref. 5]. An investigation has been made of the problem of population inversion behind a detonation wave in mixtures of H_2-F_2-He [Ref. 6-8] and H_2-Cl_2-He [Ref. 9] upon release of energy on a plane and on a straight line in a medium with constant density.

Similar problems have also been solved for shock waves propagating both in a homogeneous gas atmosphere [Ref. 7, 10] and in the supersonic part of a flared nozzle[1].

In this article a theoretical investigation is made of the problem of getting population inversion behind an overdriven detonation wave propagating through a mixture (fine particles of carbon + acetylene + air) discharged from a hypersonic nozzle. The propagation of a detonation in media with variable density and initial velocity has been considered, for example in Ref. 11, 12. Analysis of gas parameters behind a detonation wave propagating in a medium with constant density (for a given fuel mixture) has shown that the temperature differential behind the detonation front is insufficient for population inversion of vibrational levels of the CO_2 molecule.

1. Model of hypersonic discharge of a fuel mixture through a nozzle. We will take the acetylene + air mixture to be a perfect gas with constant specific heats (c_V', $c_p' = c_V' + R'$, where R' is the gas constant of the given mixture), and assume that the carbon particles are very small (characteristic diameter of the order of 1 μm). Then the equation of state can be written as [Ref. 11]

$$p/\rho=(\gamma-1)E, \quad p/\rho=RT, R=R'/(1+\alpha)$$
$$c_V=(c_V'+\alpha c)/(1+\alpha), \quad c_p=c_V+R, \quad \gamma=c_p/c_V \qquad (1.1)$$

[1]Yu. V. Tunik, "Influence of the flow characteristics of a relaxing gas on the parameters of a gasdynamic laser", author's abstract of candidate's dissertation, Institute of Mechanics, Moscow State University, 1976.

Here c is the specific heat of the carbon particles, which is taken as constant; α is the mass fraction of particles in a unit of volume as compared to the mass of the gas in that volume; E, p, ρ, T are the internal energy, pressure, density and temperature of the mixture.

Let us consider adiabatic steady-state discharge of the fuel mixture through the nozzle in the linear approximation. In this case the parameters of the medium in the nozzle are described by the Bernoulli integral and its corollaries that account for the equations of state (1.1):

$$v=v_{\max}(1+z)^{-1/2} \qquad p=p_0 z^{\gamma/(\gamma-1)}(1+z)^{-\gamma/(\gamma-1)} \tag{1.2}$$

$$\rho=\rho_0 z^{1/(\gamma-1)}(1+z)^{-1/(\gamma-1)} \qquad T=T_0 z(1+z)^{-1}$$

$$z\equiv\frac{2}{(\gamma-1)M^2}, \quad v_{\max}\equiv\sqrt{\frac{2\gamma}{(\gamma-1)}\frac{p_0}{\rho_0}} \tag{1.3}$$

Here p_0, ρ_0, T_0 are the stagnation parameters; v and M are velocity and Mach number.

Let the mixture escape from a large reservoir (in which $p=p_0$, $\rho=\rho_0$, $T=T_0$, $v=0$) into the ambient space with constant pressure through a Laval nozzle. Let us give the area of the flared part of the nozzle as $S=\sigma_\nu r^{\nu-1}$, and the area of the minimum cross section of the nozzle as $S_{\min}=\sigma_\nu r_*^{\nu-1}$ ($\nu>1$, with $\nu=2$ corresponding to cylindrical symmetry, and $\nu=3$ corresponding to spherical symmetry). Let us assume that discharge is supersonic. Then the law of mass conservation can be written as

$$\rho v S=\rho_* v_* S_{\min}\equiv G=\text{const} \tag{1.4}$$

Here ρ_*, v_* are the critical flow parameters in the minimum cross section of the nozzle.

From (1.2)-(1.4) for the supersonic part of the nozzle we get

$$z^{1/(\gamma-1)}(1+z)^{-(\gamma+1)/2(\gamma-1)}=\sqrt{\frac{\gamma-1}{\gamma+1}}\left(\frac{2}{\gamma+1}\right)^{1/(\gamma-1)}\left(\frac{r_*}{r}\right)^{\nu-1} \tag{1.5}$$

$$\rho=\frac{A}{r^{\nu-1}}\sqrt{1+z}, \quad A\equiv\rho_0\sqrt{\frac{\gamma-1}{\gamma+1}}\left(\frac{2}{\gamma+1}\right)^{1/(\gamma-1)} r_*^{\nu-1} \tag{1.6}$$

Since $\nu>1$, $\gamma>1$ and $M\geqslant 1$ or $z\leqslant 2/(\gamma-1)=\text{const}$, (1.5) implies that for any r_* there is an r_+ such that for any $r>r_+$ we can assume $z\ll 1$, and if r_* approaches zero, then r_+ will also approach zero (the stagnation parameters are not important here). Let us also assume that r_* and r_+ are small, and throughout the region of supersonic flow we will take the approximation $z\ll 1$, $r\geqslant 0$. Then for this region from (1.2) and (1.6) we get the laws of behavior of velocity and density

$$v=v_{\max}, \quad \rho=A/r^{\nu-1} \tag{1.7}$$

It should be noted that the smallness of z and formulas (1.3) do not imply smallness of p, ρ, T in the flow since p_0, ρ_0, T_0 may be large quantities.

2. Calculation of gas parameters behind a detonation wave propagating in a medium with variable density and constant velocity. The percentage of acetylene is determined both by the detonative capacity of the mixture and the percentage of water vapor in the detonation products. Detonation of coal dust in air has been experimentally studied [Ref. 14, 15]; however, in this paper we are considering a mixture with acetylene added to improve the detonative capacity. The effect of a methane additive on detonation of coal dust was studied in Ref. 16.

Let us consider perturbation of the motion of a fuel mixture escaping through a hypersonic nozzle as a result of simultaneous cessation of the delivery of fuel mixture to the nozzle and arisal of detonation at point r = 0 at time t = 0. When $t>0$, the detonation wave is propagating downstream. Let us assume that the carbon and acetylene in the detonation wave are oxidized to CO_2 and H_2O (N_2 enters as ballast), and that the gasdynamic parameters of the detonation products satisfy the following equations of state [Ref. 17]:

$$\frac{p}{\rho}=\frac{R_0}{\mu}T,\quad E=\frac{R_0}{\mu}\left[\beta T+\sum_i g_i\xi_i\theta_i e_i\right]=E(T,e_i)$$
$$e_i=[\exp(\theta_i/T_i)-1]^{-1},\quad \beta=1.5+\xi_L+1.5\xi_N \qquad (2.1)$$

Here R_0 is the universal gas constant, μ is the molecular weight of the mixture, g_i is the degree of degeneration of the i-th mode; ξ_i is the molecular fraction of the component to which the i-th vibrational mode applies; θ_i, T_i are the characteristic and instantaneous vibrational temperatures of the i-th mode; ξ_L is the molecular fraction of the component consisting of linear molecules; ξ_N is the same for nonlinear molecules; E, p, ρ, T are the internal energy, pressure, density and temperature of the detonation products.

Let us disregard the change of internal energy of the detonation products due to deviations of the vibrational energies from the equilibrium values, i. e. let us assume that $T_i = T$ in (2.1) (for all i) and hence $E = E(T)$.

Let us assume further that the gas behind the detonation front does not radiate, is not viscous, and is not thermally conductive. Then the equations of motion for quasi-one-dimensional flows are written as [Ref. 11]

$$\frac{\partial v}{\partial t}+v\frac{\partial v}{\partial r}+\frac{1}{\rho}\frac{\partial p}{\partial r}=0$$
$$\frac{\partial \rho}{\partial t}+\frac{\partial \rho v}{\partial r}+(\nu-1)\frac{\rho v}{r}=0 \qquad (2.2)$$
$$\frac{\partial E}{\partial t}+p\frac{\partial}{\partial t}\left(\frac{1}{\rho}\right)+v\left[\frac{\partial E}{\partial r}+p\frac{\partial}{\partial r}\left(\frac{1}{\rho}\right)\right]=0$$

System of equations (2.1), (2.2) is closed. Let us formulate the boundary conditions.

Taking the detonation wave as strong and "infinitesimally thin", we write the following relations on this wave [Ref. 11]:

$$\begin{aligned} &\rho_1(v_1-D)=\rho_2(v_2-D)\\ &\rho_1(v_1-D)^2=\rho_2(v_2-D)^2+p_2\\ &\frac{1}{2}(v_1-D)^2+Q=\frac{1}{2}(v_2-D)^2+\frac{p_2}{\rho_2}+E_2 \end{aligned} \tag{2.3}$$

Here Q is the amount of heat released upon combustion of a unit of mass of the fuel mixture; D is the propagation rate of the detonation wave (subscript 1 denotes quantities in front of the wave, and 2 denotes quantities behind the wave). From (1.7) we get $v_1 = v_{max}$, $\rho_1 = A/r^{\nu-1}$.

Since the gas does not enter the nozzle when $t>0$, we must set the following boundary condition:

$$(0<t\ 0=\lambda)\quad 0=a \tag{2.4}$$

From the formulation of the problem we find that the controlling parameters are: ν, Q, v_1, A, $\theta_i R_0/\mu$, μ_i, ξ_i, g_i, r, t; of these, Q and A can be taken as independent dimensional constants. In this approximate formulation, the problem is self-similar [Ref. 11].

In equations (2.1), (2.2) and boundary conditions (2.3), (2.4) we make the substitution of variables

$$v=\frac{r}{t}V(\lambda),\quad \rho=\frac{A}{r^{\nu-1}}R(\lambda),\quad p=\frac{A}{r^{\nu-1}}\left(\frac{r}{t}\right)^2 P(\lambda)$$

$$\lambda=\frac{r}{Dt},\quad 0\leqslant\lambda\leqslant 1$$

The equations are transformed to a system of ordinary differential equations for the quantities V, R and P analogous to those written in Ref. 11. Solving this system, we find the functions $V(\lambda)$, $R(\lambda)$ and $P(\lambda)$, and hence $v(r,t)$, $\rho(r,t)$ and $p(r,t)$ as well. $T(r,t)$ is determined through the equation of state. For the given system of differential equations there is an integral of masses [Ref. 11]

$$M_+=\sigma_\nu R(1-V) \tag{2.5}$$

Here $m = \lambda r M_+(\lambda)$ is mass. By using (2.5) we can easily follow the change in gasdynamic parameters of any gas particle. The system also assumes an integral of adiabaticity [Ref. 18].

3. Kinetic processes and population inversion behind a detonation wave. In section 2 we disregarded the effect that nonuniformity of vibrational energies has on gasdynamic flow parameters; however, we cannot disregard the reverse influence. Hence we must study the relaxation pattern against the "background" of the gasdynamic parameters considered in section 2.

Changes in the numbers of vibrational quanta in a gas particle are described by the following equations:

$$\frac{\partial e_i}{\partial t} = pF_i(T, e_j) \quad (i, j = 1, 2, 3, 4) \tag{3.1}$$

Here the F_i are functions defined in Ref. 17.

The beginning of observation of a gas particle is determined by the time t_0 of entrainment of the particle by the detonation wave at distance $r_0 = Dt_0$ from the beginning of the hypersonic part of the nozzle. Let us assume that at the instant of entrainment all the vibrational energies in the particle are at their equilibrium values.

For a fixed composition of the fuel mixture, Q = const. If ν and T_0 are also given, then D and the functions $V(\lambda)$, $R(\lambda)$, $P(\lambda)$ will be the same for any values of A and r_0. Then from (2.5) and solution of the system of ordinary differential equations we get the ratio $r/r_0 = f(\lambda)$, but $\lambda = (r/r_0)/(t/t_0)$, and therefore $\lambda = f_1(t/t_0)$. Now we rewrite (3.1) as

$$\frac{\partial e_i}{\partial (t/t_0)} = t_0 \frac{A}{r_0^{\nu-1}} D^2 \frac{\lambda^2 P(\lambda)}{(r/r_0)^{\nu-1}} F_i(T(\lambda), e_j)$$
$$\lambda = f_1(t/t_0), \; r/r_0 = f(\lambda)$$

These equations yield a dimensionless law for the e_i as functions of t for different gas particles and for different values of A (at constant ν, T_0 and gas makeup). The expressions $e_i = e_i(t/t_0)$ will be the same if $t_0 D^2 A / r_0^{\nu-1} = \text{const}$. The quantity D is independent of A and of the choice of particle, and $t_0 = r_0/D$; therefore

$$A/r_0^{\nu-2} = \text{const}.$$

Consequently when $\nu = 2$ (cylindrical symmetry) the relations $e_i = e_i(t/t_0)$ for any gas particle (at fixed A) are the same, and therefore the relative population inversion for different gas particles behaves in the same way as a function of the variable t/t_0. However, there is no such dimensionless number for weak-signal optical gain since pressure enters nonlinearly into the expression for this parameter [Ref. 17]. Therefore in the case of a constant ratio of fuel components and constant T_0, it is necessary for $\nu = 2$ to optimize the gain in the gas particle with respect to the two parameters A and r_0.

4. Methods of solution and discussion of results. The system of ordinary differential equations described in section 2 was solved numerically for the following parameters: $\xi_{C_2H_2} = 0.025$, $\xi_{O_2} = 0.205$, $\xi_{N_2} = 0.77$, $\alpha = 0.06$, $Q = 2.9$ kJ/g, $\gamma = 1.37$ and $\xi_{C_2H_2} = 0.077$, $\xi_{O_2} = 0.194$, $\xi_{N_2} = 0.729$, $\alpha = 0$, $Q = 3.5$ kJ/g, $\gamma = 1.38$; for both sets of parameters $T_0 = 293$ K. The quantity ν was taken as equal to several values: 1.5, 2, 2.5, 3. Analysis of the field of integral curves showed that for given ν, T_0 and the two sets of parameters of the fuel mixture (for any A) there are unique solutions for this system of equations, where the detonation wave is overdriven (there is an analogy with the case $v_1 = 0$ [Ref. 11]).

Figures 1-5 correspond to the first set of parameters of the fuel mixture. Calculations for the second set show the same qualitative behavior of the curves, although the absolute values of gain are lower.

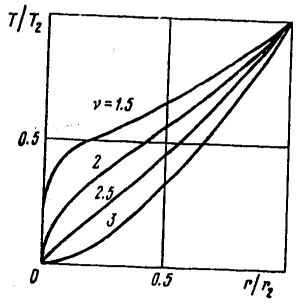

Fig. 1

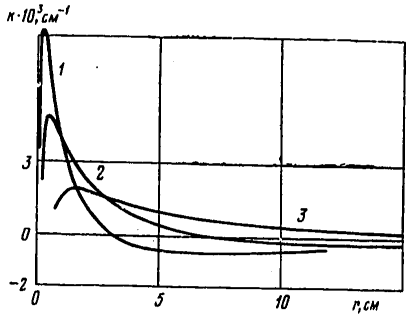

Fig. 2

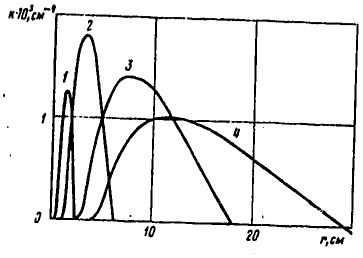

Fig. 3

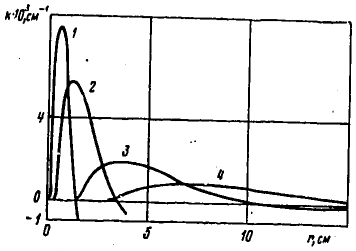

Fig. 4

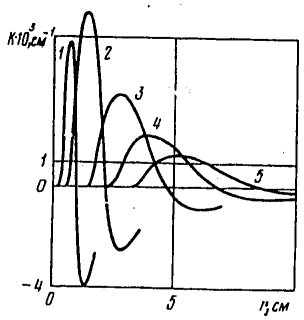

Fig. 5

Fig. 1 shows the temperature distribution behind the detonation front for different ν. It can be seen that as ν increases there is an increase in the temperature gradient immediately behind the detonation wave, and a concomitant drop in the beginning of the hypersonic part of the nozzle. The temperature on the detonation front reached levels of the order of 3000 K.

The theoretical investigation of detonation in nozzles also requires an experimental comparison since there is actually a limit of existence of detonation with respect to density of the fuel mixture in front of the wave [Ref. 19], which imposes a lower limit of the choice of A. Therefore in theory Λ cannot be taken too low.

Theoretical research is also being done in this area. For example, Ref. 10 sets limits with respect to pressure and concentration for direct initiation of detonation in a mixture of gases H_2-Cl_2.

System of kinetic equations (3.1) was solved by an implicit scheme of the second order of accuracy by the Newton method [Ref. 20], the optical weak-signal gain K being calculated on transition P20 (001-100) of the CO_2 molecule ($\lambda = 10.6$ μm) [Ref. 17].

Calculations for $\nu = 1.5$ show that population inversion takes place in a very narrow zone near the beginning of the hypersonic part of the nozzle and for small values of A.

Fig. 2 shows the distributions of gain as a function of distance from the beginning of the hypersonic part of the nozzle for different times, with $\nu = 2$, $A = 1.24 \cdot 10^{-4}$ (A has dimensions of $g/cm^{\nu-2}$). Lines 1-3 correspond to values of t of 284, 636 and 1873 μs, detonation rate D being 258,060 cm/s. The reduction in maximum gain with time and the increase in the inversion zone show up well. The gain reaches usable levels.

Fig. 3 and 4 show the same dependences for the case $\nu = 2.5$. Lines 1-4 in Fig. 3 correspond to values of t of 71, 165, 443 and 708 μs and $A = 2 \cdot 10^{-3}$, and on Fig. 4 they correspond to values of t of 36, 94, 326 and 667 μs and $A = 2 \cdot 10^{-4}$. Here D = 259,580 cm/s. It can be seen that as A increases there is a drop in maximum gain; however, the inversion zone with acceptable gain increases, reaching a size of several centimeters.

Fig. 5 shows the distributions of gain for $\nu = 3$, $A = 3 \cdot 10^{-4}$. Lines 1-5 correspond to values of t of 14, 31, 76, 121 and 169 μs, and D = 261,480 cm/s. It should be noted that as ν increases the inversion zone is displaced closer toward the detonation wave, and the maximum gain appears earlier.

A change in composition of the fuel mixture also has a considerable effect on gain. Calculations for $\nu = 3$, $A = 3 \cdot 10^{-4}$ and the second fuel mixture show that the absolute values of gain are approximately half the values shown in Fig. 5 for the same times and distances and D = 281,310 cm/s.

In conclusion the author thanks V. P. Korobeynikov for constructive discussion of the results.

REFERENCES

1. V. M. Marchenko, A. M. Prokhorov, "On the Feasibility of Producing an Inverse Medium for Lasers by Explosion", PIS'MA V ZHURNAL EKSPERIMENTAL'NOY I TEORETICHESKOY FIZIKI Vol 14, No 2, 1971.

2. J. Tulip, H. Seguin, "Explosion-Pumped Gasdynamic CO_2 Laser", APPL. PHYS. LETT., Vol 19, No 8, 1971.

3. B. A. Armstrong, B. Ahlborn, S. Mikoshiba, J. Tulip, "CO Laser Gain Measurements in Acetylene-Oxygen Detonation Products", CANAD. J. PHYSICS Vol 56, No 1, 1978.

4. M. I. Poddu'yev, "On a Method of Inversion of Vibrational Populations in a CO_2-N_2-He(H_2O) Gas Mixture", KVANTOVAYA ELEKTRONIKA Vol 6, No 2, 1979.

5. R. W. F. Gross, R. R. Giedt, T. A. Jacobs, "Stimulated Emission Behind Overdriven Detonation Waves in F_2O-H_2 Mixtures", J. CHEM. PHYS. Vol 51, No 3, 1969.

6. H. Guenoche, J. H. S. Lee, C. Sedes, "Population Inversion in Blast Wave Propagating in H_2-F_2-He Mixtures", COMBUSTION AND FLAME Vol 22, No 2, 1974.

7. J. H. S. Lee, T. D. Bui, R. Knystautas, "Population Inversion in Blast Waves", ACTA AERONAUTICA Vol 1, No 7/8, 1974.

8. H. Guenoche, J. H. S. Lee, C. Sedes, "Population Inversion Behind a Shock in a Mixture: H_2, F_2, He", ACTA AERONAUTICA Vol 3, No 1/2, 1976.

9. H. Guenoche, C. Sedes, "Calcul de l'inversion de population entre les niveaux de vibration de HCl en aval d'une onde de choc droite et d'une onde de souffle cylindrique", COMPT. REND. ACAD. SCI. SÉR. B Vol 282, No 20, 1976.

10. V. A. Levin, V. V. Markov, S. F. Osinkin, Yu. V. Tunik, "Numerical Modeling of Explosive Phenomena with Consideration of Nonequilibrium Physicochemical Processes", Sixth International Conference on Numerical Methods in Hydrodynamics held in Tbilisi, 1978., Collected Papers Vol 2, Moscow, 1978.

11. L. I. Sedov, "Metody podobiya i razmernosti v mekhanike" [Scaling and Dimensional Analysis in Mechanics], Moscow, "Nauka", 1977.

12. N. S. Zakharov, V. P. Korobeynikov, "Self-Similar Motions of Gas in the Case of Localized Inlet of Mass and Energy in a Fuel Mixture", IZVESTIYA AKADEMII NAUK SSSR: MEKHANIKA ZHIDKOSTI I GAZA No 4, 1979.

13. L. I. Sedov, "Mekhanika sploshnoy sredy" [Mechanics of a Continuous Medium], Vol 2, Moscow, "Nauka", 1973.

14. W. B. Cybulski, "Detonacja pylu weglowego", PRZEGLAD GÓRNICZY, Vol 30, No 3, 1974.

16. A. G. Abinov, A. M. Chekhovskikh, "Experimental Investigation of Detonation that Arises Upon Explosions of Methane and Coal Dust in Mines" in: "Detonatsiya. Kriticheskiye yavleniya. Fiziko-khimicheskiye prevrashcheniya v udarnykh volnakh" [Detonation. Critical Phenomena. Physicochemical Transformations in Shock Waves], Chernogolovka, 1978 (Soviet Academy of Sciences, Division of the Institute of Chemical Physics).

17. S. A. Losev, "Gazodinamicheskiye lazery" [Gasdynamic Lasers], Moscow, "Nauka", 1977.

18. V. P. Korobeynikov, "Problems of the Theory of a Point Explosion in Gases", Proceedings of the Mathematics Institute, Soviet Academy of Sciences, Vol 119, 1973.

19. J. H. Lee, R. I. Soloukhin, A. K. Oppenheim, "Current Views on Gaseous Detonation", ASTRONAUTICA ACTA, Vol 14, No 5, 1969.

20. A. A. Samarskiy, "Teoriya raznostnykh skhem" [Theory of Difference Schemes], Moscow, "Nauka", 1977.

6610
CSO: 8144/0812

LASERS AND MASERS

UDC 621.375.826

CHEMICAL LASERS

Moscow KHIMICHESKIYE LAZERY in Russian 1980 (signed to press 5 Sep 80) pp 2, 171-224

[Annotation, chapter 7 and table of contents from book "Chemical Lasers", by Valeriy Konstantinovich Ablekov, Yuriy Nikiforovich Denisov and Viktor Vasil'yevich Proshkin, Atomizdat, 2850 copies, 224 pages]

[Text] The book presents the principles of gas-phase reactions typical of chemical lasers, gives fundamentals of the quantum mechanical description of molecular systems, and outlines processes of formation of excited particles in the course of nonequilibrium chemical reactions. An examination is made of the kinetics of processes in chemical lasers classified according to their hydrogasdynamic characteristics into devices with a stationary medium, with subsonic and supersonic flow, and with detonation processes in the medium. Designs and working principles of present-day chemical lasers are described.

For engineers and scientists working in laser research and development. May be of use to undergraduate and graduate students majoring in physics and in engineering physics.

CHAPTER 7: CHEMICAL DETONATION LASERS

§7.1. General Information on Detonation Processes

We know that the process of detonation of solid [Ref. 1] and gaseous [Ref. 2, 3] explosives can be used for optical pumping of lasers. In this process the chemical energy of the explosive is converted directly to luminous pumping energy, and then to the energy of stimulated emission. Chemical energy conversion should be still more efficient in chemical detonation lasers with working principle based on stimulating emission directly from the zone of chemical reaction behind the detonation front [Ref. 4, 5], or from the region of free dispersal of the detonation products [Ref. 6], or from the region of discharge of the detonation products through the nozzle [Ref. 7]. In general we will apply the term *detonation* laser to a chemical laser in which detonation products serve as the active medium or as a component of this medium.

Let us give some information of a general nature on detonation.

Detonation is an explosive combustion wave for which one of the major well known properties is propagation at a constant supersonic velocity characteristic of the

given explosive and given initial parameters. If we take a coordinate system fixed on the detonation wave front, then in accordance with the one-dimensional theory of detonation the flow can be represented as shown in Fig. 7.1. The gas flows along

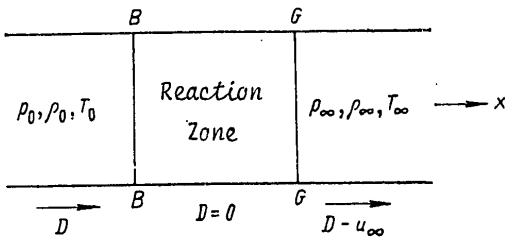

Fig. 7.1. Flow in coordinate system tied to the velocity D of the detonation front

the x-axis in the positive direction, and the wave parameters remain constant in planes perpendicular to the x-axis. Equations that describe such flow are given in Ref. 8. From these equations in coordinates of p vs. V we get a curve -- the Hugoniot adiabat -- that describes the solution for any values of the wave velocity D (Fig. 7.2):

$$V/V_0 = \frac{(p/p_0)+[(\gamma+1)/(\gamma-1)]+(2\gamma Q/c_0^2)}{[(p/p_0)(\gamma+1)/(\gamma-1)]+1}. \qquad (7.1)$$

Here $V = 1/\rho$ is specific volume; $\gamma = c_p/c_V$ is the ratio of specific heats; Q is the heat of combustion of a unit mass of the system; c_0 is the speed of sound in the initial mixture.

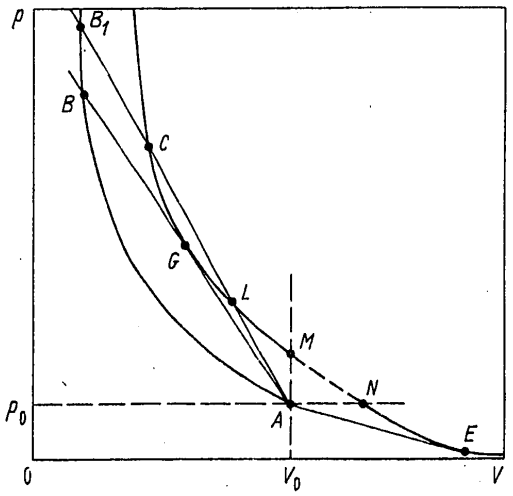

Fig. 7.2. Hugoniot adiabat

The condition of uniqueness of the detonation rate is demonstrated in Ref. 9, and has come to be called the Chapman-Jouguet rule:

$$(p - p_0)/(V_0 - V) = -(\partial p/\partial V)_S. \tag{7.2}$$

This rule implies that *normal* detonation corresponds to the minimum velocity D of all posible velocities, which is shown on the curve of p(V) (see Fig. 7.2) by the Michelson line AB tangent to the Hugionot curve CMNE at point G, known as the Jouguet point. It is typical of the process that in the state corresponding to point G, the detonation rate is equal to the sum of the flow velocity and the rate of propagation of the disturbance in the blast products, i. e.

$$D = u + c. \tag{7.3}$$

In addition to the mode of normal detonation corresponding to line AB tangent to the adiabatic curve of the detonation products, there are two other detonation modes described by curve CM: *overdriven* (CG) and *underdriven* (GM) detonations. For the former mode $u + c > D$, and for the latter $u + c < D$.

According to the *classical one-dimensional theory of detonation* [Ref. 10, 11], after the initial mixture has been compressed by the shock wave, its state corresponds to point B (see Fig. 7.2) in the case of normal detonation, and to point B_2 in the mode of overdriven detonation. Thereafter in the course of the chemical reaction the state of the medium shifts along Michelson curve BG or B_1C. States described by points G or C respectively correspond to completion of the chemical reaction. Thus the pressure should increase at points B or B_1.

The detonation wave theory that assumes the presence of a smooth wave front is based on solution of one-dimensional equations of gas dynamics and chemical kinetics.

There is a departure from this one-dimensional model in what is called *spin* detonation [Ref. 12]: the phenomenon of helical motion near the wall of a tube on the part of a single focus of a chemical combustion reaction, this focus being formed upon splitting of the wave front [Ref. 13]. Spin detonation always occurs at the limits of propagation of the detonation wave [Ref. 14].

The limits of propagation of the detonation are critical initial conditions with respect to pressure p_0 or density ρ, explosive charge diameter d, and also with respect to the concentration of components and the composition of the initial mixture, such that a change in these parameters either toward a reduction in pressure or diameter, or toward an initial mixture that is richer or leaner in the fuel component, makes it impossible for the detonation process to propagate.

According to the classical concept, the detonation wave should have a flat, smooth front far from the limits of propagation. However, the results of high-resolution photography and the wake method under these conditions have shown [Ref. 15, 16] an *inhomogeneous high-frequency structure* of real detonation waves with periodic inhomogeneities in the uneven leading edge of the wave.

Spin detonation close to its limit of propagation corresponds to the wake print of Fig. 7.3a [not included in the translation] with a thickened helical wake of

only one combustion focus moving with a trajectory at an angle χ to the generatrix of the detonation channel. With increasing distance from the limits of propagation there is a stepwise restructuring of the process: instead of a single combustion focus in the detonation front, there are 2n (n = 1, 2, 3...) combustion foci moving in contrary motion over the front with spacing Δx, undergoing collisions and reflections. A time photoscan gives the frequency of pulsations of the process:

$$\nu = D/\Delta x. \tag{7.4}$$

It is convenient to characterize such a periodic process by the *detonation mode*

$$\Omega = \nu/\nu_0 \ (\Omega \approx n), \tag{7.5}$$

where ν_0 is the minimum frequency of pulsations in the near-limit region of existence of the detonation wave with $\Omega \approx n - 1$. The spacing of the pulsations decreases with an increase in the initial pressure p_0 of the mixture or in its reactivity, e. g. by changing the chemical composition (Fig. 7.4) [Ref. 15-19]. Here the results of extrapolation of data of Ref. 20 correspond to $\Delta x \approx 5 \cdot 10^{-3}$ and $2 \cdot 10^{-3}$ mm, and $\nu \approx 7 \cdot 10^8$ and $11 \cdot 10^8$ Hz.

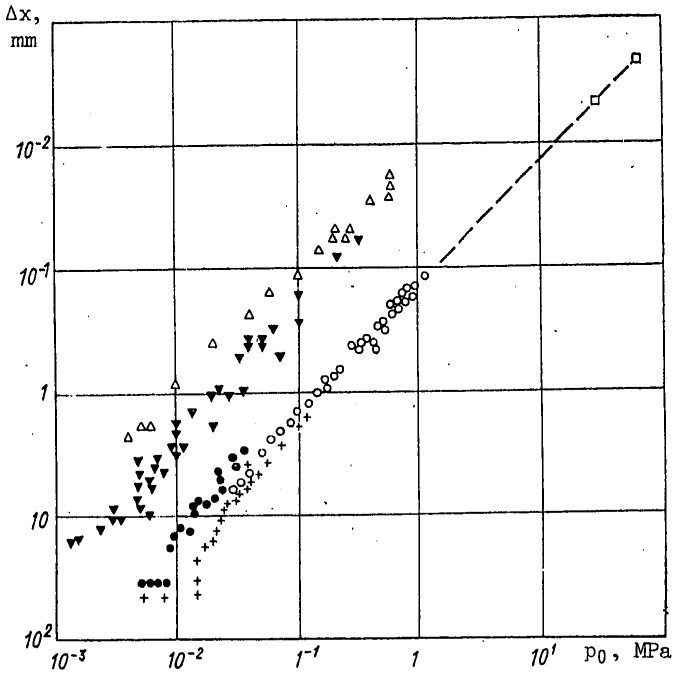

Fig. 7.4. Scale of pulsations Δx as a function of initial pressure p_0 of explosive mixtures $2H_2/O_2$ (○ [18], + [15, 16] ● [19]); $2C_2H_2/O_2$ (▼ [17-19]); C_2H_2/O_2 (△ [18]); $2H_2/O_2$ (□--extrapolation of data of Ref. 20)

Pulsations also occur in spherical detonation waves [Ref. 20], which is further evidence of the general nature of the pulsating mechanism as a property of detonation waves.

One of the peculiarities of detonation is the phenomenon of *discreteness* of the pulsation spacing Δx, frequency ν and other parameters that characterize the structure of the detonation wave as functions of initial pressure p_0.

Analysis of sequences of Δx for successive n in Ref. 22 gave an expression for the discrete spectrum of Δx in the form

$$\pi d/\Delta x = 1/n + \zeta_* (1 + 1/n)(n-1), \quad n = 1, 2, 3, \qquad (7.6)$$

Here $\zeta_* = \tan(\chi)_{min}$, i. e. the tangent of the smallest angle χ reached far from the detonation limits.

Each of the intersecting lines on the wake prints of Fig. 7.3b, c [not included in the translation] in Ref. 15, 16 is interpreted as a trajectory of a so-called *kink*. The kink was examined in Ref. 23 in the form of three intersecting shock discontinuities: an *oblique* compression shock, a *head-on* shock wave normal to the generatrix of the detonation channel, and a shock wave that moves *tangentially* to the head-on shock wave. Gasdynamic calculation of such a model, which is the *Mach configuration*, leads to the necessity of existence of a fourth discontinuity as well: a *tangential discontinuity* emanating from the point of intersection of the other three, the *triple point*.

And indeed, a triple point delineates each of the wake lines of the kinks [Ref. 24]. The space structure of an actual detonation wave for the case with n = 2 recorded on the wake print of Fig. 7.3b [not included in the translation] is graphically shown in Fig. 7.5 [Ref. 24] for three successive times t_0, t_1, t_2. Concavity of the

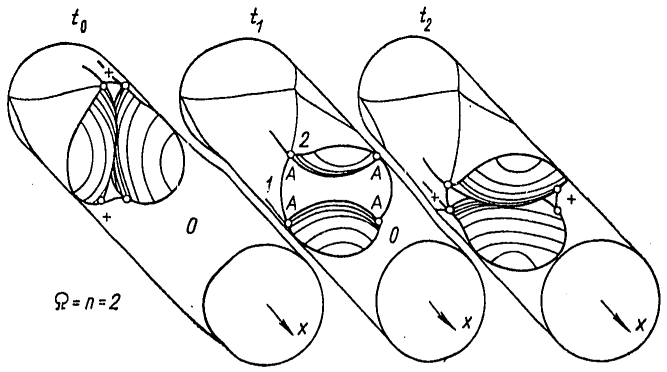

Fig. 7.5. Diagram of three-dimensional structure of detonation for $\Omega \approx n = 2$: light lines are the trajectories of triple points; heavy lines are shock discontinuities; circles indicate the triple points A; 0, 1, 2 -- states of the gas: initial, and behind oblique and head-on compression shocks respectively

wave front is replaced by convexity at collisions of triple points marked with the crosses. Pulsating behavior of the leading edge of a detonation wave has also been observed in Töpler schlieren photographs of the process of detonation in a flat

channel [Ref. 25, 17]. However, as shown in Ref. 25, the flow structure behind the leading edge for detonation at low n is still more complicated, and includes a *transverse detonation wave* suggested in Ref. 26 for spin detonation, experimentally observed in the structure of this detonation in Ref. 27-29, and studied in Ref. 30-32.

Flat Mach configurations in a detonation wave and their collision with one another were first analyzed by the method of *shock and detonation polar curves* in Ref. 24, 33 and 34. To do this, equations were derived that relate the relative pressure change ΔP in the i-th shock, $\Delta P = (p_i - p_0)/p_0 = \Delta p/p_0$, to the angle of deflection η of the flow behind the shock:

for the detonation polar curve

$$\operatorname{tg}\eta = \frac{\Delta P}{\gamma M^2 - \Delta P}\sqrt{\frac{M^2(1-q/\Delta P)}{\Delta P/(\mu^2+1)+1} - 1} \tag{7.7}$$

[M is the Mach number, $q = Q/E_0 = Q(\gamma-1)(p_0/\rho_0)^{-1}$ is the effective energy release as a fraction of the internal energy of the gas, $\mu^2 = (\gamma-1)/(\gamma+1)$];

for the shock polar curve

$$\operatorname{tg}\eta = \frac{\Delta P}{\gamma M^2 - \Delta P}\sqrt{\frac{M^2}{\Delta P/(\mu^2+1)+1} - 1}\,. \tag{7.8}$$

Solution showed that for detonation with $\Omega > 1$, collisions of Mach configurations and the resultant formation of new pulsations in the wave should be important. However, the actual process of interaction of perturbations in the detonation wave far from the limits of propagation is even more complicated than that usually considered in the plane model, and involves the influence of a *volumetric effect* on the structure of the detonation front [Ref. 35]. What is really important is that the process is three-dimensional, and that the most intense sources of disturbances that renew pulsations with Mach configurations in the wave are points of "triple" or higher multiple collisions of the Mach configurations. As a result, the pulsation multiplication factor

$$K = 1 + [(1 + N)/(n^* + N)] \tag{7.9}$$

at a sufficiently large number of initial pulsations N approaches two ($n^* = 3$ for detonation in channels of circular cross section, $n^* = 5$ for spherical detonation). The feasibility of such multiplication is implied by the reaction-kinetic data of a detonating medium [Ref. 21]. When the number of pulsations in the wave is small ($<n^*$) they may multiply by the formation of new triple points when there is an uneven change in the intensity of the discontinuities making up the Mach configuration [Ref. 36].

The question of *localization of controlling factors of the combustion zone* is an important one for an understanding of the detonation mechanism. Ref. 37 suggests a mechanism of chemical reaction under conditions of adiabatic explosion where the induction zone is a compression shock in which a few collisions between atoms or

molecules lead to chemical conversion of a small part of the explosive, and this brings about conditions for the concluding stages of the reaction. Hence we can assume that during detonation there is a thin layer (a shock-wave film) in which combustion foci are imbedded. That such a reaction zone structure is present in the detonation wave is demonstrated by methods of correlation analysis, experimental investigation of disturbances of the fine structure of spin detonation and comparison of the resultant data with calculated dimensions of the zone of vibrational relaxations of molecules [Ref. 38, 39]. The controlling factors of the combustion zone during detonation are localized in the narrow forward layer of the detonation wave with thickness of the order of the size of the zone of vibrational relaxations of the mixture; consequently, the scale of detonation pulsations may also reach values of this same order of magnitude.

§7.2. "Optical" Properties of Detonation Waves, and the Phase Nature of Their Propagation

In accordance with Fig. 7.5, the detonation wave front can be treated as consisting of elementary fronts that oscillate about some average position propagating at constant velocity. The interactions between neighboring elementary fronts are sources of new fronts. If the initial explosive is isotropic, the propagation of such a wave front should conform to laws of geometric and physical optics.

On this basis, the Fermat analytical principle and the Huygens-Fresnel principle can be applied to the process of propagation of detonation waves in an inorganic medium [Ref. 40].

The first of these states that propagation of a wavefront f in an isotropic medium from point $P_1(x_1,y_1)$ to point $P_2(x_2,y_2)$ corresponds to the extremum value of the integral

$$T=\int_{P_1}^{P_2}\frac{ds}{D(x,y)}, \tag{7.10}$$

where T is the time required for passage of the section of wave front from P_1 to P_2 and s is the length of arc of the trajectory of a point of the wave front.

The integral curve is determined from the differential equation of Euler for the extremum

$$\frac{d}{dx}\frac{y'}{D(x,y)\sqrt{1+(y')^2}}+\frac{\sqrt{1+(y')^2}}{D^2(x,y)}\frac{\partial D(x,y)}{\partial y}=0. \tag{7.11}$$

The constants of general solution $y\ (x, C_1, C_2)$ are determined from the conditions

$$\left.\begin{aligned} y_1&=y(x_1, C_1, C_2),\\ y_2&=y(x_2, C_1, C_2).\end{aligned}\right\} \tag{7.12}$$

In many cases the Fermat principle reduces to simple algebraic expressions for conditions of minimum time of propagation of the wave fronts, as shown for example

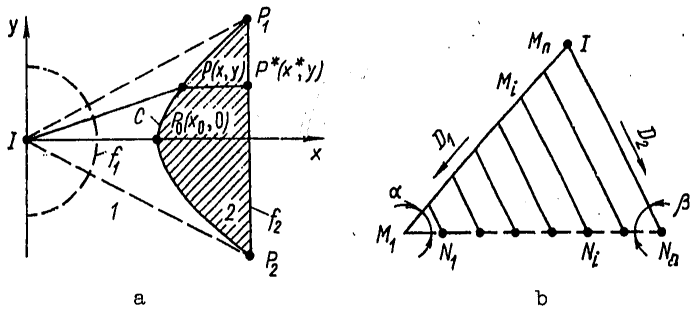

Fig. 7.6. Examples of application of the Fermat principle to the detonation process (detonation collimators): a--with two continuous explosive media 1 and 2 ($D_1/D_2>1$); b--with separate explosive channels

in Fig. 7.6a, b. In the two-dimensional case, for simultaneous emergence of all points of the detonation front f_1 emanating from a single initiation point I at straight line P_1P_2 (see Fig. 7.6a) when a compound charge is used with two media 1 and 2 having different detonation rates D_1 and D_2, the shape of the boundary between media 1 and 2 is calculated from the equations:

$$T = \sqrt{x^2+y^2}/D_1 + (x^*-x)/D_2; \tag{7.13}$$

$$T_{\min} = x_0/D_1 + (x^* - x_0)/D_2. \tag{7.14}$$

When $D_1/D_2>1$, the boundary C between the media is a hyperbola. Such a generator of a straight wave front (collimator) may be important for chemical detonation lasers as a device for simultaneous input of gaseous detonation products into the optical cavity. The detonation wave generator shown in Fig. 7.6b can serve the same purpose.

Here the line M_1M_n is a channel filled with a detonating medium having detonation rate D_1, and the lines M_iN_i ($i=1, 2,\ldots, n$) are channels with a medium detonating at rate D_2. The condition of simultaneous arrival of the detonation fronts in all channels M_iN_i at the level of straight line M_1N_n is

$$T = \frac{IM_i}{D_1} + \frac{M_iN_i}{D_2} \text{ or } T = \frac{IM_1}{D_1}\Big|_{M_iN_i=0} = \frac{IN_n}{D_2}\Big|_{IM_i=0}, \tag{7.15}$$

whence

$$D_1 = D_2 \sin\beta/\sin\alpha. \tag{7.16}$$

If $\alpha=\beta$, then $D_1=D_2$ and $IM_1=IN_n$. An example of realization of such a scheme is linear detonation generators filled with gaseous explosive and made in the form of detonation channels of the same length [Ref. 3]. A device based on an analogous principle focuses the detonation wave by using hollow cylindrical shaping lenses made in the form of a stack of cylindrical diaphragms that are roughened in the central part and smooth on the edges.

A number of wave generator designs based on the Fermat principle are shown in Fig. 7.7a-r [Ref. 40]. Shown are: a, b, i, o -- designs with focusing of detonation

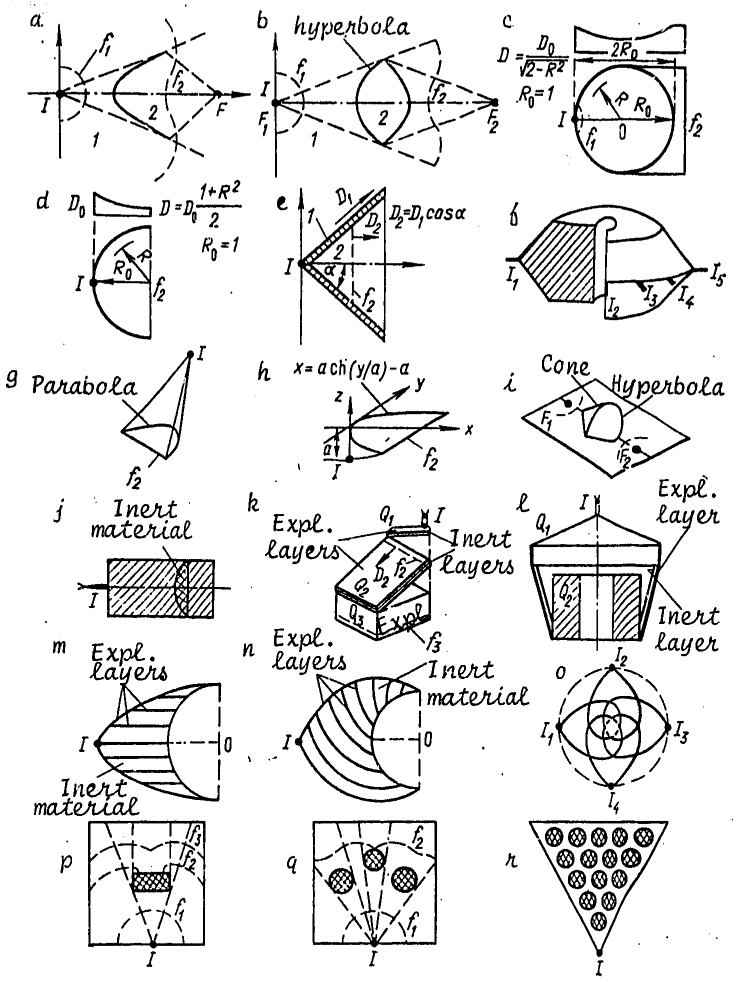

Fig. 7.7. Diagrams of detonation wave generators

fronts at a point; c, d, e, g, h, r -- linear detonation front; f, l -- focusing of detonation on the axis of the system; j, k -- generation of a planar detonation front; m, n -- generation of a curvilinear detonation front; p, q -- diffraction of detonation fronts. Designs p, q and r are based on the diffraction properties of detonation waves occasioned by the physical rather than the geometric optics of the system.

Within the framework of physical optics of detonation, the Huygens-Fresnel principle enables construction of the detonation wave front for some instant if the wave front is known at a preceding time. Such a construction is based on the fact that each point of the medium reached by the wave front is treated as a new source of oscillations.

The regions of collisions of kinks -- triple Mach configurations -- act as such new sources of pulsations in a detonation wave. The sources of new pulsations in the detonation front are responsible for the *phase nature* of propagation. After each collision of kinks, a new pulsation arises with parameters that depend only on the initial conditions. This can explain the effect of detonation wave diffraction that takes place for example when detonation waves flow around corners, or the effect of refraction on interfaces [Ref. 41]. The pattern of phase propagation of a detonation front is shown schematically in Fig. 7.8, where the numbers 1-8 denote positions of pulsation fronts corresponding to times from t_1 to t_8. The heavy lines depict regions of maximum energy release that renew pulsations in the wave.

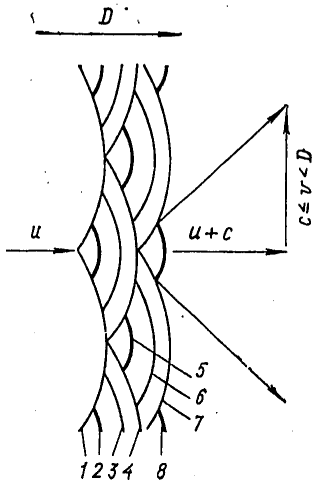

Fig. 7.8. Diagram of phase propagation of a detonation wave. For tangential velocity of development of pulsation $c \leqslant v < D$ ($v = D$ -- spin detonation, $n = 1$)

Phase propagation of such a structure at velocity D, as can be seen from Fig. 7.3b, c [not included with the translation] forms patterns similar to those observed in hydrodynamics during flow of shallow water (motion in a field of gravity of an incompressible liquid with a free surface and with depth of a layer of this liquid that is small compared with the characteristic dimensions of the flow). It is known (see for example Ref. 42) that wave processes on shallow water are described by the Kortweg – de Vries equation

$$\psi_t + D\psi_x + b\psi_{xxx} + \psi\psi_x = 0 \qquad (7.17)$$

(D is wave velocity, $b = Dl^2$, l is the scale factor). Special cases of this equation for propagation of small and finite perturbations in a medium with a chemical reaction were considered in Ref. 43.

Long-wave perturbations for the case of acoustic detonation in reacting media have been analyzed to derive an equation that describes the structure of a finite perturbation propagating in one direction in a reacting medium. The general system of equations of a reacting gas presented in §1.7 is reduced in Ref. 43 to a single equation from which the Kortweg - de Vries - Burgers equation is derived for waves on the surface of a liquid with positive viscosity in limiting cases $\tau_{ch}/T < 1$ (τ_{ch} is the time of the chemical reaction, T is the characteristic period of the initial disturbance). In this connection, condition $\tau_{ch} \sim 1$ corresponds to medium frequencies, while $\tau_{ch} > 1$ corresponds to the high-frequency approximation. The analysis implies that when a long-wave perturbation propagates through a medium with an exothermic reaction, it increases in amplitude and decreases in duration, i. e. signal amplification takes place.

The frequency response of wave bursts in each of the possible detonation modes for given initial conditions of the explosive medium can be derived by the energy method and the formalism of elementary quantum mechanics [Ref. 42] in which the state of the medium is described by a normalized function $\psi(x,t)$ that satisfies an equation of Schrödinger type as a special case of (7.17). Such a set of possible

normal frequencies of the detonation process can be obtained in the following way [Ref. 44]. Energy release Q(T) is accounted for by the equation of the second law of thermodynamics:

$$Tds = dT - (\gamma - 1)Td\rho/\rho = (1/c_V)Q(T)dt. \tag{7.18}$$

Here $s = S/c_V R$ is the dimensionless specific entropy.

To simplify the problem, we will assume that Q is a linear function of T, i. e. $Q(T) = (\partial Q/\partial T)T$, where $\partial Q/\partial T = \text{const}$. Then from equation (7.18)

$$T = T_a \exp(\omega t), \tag{7.19}$$

where $\omega = ds/dt = \frac{1}{c_V}\frac{\partial Q}{\partial T} = \frac{1}{\tau}$; τ is the ignition induction period; $T_a = T_0(\rho/\rho_0)^{\gamma-1}$ is flash point.

Each wave burst in the detonation wave is described on the average by the transported mass m, momentum $\vec{p} = m\vec{u}$ and energy E in phase space $\vec{r}$, t. By analogy with quantum mechanical formalism [Ref. 42] we write

$$ih_D\frac{\partial\psi}{\partial t} = -\frac{h_D^2}{2m}\nabla^2\psi + \left(\frac{\gamma T_a e^{\omega t}}{\gamma - 1} - \int Tds\right)\psi. \tag{7.20}$$

Here h_D is a constant that depends on the thermodynamic properties of the medium, $\psi(\vec{r},t)$ is the wave function that characterizes the wave burst in the detonation front.

To determine the constant h_D, we use one of the solutions of equation (7.20) in the form of a plane wave

$$\psi(\mathbf{r}, t) \sim \exp[-(i/h_D)(Et - \mathbf{pr}) - is_0(t)], \tag{7.21}$$

where s_0 is the initial phase of the wave.

The law of conservation of energy in such a wave is

$$E = mu^2/2 + [T_a/(\gamma - 1)]\exp\omega t. \tag{7.22}$$

We determine constant h_D by substituting (7.21) in equation (7.20). We get

$$E + h_D ds_0/dt = mu^2/2 + [T_a/(\gamma - 1)]\exp(\omega t) + T_a. \tag{7.23}$$

From expressions (7.22) and (7.23) we get

$$ds_0/dt = T_a/h_D = \omega \text{ or } h_D = T_a/\omega. \tag{7.24}$$

In a physical sense, the initial phase of the wave s_0 coincides here with the idea of specific entropy, and therefore when a new wave burst is formed by a discontinuity, not only the phase changes, but the entropy as well.

Now let us verify whether equation (7.20) satisfies the principal laws of conservation of mass and momentum. The expressions for these laws can be obtained from

expression (7.20) by averaging. For instance the law of conservation of mass

$$\frac{\partial |\psi|^2}{\partial t} = -\operatorname{div} \mathbf{j} \tag{7.25}$$

is written as $\frac{\partial}{\partial t}\int |\psi|^2 d\mathbf{u} = -\operatorname{div}\int \mathbf{j} d\mathbf{u}$, where $|\psi|^2 \sim \rho/\rho_0$, and $\vec{j} = \frac{ih_D}{2m}(\psi \nabla \psi^* - \psi^* \nabla \psi)$ is the probability flux density. Integration with respect to physical volume $\vec{r}$, t gives the averaged law of conservation of mass. The law of conservation of momentum is written as

$$\frac{\partial j_i}{\partial t} = -\frac{\partial}{\partial x_j}\hat{\Pi}_{ij}. \tag{7.26}$$

Here the momentum probability flux density tensor is

$$\hat{\Pi}_{ij} = \frac{h_D^2}{4m}[(\nabla_i \psi \nabla_j \psi^* + \nabla_i \psi^* \nabla_j \psi) - (\psi \nabla_i \nabla_j \psi^* + \psi^* \nabla_i \nabla_j \psi)] + \delta_{ij}(p_0/\rho_0)\gamma \exp(\omega t)/(\gamma - 1). \tag{7.27}$$

Analogously upon integration of (7.26) with the use of (7.21) we get an expression for the law of conservation of momentum.

Let us analyze the structure of the detonation front on the basis of equation (7.20). To do this, we consider the two-dimensional problem with longitudinal transport of wave energy in the direction of the x-axis, and along the y-axis in the transverse direction. We will look for periodic solutions with respect to y, and derivatives with respect to x, t in the form

$$\psi = \psi(x, t)\exp(iky), \tag{7.28}$$

where $k = 2\pi/\Delta y$ is the wave number, Δy is the transverse scale of the pulsations in the detonation front. From (7.20) we get

$$ih_D \frac{\partial \psi}{\partial t} = -\frac{h_D^2}{2m}\frac{\partial^2 \psi}{\partial x^2} + \left[T_a\left(\frac{e^{\omega t}+\gamma-1}{\gamma-1}\right) + \frac{k^2 h_D^2}{2m}\right]\psi. \tag{7.29}$$

Let us look for self-similar solutions of (7.29) for steady-state motion by a procedure analogous to that used in the theory of steady-state shock waves [Ref. 45]:

$$\psi(x, t) = \psi(x - Dt).$$

Making the self-similar substitution $\frac{\partial}{\partial x} \to -\frac{1}{D}\frac{\partial}{\partial t}$, we get

$$\frac{\partial^2 \psi}{\partial t^2} + \frac{2imD^2}{h_D}\frac{\partial \psi}{\partial t} - \frac{2mD^2}{h_D^2}\left[T_a\frac{\exp(\omega t)+\gamma-1}{\gamma-1} + \frac{k^2 h_D^2}{2m}\right]\psi = 0 \tag{7.30}$$

To solve this equation for eigenvalues, we use the conditions $|\psi|^2_{t=0} = 1$, $|\psi|^2_{t\to\infty} = 0$.

After the substitution

$$\psi(x, t) = \Phi(x, t)\exp(-imD^2 t/h_D) \tag{7.31}$$

(7.30) is transformed to

$$\Phi_{tt}''-\Phi\left(\frac{2mD^2}{h_D^2}\right)\left[\frac{T_a(e^{\omega t}+\gamma-1)}{\gamma-1}-\frac{1}{2}mD^2+\frac{k^2h_D^2}{2m}\right]=0. \tag{7.32}$$

We solve this equation at $\Phi_{t=0}=1$, $\Phi_{t\to\infty}=0$. The solution can be represented as a cylindrical function of the imaginary argument $K_\nu(z)$, and then

$$\psi(x,t)=\exp\left[-\frac{imD^2}{h_D}\left(t-\frac{x}{D}\right)\right]CK_\nu\left\{a\exp\left[\frac{\omega}{2}\left(t-\frac{x}{D}\right)\right]\right\}, \tag{7.33}$$

where $a=\frac{2D}{\omega h_D}\left(\frac{2mT_a}{\gamma-1}\right)^{1/2}$, and C is found from the normalization condition

$$\int_{-\infty}^{+\infty}|\psi|^2\,dv=1.$$

From the solution we get a dispersion relation for the pulsating process

$$\Omega=\frac{2D}{\omega}\left(\frac{2mT_a}{h_D^2}+k^2-m^2\frac{D^2}{h_D^2}\right)^{1/2}. \tag{7.34}$$

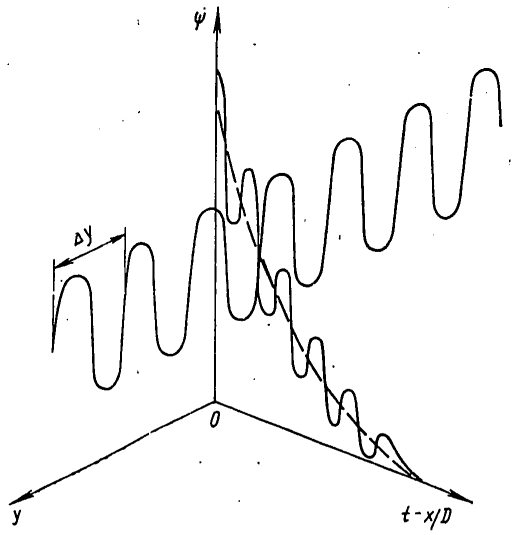

Fig. 7.9. Model of wave burst of the detonation process

Fig. 7.9 shows the resultant model of the wave burst in the form of the function ψ in coordinates y vs. t - x/D at a fixed value of Ω. Estimation of the time scale of the pulsation with respect to x in the detonation wave gives

$$\Delta t \simeq \frac{2}{\omega} \ln \left[\frac{8mD^2}{(\gamma-1)T_a} \right]^{-1/2}. \tag{7.35}$$

Using expression (7.33) for the wave function ψ and taking the representation of energy in accordance with formula (7.22) in operator form, we get after averaging

$$\bar{E} = \rho_0 T_a + \rho_0 D^2 \left[1 - \frac{\Omega^2 T_a^2}{4\rho_0^2 D^4} \right]. \tag{7.36}$$

This implies for example that for $\Omega > \bar{\varepsilon} - 1$ the Mach number of the detonation wave is

$$M = \left[\frac{\Omega}{2\gamma} + \frac{\bar{\varepsilon}-1}{2\gamma} \right]^{1/2} (\rho/\rho_0)^{\frac{\gamma-1}{2}}, \tag{7.37}$$

where $\bar{\varepsilon} = Q\bar{\mu}/RT_a^{(0)}$; $Q = \bar{E}/\rho_0$.

If the spectrum of detonation frequencies is represented in accordance with (7.5) as $\nu = \Omega\nu_0$, where ν_0 is the minimum frequency of pulsations in the near-limit region of existence of the detonation, and the specific energy release of the chemical reaction of ignition, the flash point and the average molar mass of the mixture are taken as Q, $T_a^{(0)}$ and $\bar{\mu}$ respectively, then relation (7.37) qualitatively follows the spectrum of the experimentally observed relation between the longitudinal mode and the Mach number M. This can be seen for example from a comparison on Fig. 7.10 of the experimental discrete detonation frequency spectrum (shown by the vertical lines and the broken curve; the cross shows the value calculated from the data of Ref. 18) with the results calculated by relation (7.37) (short lines and dot-and-dash curve) for a stoichiometric oxygen-hydrogen mixture.

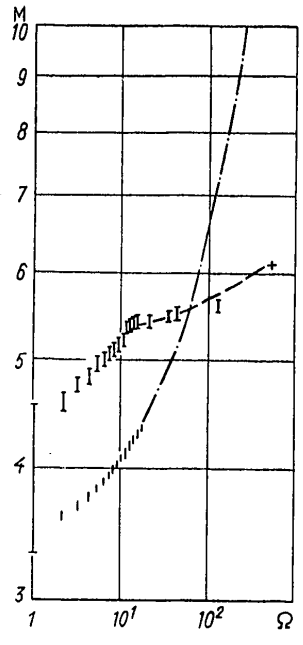

Fig. 7.10. Comparison of experimental and theoretical discrete detonation spectra

Although the comparison of theory and experiment on Fig. 7.10 shows only the qualitative correspondence between the directions of changes in parameters, nevertheless the theoretical concept that has been developed can serve as an illustration of the phase process of detonation wave propagation based on the "physical optics" of detonation waves. A condition of applicability of such consideration, of course, must be the fact that the frequency of the process $\nu = \Omega\nu_0$ must be less than the natural frequency of vibrations of the molecules.

The fundamental harmonics of detonation pulsations were also found in Ref. 46 by examining

periodic instability as a theoretical basis of the internal property of detonation -- pulsation wave structure.

A detailed mechanism of phase propagation of detonation is proposed in Ref. 47. It is based on equality of the average tangential velocities of collision D_2 and reflection D_3 of triple points A treated as *ignition points* (*ignition lines*) in the relaxation layer (film).

Actually, conditions of stable existence of detonation should be

$$D_3/D_2 = 1, \tag{7.38}$$

$$M_2 = D_2/c_1 \gtrsim 1, \tag{7.39}$$

where the latter condition means that the tangential velocity of point A is close to the speed of sound in the initial shock-compressed gas in state 1.

Suppose that shock waves collide, and Chapman-Jouguet waves are reflected. When condition (7.38) is satisfied, the conservation equations yield

$$M_2^2 = \frac{\gamma_1+1}{2\gamma_1}\,\frac{2\gamma_3(3-\gamma_1)+\gamma_1(4-\gamma_1)-3}{\{[\gamma_3(\gamma_1-1)+2\gamma_1(\gamma_1-2)]^2-4\gamma_1(\gamma_1-3)[2\gamma_3(\gamma_1-3)+} \rightarrow$$

$$\rightarrow \frac{}{+\gamma_1(\gamma_1-4)+3]\}^{1/2}-\gamma_3(\gamma_1-5)+\gamma_1^2-3} + \frac{\gamma_1-1}{2\gamma_1}. \tag{7.40}$$

In Ref. 38, 47, the motion of ignition point A during detonation is treated in a coordinate system fixed to this point as supersonic flight of a pointed wedge in a gas mixture with an exothermal reaction in the wedge. Let us represent the flow in the near vicinity of the point A as shown in Fig. 7.11. Since the collisions of ignition points (lines) are symmetric relative to the directed average velocity D, the absolutely rigid wall x-x can be taken as the axis of symmetry of the process. We will take AB as the incident wave front of oblique Mach reflection, AN as the Mach disk of this reflection, the dot-and-dash line indicating the direction of "flight" of ignition point A with dispersal of the products of isothermic reaction to both sides of this line at angles $\phi_1 \approx \phi_2$, and AK indicating the limit of dispersal in the form of a compression shock that changes into a Mach wave. In order for an oblique Mach reflection to form again after collision with x-x, the condition

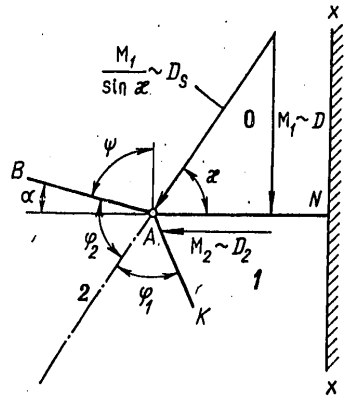

Fig. 7.11. Diagram of flow in the vicinity of an ignition point in the detailed structure of a detonation wave

$$\psi \geqslant \operatorname{arcctg} \sqrt{\frac{\gamma_2+1}{2}\frac{\rho_0}{\rho_2}\left(1-\frac{\rho_0}{\rho_2}\right)}. \tag{7.41}$$

must be satisfied.

Taking the equal sign, and assuming that the transition 0-2 is strong enough that $\rho_0/\rho_2 \approx (\gamma_2 - 1)/(\gamma_2 + 1)$, we get from (7.41)

$$\psi = \operatorname{arcctg} \sqrt{(\gamma_2-1)/(\gamma_2+1)}. \tag{7.42}$$

For angles ϕ_1 and ϕ_2 we have

$$\varphi_1 \approx \varphi_2 = \alpha + \varkappa = \frac{\pi}{2} - \psi + \varkappa \approx \varphi, \tag{7.43}$$

where

$$\varkappa = \operatorname{arctg}(D/D_2) = \operatorname{arctg}(M_1 c_0 / M_2 c_1); \tag{7.44}$$

$$c_0/c_1 = \{(\gamma_1 + 1)^2 (\gamma_0 - 1)/2\gamma_1 (\gamma_1 - 1)[2 + (\gamma_0 - 1)M_1^2]\}^{1/2}. \tag{7.45}$$

From (7.44 and (7.45) with consideration of (7.43) we get

$$\varphi = \operatorname{arctg}\left\{\left(\frac{\gamma_1+1}{m} + \mu_2\right) \Big/ \left[1 - \frac{(\gamma_1+1)\mu_2}{m}\right]\right\}, \tag{7.46}$$

where

$$m = M_2\{2\gamma_1 (\gamma_1 - 1)[1 + 2/M_1^2 (\gamma_0 - 1)]\}^{1/2};$$
$$\mu_2 = [(\gamma_2 - 1)/(\gamma_2 + 1)]^{1/2}.$$

For the pressure in region 2 we have [Ref. 48]

$$p_2 = \frac{2}{n_2+1} \rho_0 D_s^2 \sin^2 \varphi, \tag{7.47}$$

which with consideration of the fact that $D_S = D/\sin\kappa$ (see Fig. 7.11) becomes

$$n_2 = \gamma_2 \frac{1+(\gamma_2-1)q/2\gamma_2}{1+(\gamma_2-1)q/2} \quad \left(q = \frac{2Q}{p_2/\rho_2}\right). \tag{7.48}$$

Here, in accordance with Ref. 48,

$$\frac{p_2}{p_0} = \frac{2\gamma_0 M_1^2}{n_2+1} \frac{\sin^2\varphi}{\sin^2\varkappa}. \tag{7.49}$$

In the given calculations, p_1/p_0 and ρ_1/ρ_0 are related to M_1 by the respective formulas

$$\frac{p_1}{p_0} = \frac{\gamma_0 M_1^2 + 1}{\gamma_1 + 1} + \left[\left(\frac{\gamma_0 M_1^2 + 1}{\gamma_1 + 1}\right)^2 + \frac{2\gamma_0 M_1^2 (\gamma_0 - \gamma_1)}{(\gamma_1+1)(\gamma_0-1)} - \frac{2\gamma_0 M_1^2 - (\gamma_1 - 1)}{\gamma_1 + 1}\right]^{1/2}; \tag{7.50}$$

$$\rho_1/\rho_0 = \left\{1 + \frac{\gamma_1+1}{\gamma_1-1}\left[\left(\frac{2\gamma_0 M_1^2}{\gamma_0+1}\right) - \frac{\gamma_0-1}{\gamma_0+1}\right]\right\}\left[\frac{4\gamma_0}{\gamma_0^2-1} + \frac{2\gamma_0 M_1^2}{\gamma_0+1}\right]^{-1}. \tag{7.51}$$

There are analogous formulas for p_2/p_1 and ρ_2/ρ_1.

From (7.40), (7.44), (7.45) for a stoichiometric hydrogen-oxygen mixture at $\gamma_0 = 7/5$, $\gamma_1 = 8/6$, $\gamma_2 = 9/7$ we get calculated values of $\kappa = 55\text{-}56^\circ$ close to the experimental results at Mach numbers $M_1 = 5\text{-}6$ typical of pulsating detonation.

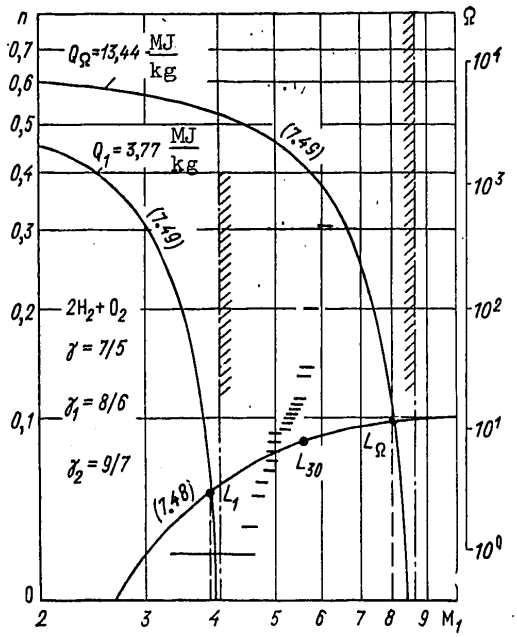

Fig. 7.12. Graphic solution of equations (7.48), (7.49) for $Q_1 = 3.77$ and $Q_\Omega = 13.44$ MJ/kg, and comparison with the limits of the experimental spectrum of detonation frequencies

The Mach number M_1 of the detonation wave in this same mixture can be conveniently determined from the graphic solution of equations (7.48) and (7.49) on Fig. 7.12, which also shows for comparison the experimental spectrum of detonation frequencies in coordinates M_1, $\Omega = \nu/\nu_0$. For pulsating detonation the region of this spectrum on the graph is bounded by the shaded dot-and-dash line. Solutions L_1 and L_Ω of equations (7.48) and (7.49) for $Q_1 = 3.77$ and $Q_\Omega = 13.44$ MJ/kg respectively show little difference from the indicated region of the experimental spectrum of detonation frequencies. Here Q_1 is the energy release for near-limit pulsating detonation with fundamental mode $\Omega = 1$, Q_Ω is the maximum theoretically possible energy release accompanying a chemical reaction in a detonation wave. The point L_{30} corresponds to detonation of a mixture of $2H_2 + O_2$ under normal initial conditions with natural frequency characterized by the mode $\Omega = 30$ and $\nu = 1.5$ MHz.

In the fan of rarefaction waves that is formed in region 2 as the reaction products disperse from ignition point A, the incoming flux may be deflected to the point where compression takes place in region 1 (see Fig. 7.11), and self-regulation is effected by this kind of "feedback". It is by this that the detonation wave

"knows" in what tangential geometry it is propagating: in channels of circular or perhaps rectangular cross section, and at the same time does not "know" the geometry of the space in the direction normal to its flow, for example whether the ends of the channel are closed or open.

§7.3. Overdriven Detonation

Of interest in application to chemical lasers of detonation type is an examination of conditions of overdriven detonation, since it is in just such modes that the effect of direct stimulation of coherent emission has so far been realized [Ref. 4]. Corresponding to modes of overdriven detonation are states on the Hugoniot adiabat lying above the Chapman-Jouguet point, e. g. on curve CG (see Fig. 7.2). Such modes can be realized by preventing the formation of a rarefaction wave behind the detonation wave front, e. g. by using a piston or some other method to compress the reaction products [Ref. 10]. Overdriven detonation is realized for example by a change in the channel geometry tangential to the wave in a narrow tube as detonation passes to it from a wide tube, by setting up an electric discharge current layer in the explosive mixture to act as an impermeable piston that pushes the shock wave [Ref. 49].

Overdriven detonation can also be realized by "driving" the detonation wave out of a high-pressure section into a section with a low-pressure explosive medium that is separated from the high-pressure section by a breakable diaphragm.

Unless they are maintained, overdriven waves have a damped velocity, and in essence should not be considered detonation waves, for which one of the major properties is steady-state propagation under fixed initial conditions.

However, there is another feature of detonation that must be taken into account -- the periodic structure identified by the wake method [Ref. 15]. The presence of such a structure in a reactive medium is evidence of energy release immediately in the wave front, and in particular during overdriven detonation.

From the way that pulsation spacing Δx changes on wake prints for known initial conditions p_0, d_{tube}, one can judge whether overdriven detonation occurs, and can select structures with a smooth front that are of interest for chemical lasers. Fig. 7.13 shows diagrams of such wake prints for some methods of exciting overdriven detonation, and graphs of the change in pulsation spacing Δx as the detonation waves from overdriving are reaching the steady Chapman-Jouguet state on length L_{CG} from the cross section in the detonation channel that corresponds to overdriving at point C of the Hugoniot adiabat until the steady state of detonation is reached, corresponding to point G (see Fig. 7.2). The overdriven detonation mode with velocity D_C was realized both by stimulated excitation (broken curves on Fig. 7.13) and by the natural onset of detonation from the unsteady combination of an accelerated flame G preceded by a shock wave S (solid curves) propagating at velocity D_y.

We can see from these diagrams that chemical detonation lasers can utilize processes shown in diagrams I, III and V on sections corresponding to overdrive compressions beyond the limit values, i. e. downstream from cross section C to points where high-frequency detonation pulsations arise. Use can also be made of the overdriven processes with smooth fronts found in Ref. 52.

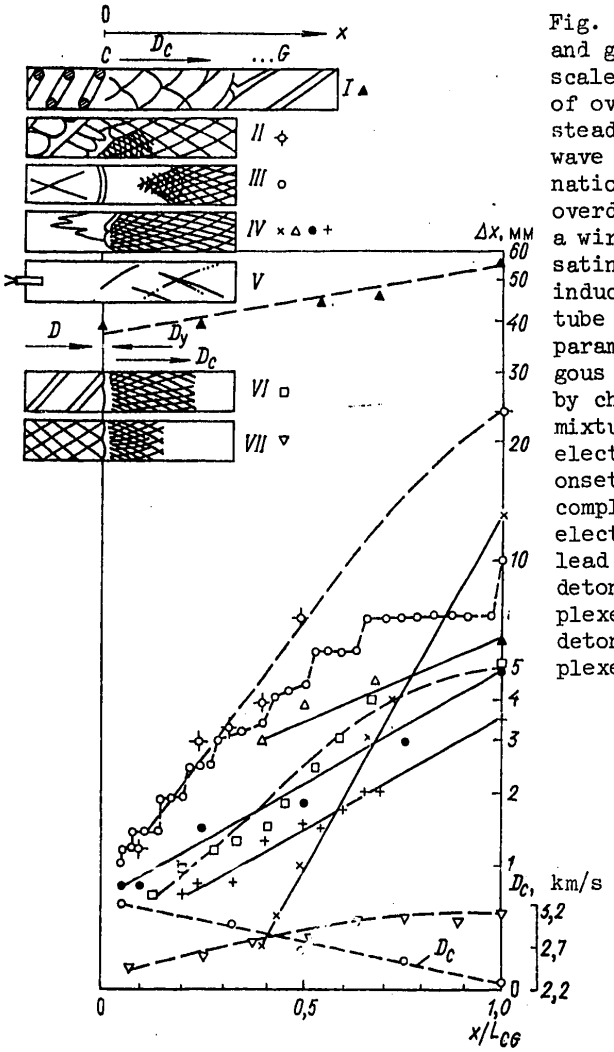

Fig. 7.13. Diagrams of wake prints and graphs of the change in pulsation scale Δx on the length of transition of overdriven detonations to the steady state, L_{CG}: I--spin detonation wave transition of a pulsating detonation artificially produced under overdriving conditions in a tube with a wire helix [Ref. 24, 50]; II--pulsating detonation transition of an induced spin detonation produced in a tube with a helix at fixed initial parameters of the mixture (an analogous result was obtained in Ref. 36 by changing the initial density of the mixture); III--strong initiation by an electric discharge [Ref. 51]; IV--onset of detonation from unsteady G-S complex; V--strong initiation by an electrodetonator or a suspension of lead azide; VI--collision of spin detonation with unsteady G-S complexes; VII--collision of pulsating detonation with unsteady G-S complexes

Mixture	Experiment	p , kPa	d_{tube}, mm	L_{CG}, mm
$CH_4/2O_2$	×	40	20	90
$2H_2/O_2$	▲	13,3	16	400
	-○-	17,3	18	50
	○	26,6	18	800
	△	40	20	30
	●	53,3	20	40
	+	66,6	20	50
	□	9,3	16	30
	▽	40	16	8

The process by which detonation arises under conditions of overdriving is identical to the process of stimulated emission in lasers and masers, and is characterized by shock wave amplification and coherent energy release (for example, IV on Fig. 7.13) -- called the "swaser" effect in Ref. 53.

§7.4. Mechanisms of Population Inversion in Chemical Detonation Lasers

Pumping the active substance by the energy of the chemical bond. To increase the coefficient of utilization of pumping energy, it is suggested in Ref. 4 that explosion energy be converted directly by dissociation, including by photolysis, impact dissociation or some other chemical reaction through the process of premixing the working substance of the laser with the initial explosive. Such a method of producing a medium with negative absorption factor is based on the fact that any explosive in the initial state can be treated as a medium with population inversion for which the state of the combustion products is a stable state. Inversion upon detonation of an explosive can be realized by a variety of reactions in the detonating explosive medium. Let us consider some of these reactions.

a. *Two-component mixture*: explosive + working (emitting) substance.

For this case, energy conversion is realized as follows. The explosive XY dissociates:

$$XY \rightarrow \sum_{j=1}^{m} (XY_j + \Delta E_j + h\nu_j), \tag{7.52}$$

where the XY_j are products of dissociation of the initial substance; ΔE_j is the kinetic energy of the reaction products; $h\nu_j$ is the energy of a quantum emitted upon dissociation of the intial substance XY into components XY_j; m is the number of terminal products.

Upon explosion, the energy of the products of dissociation is expended on decomposition and emission of the introduced working substance AB:

$$AB + \Delta E_j \rightarrow AB^*; \tag{7.53}$$
$$AB + h\nu_j \rightarrow AB^*. \tag{7.54}$$

AB* in turn may emit a quantum as a result of reactions

$$AB^* \rightarrow A + B^* \rightarrow A + (B + h\nu); \tag{7.55}$$
$$AB^* \rightarrow A + B + h\nu + \Delta E. \tag{7.56}$$

Reaction (7.55) corresponds to emission of a product of dissociation (B*) of the excited AB* molecule, and reaction (&.56) corresponds to conversion of the working substance from the excited to the dispersed state.

Instead of the diatomic working molecule AB, the working substance may contain a monatomic substance A that in the excited state forms a metastable molecule with a dispersed lower state. The reaction scheme for this case is as follows:

$$\left.\begin{matrix} A + \Delta E_j \\ A + h\nu_j \end{matrix}\right\} A^*; \tag{7.57}$$

$$A + A^* \rightarrow A_2^*; \tag{7.58}$$
$$A_2^* \rightarrow A + A + \Delta E + h\nu. \tag{7.59}$$

From an energy standpoint it is more advantageous to use substances with low dissociation potentials such as metal salts in reactions (7.35)-(7.56). On the other hand, reactions (7.57), (7.58) can utilize noble gases or metals such as Zn, Cd and Hg that are capable of forming dispersed molecules as the substance A.

b. *Pure explosive.* The most interesting method of energy conversion is that in which the initial substance XV, one of the fission fragments XY_j and intermediate dissociation fragment XY^j are excited or deactivated according to reactions (7.53)-(7.56) or (7.57)-(7.59).

Let us examine each reaction individually. The initial substance XY dissociates into

$$XY \rightarrow \sum_{j=1}^{m} (XY_j + \Delta E_j). \tag{7.60}$$

Upon collision of the initial substance with fission fragment XY_j, a molecule XY of this substance is excited:

$$XY + \Delta E_j \rightarrow XY^* \tag{7.61}$$

and emits a quantum of light with transition of the molecule to the dispersed state:

$$XY^* \rightarrow XY^1 + XY^2 + h\nu + \Delta E_1 + \Delta E_2. \tag{7.62}$$

As the dispersing fragments interact with each other, they are converted to the terminal products of the dissociation reaction of the initial substance XY, i. e.

$$XY^1 + XY^2 \rightarrow \sum_{j=1}^{m} (XY_j + \Delta E_j). \tag{7.63}$$

The dissociation reaction products XY_j in turn enter into reaction with the initial substance XY, and the chain reaction continues until the initial reserves of substance XY are completely exhausted, the greater part of the energy stored in the substance being converted to emission energy in reaction (7.61). The terminal products of such a reaction have a low temperature since the kinetic energy of the reaction products XY_j is converted to luminous radiation in reaction (7.61).

Another mechanism of transformation of the energy of the chemical bond to luminous radiation is dissociation of the initial explosive XY in accordance with scheme (7.60). One of the fission fragments, for example XY_i that has sufficiently low dissociation energy emits a photon by reaction scheme (7.53)-(7.56), i. e.

$$XY_i + \Delta E_j \rightarrow XY_i^* \rightarrow X_i + Y_i^*; \tag{7.64}$$
$$Y_i^* \rightarrow Y_i + h\nu_i; \tag{7.65}$$
$$X_i + Y_i \rightarrow XY_i. \tag{7.66}$$

Thus the kinetic energy of fission fragments is transformed to luminous emission, and the final chemical makeup of the mixture remains unaltered.

Also of some interest may be the following reaction mechanism that leads to conversion of the energy of the chemical bond to luminous radiation, and that is: the initial explosive is divided into several intermediate fission fragments (taken as two in our case for the sake of simplicity):

$$XY \rightarrow XY^{(1)} + XY^{(2)}. \tag{7.67}$$

The fragments dissociate further into the terminal products of the decomposition reaction

$$XY^{(1)} \rightarrow \sum_{j=1}^{k} (XY_j + \Delta E_j); \tag{7.68}$$

$$XY^{(2)} \rightarrow \sum_{j=k+1}^{m} (XY_j + \Delta E_j). \tag{7.69}$$

The unstable intermediate dissociation products (complexes) may emit a light quantum with the following reaction schemes in the medium:

one of the complexes $XY^{(j)}$ is formed in the electron-excited state, and its deactivation takes place upon radiative transition of the complex to the dispersed state:

$$XY^{(j)*} \rightarrow \sum_{j=1}^{k} (XY_j + \Delta E_j) + h\nu \tag{7.70}$$

or as a result of spontaneous emission with transition to the ground state

$$XY^{(j)*} \rightarrow XY^{(j)} + h\nu \tag{7.71}$$

with subsequent dissociation in accord with reaction scheme (7.68), (7.69);

the intermediate complex is formed during collisions with the terminal reaction product

$$XY^{(j)} + \Delta E_j \rightarrow XY^{(j)*} \tag{7.72}$$

and emits a quantum upon transition to the dispersed state

$$XY^{(j)*} \rightarrow \sum_{j=1}^{k} (XY_j + \Delta E_j) + h\nu \tag{7.73}$$

or with transition to the ground state

$$XY^{(j)*} \rightarrow XY^{(j)} + h\nu \tag{7.74}$$

with further dissociation

$$XY^{(j)} \rightarrow \sum_{j=1}^{k} (XY_j + \Delta E_j). \tag{7.75}$$

These cases do not cover all possible reactions that convert the energy of the chemical bond to radiation. The given reactions are typical in that they are nonequilibrium, and that population inversion with stimulation of coherent radiation may take place in the medium in which they occur.

Feasibility of lasing on the CO molecule behind an overdriven detonation front [Ref. 54]. The detonation process, as we pointed out in §7.1, is characterized by constant average parameters that are high inside the limits of detonation propagation. This makes it difficult to vary temperature or density of the reaction products for example when using mixtures in which the ratios of components are outside the concentration limits of detonation. So far no methods have been found for chemical laser utilization of the high-frequency processes in detonation wave structure described in §7.1. Accounting for them is quite complicated, and so far it can only be assumed that the nonlinearity of the detonation structure, the local inhomogeneities of temperature and density fields, and alternation of zones of unreacted mixture and combustion products must reduce the maximum possible gain of emission. These constraints can be removed by using a mode of overdriven detonation from plane shock wave S and trailing combustion zone G. In this case, the induction time of chemical reactions may be more than five times as long as the period for reaching the thermodynamically equilibrium state of the gas behind the shock wave. It was shown by calculation in Ref. 54 that under such conditions it is possible to make CO chemical detonation lasers based on a $CS_2 + O_2$ mixture.

First the parameters behind the shock wave front are calculated without consideration of chemical transformations. The Runge-Kutta method is used with a computer to calculate the concentrations of all components from the equations of chemical kinetics. Each vibrational level of the CO(v) molecule from zero-energy to the seventeenth was taken as an individual component. The thermodynamic quantities p, ρ, T and wave velocity were taken as constant at energy release Q less than some predetermined value Δq. After calculating the new values of the thermodynamic quantities and velocity corresponding to the calculated concentrations, the rate constants of the chemical reactions were found at the new temperature values. The method of iterations was used to account for the temperature dependence of specific heats.

The principal reactions among more than 40 elementary reactions known from data in the literature for the given mixture were selected from consideration of their role in the first 75 μs from the instant when the shock wave acts on the mixture. Reactions were not considered if their elimination during this period caused no more than 0.1% deviations in the concentrations of components. The given time interval completely covers the time of existence of inversion under the conditions assumed for the given problem with respect to: a) composition of the mixture $CS_2/O_2/Ar$ = 1/2.5/40, 1/1/30, 2.5/1/10; b) temperature range T = 1400-3400 K; c) pressure p ~ 0.1 MPa; d) chemical kinetics in the given initial time interval of 75 μs determined by 16 selected principal equations of reactions with the following rate constants of these reactions (k, $cm^3 \cdot mole^{-1} \cdot s^{-1}$; E, $kJ \cdot mole^{-1}$; R, $kJ \cdot mole^{-1} \cdot K^{-1}$):

1. $CS_2 + CS_2 \rightleftarrows CS + S + CS_2$, $k_1 = 0{,}166 \cdot 10^{15} \times \exp(-183/RT)$; [55]
2. $CS_2 + Ar \rightleftarrows CS + S + Ar$, $k_2 = 0{,}364 \cdot 10^{16} \times \exp(-336/RT)$; [55]
3. $CS_2 + O \rightleftarrows CS + SO$, $k_3 = 0{,}12 \cdot 10^{14} \times \exp(-4{,}4/RT)$; [56]

$$
\begin{array}{ll}
4.\ CS_2 + O \rightleftarrows OCS + S, & k_4 = 0{,}1\cdot 10^{15} \times \\
& \times \exp(-33{,}6/RT);\ [58] \\
5.\ CS_2 + S \rightleftarrows CS + S_2, & k_5 = 0{,}1\cdot 10^{15} \times \\
& \times \exp(-16{,}7/RT);\ [58] \\
6.\ O_2 + SO \rightleftarrows SO_2 + O, & k_6 = 0{,}35\cdot 10^{12} \times \\
& \times \exp(-27{,}2/RT);\ [57] \\
7.\ O_2 + S \rightleftarrows SO + O, & k_7 = 0{,}1\cdot 10^{14} \times \\
& \times \exp(-23{,}4/RT);\ [57] \\
8.\ O + OCS \rightleftarrows CO + SO, & k_8 = 0{,}19\cdot 10^{14} \times \\
& \times \exp(-18{,}9/RT);\ [58] \\
9.\ O + S_2 \rightleftarrows SO + S, & k_9 = 0{,}4\cdot 10^{13} \text{ при } T = \\
& = 1100\ \text{K};\ [57] \\
10.\ O + OCS \rightleftarrows CO_2 + S, & k_{10} = 0{,}16\cdot 10^{13} \text{ при } T = \\
& = 1270\ \text{K};\ [58] \\
11.\ CS + O_2 \rightleftarrows OCS + O, & k_{11} = 0{,}1\cdot 10^{14} \times \\
& \times \exp(-50{,}3/RT);\ [58] \\
12.\ S + OCS \rightleftarrows CO + S_2, & k_{12} = 0{,}19\cdot 10^{14} \times \\
& \times \exp(-18{,}9/RT);\ [58] \\
13.\ SO + SO \rightleftarrows SO_2 + S, & k_{13} = 0{,}45\cdot 10^{12} \times \\
& \times \exp(-15{,}9/RT);\ [57] \\
14.\ OCS + Ar \rightleftarrows CO + S + Ar, & k_{14} = 0{,}398\cdot 10^{20} T^{-1{,}37} \times \\
& \times \exp(-299/RT);\ [55] \\
15.\ O_2 + CS \rightleftarrows CO^*(v) + SO, & k_{15} = 0{,}55\cdot 10^{11} \times \\
& \times \exp(-8{,}36/RT);\ [58] \\
16.\ O + CS \rightleftarrows CO^*(v) + S, & k_{16} = 0{,}24\cdot 10^{15} \times \\
& \times \exp(-8{,}36/RT).\ [58]
\end{array}
\qquad (7.76)
$$

Equations (1)-(16) characterize a complex chain reaction for which curves are shown on Fig. 7.14 obtained in Ref. 54 for the way that the concentration of reagents c_i and temperature T depend on the time t of motion of the gas volume relative to the leading shock front of overdriven detonation. The calculations were done for a mixture of $CS_2/O_2/Ar = 1/2.5/40$ at an initial gas pressure of 2 kPa and shock wave velocity of 1500 m/s. It can be seen that the temperature in the reaction zone changes insignificantly. The broken curves show the change in concentrations of O_2, CS_2, CS and CO; in calculating these concentrations, the rate constants for dissociation of CS_2 (k_1, k_2) were assumed to be zero beginning at 6 μs. After this instant the reaction may be maintained by chain branching processes, but chain initiation processes considerably accelerate combustion. With weaker dilutions, or in the undiluted working mixture the temperature may rise during reactions. For example Fig. 7.15 shows the calculation of the chemical kinetics of reaction in a mixture of $CS_2/O_2 = 1/9$ at initial pressure of the mixture of 2 kPa and shock wave velocity of 1700 m/s. Here the temperature changes from 1510 to 2800 K during the course of the reaction.

Reactions (15) and (16) determine the populations of vibrational levels of CO molecules [Ref. 59] in the same way as processes of V-V exchange with molecules of CO(v), O_2, OCS, CS_2 and V-T exchange with molecules of CO, O, Ar. Molecules of O_2, $OCS(v_3)$ and $CS_2(v_3)$ may make a transition from the ground state to the first

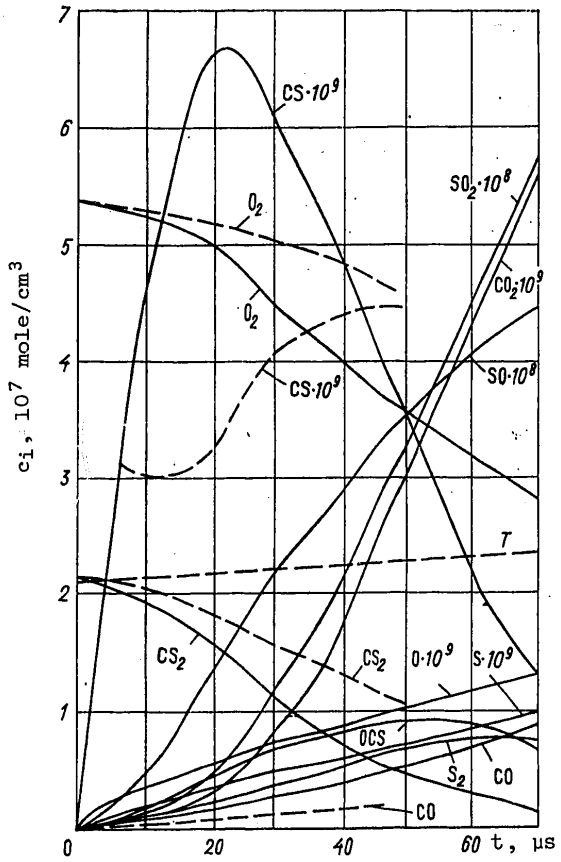

Fig. 7.14. Calculation of the change in concentration of reagents c_i and temperature T as a function of the time t in the overdriven detonation wave

excited vibrational level upon collisions with CO(v). This calculation did not consider transfer of excitation from O_2, OCS(001) and CS_2(001) to CO.

Numerical computer solution of the system of equations for chemical, relaxation and gasdynamic processes gave the time dependences of the population of vibrational levels of CO molecules behind the leading shock front of the overdriven detonation wave. The results of calculation of this dependence for complete inversion of the vibrational levels of CO are shown on Fig. 7.16. The rate constants of relaxation as a function of vibrational number v were calculated by using formulas from Ref. 60, and the emission gain in the center of the line for individual V-R transitions of $\mathcal{P}$- and $\mathcal{R}$-branches was calculated at times corresponding to the maximum complete inversion between each pair of vibrational levels. Maxwell-Boltzmann population of rotational levels was assumed at a temperature equal to the translational temperature, the half-width of the line was taken as corresponding to impact broadening, and the linewidth was assumed to be independent of quantum numbers or the kind of molecules responsible for broadening. The resultant maximum values of gain α_{max}

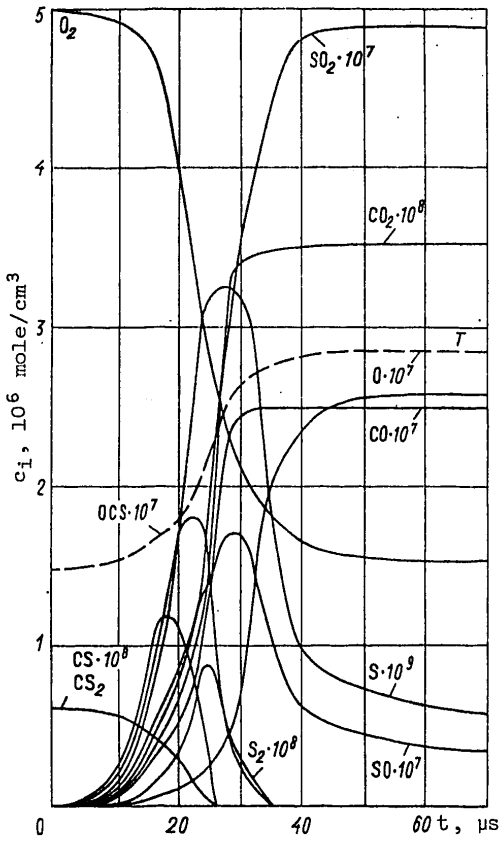

Fig. 7.15. Results of calculation of the chemical kinetics of a reaction behind the leading shock front of an overdriven detonation

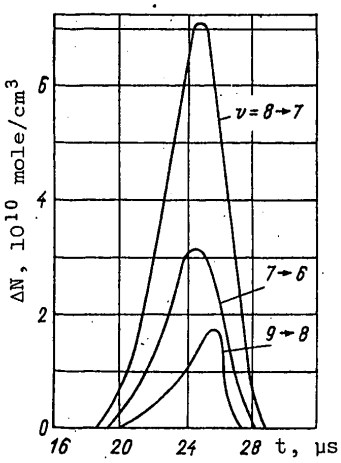

Fig. 7.16. Calculated time dependences of vibrational levels of the CO molecule behind the leading shock front of an overdriven detonation

on a given vibrational level v for a mixture of $CS_2/O_2 = 1/9$ at T = 2495 K are shown in Table 7.1. This same table gives the populations of vibrational levels n_V, n_V/n_{V-1}, and the corresponding rotational quantum number J and wave number $\omega_{v-1,J+1}^{v,J}$ of the transition on which α_{max} is reached for the $\mathcal{P}$- and $\mathcal{R}$-branches.

Analysis of the calculated data shows that during the first 1.5 μs the first inversion wave passes through all vibrational levels from 1 to 13. As we can see from Table 7.1, this wave is characterized by low populations of vibrational levels of the CO molecules and low gains ($10^{-7}-10^{-5}$ cm^{-1}). The second inversion wave is due to the intense process of chemical reactions, and under the given conditions propagates to only three vibrational levels (7, 8, 9). This wave is characterized by high values of the maximum gain ($10^{-3}-10^{-2}$ cm^{-1}) and long durations of inversion. The calculated maximum gains α_{max}, the duration of inversion τ_i, the dimensions of the inversion zone Δx_i that correspond to this duration, velocities D, temperature in the inversion zone and the transition vibrational and rotational quantum numbers corresponding to α_{max} are given in Table 7.2 for p_0 = 2 kPa.

TABLE 7.1

Results of calculation of kinetics of populations and gain [Ref. 54]

time from start of reaction, μs	v	n_v, см$^{-3}$	$\frac{n_v}{n_{v-1}}$	$J_{\mathcal{P}}$	$\omega^{v, J_{\mathcal{P}}}_{v-1, J_{\mathcal{P}}+1}$, см$^{-1}$	$\alpha_{\mathcal{P}\max}$, см$^{-1}$	$J_{\mathcal{R}}$	$\omega^{v, J_{\mathcal{R}}}_{v-1, J_{\mathcal{R}}-1}$, см$^{-1}$	$\alpha_{\mathcal{R}\max}$, см$^{-1}$
0,04	13	$0,42\cdot10^{-7}$	1,004	32	1699,31	$1,7\cdot10^{-7}$	—	—	—
0,08	12	$0,19\cdot10^{-6}$	1,044	28	1741,71	$1,2\cdot10^{-6}$	8	1882,08	$1,4\cdot10^{-7}$
0,11	12	$0,37\cdot10^{-6}$	1,062	27	1770,91	$2,5\cdot10^{-6}$	12	1920,64	$5,4\cdot10^{-7}$
0,15	10	$0,73\cdot10^{-6}$	1,075	26	1800,22	$4,9\cdot10^{-6}$	14	1953,02	$1,4\cdot10^{-6}$
0,22	9	$0,17\cdot10^{-5}$	1,092	25	1829,64	$1,2\cdot10^{-5}$	15	1982,47	$4,2\cdot10^{-6}$
0,31	8	$0,36\cdot10^{-5}$	1,109	25	1854,74	$2,5\cdot10^{-5}$	17	2015,01	$1,1\cdot10^{-5}$
0,38	7	$0,54\cdot10^{-5}$	1,127	24	1884,36	$3,7\cdot10^{-5}$	17	2041,68	$1,8\cdot10^{-5}$
0,43	6	$0,67\cdot10^{-5}$	1,147	24	1909,63	$4,4\cdot10^{-5}$	18	2071,44	$2,3\cdot10^{-5}$
0,48	5	$0,81\cdot10^{-5}$	1,169	23	1939,47	$4,9\cdot10^{-5}$	19	2101,30	$2,8\cdot10^{-5}$
0,57	4	$0,17\cdot10^{-4}$	1,176	23	1964,92	$6,1\cdot10^{-5}$	19	2128,25	$3,6\cdot10^{-5}$
0,67	3	$0,18\cdot10^{-4}$	1,203	23	1990,43	$7,5\cdot10^{-5}$	19	2165,26	$4,8\cdot10^{-5}$
0,81	2	$0,30\cdot10^{-4}$	1,258	22	2020,58	$1,0\cdot10^{-4}$	20	2185,43	$7,2\cdot10^{-5}$
5,49	7	$0,22\cdot10^{-3}$	1,220	23	1888,80	$2,2\cdot10^{-3}$	20	2050,51	$1,5\cdot10^{-3}$
5,74	8	$0,31\cdot10^{-3}$	1,417	22	1867,93	$5,0\cdot10^{-3}$	21	2026,57	$4,1\cdot10^{-3}$
6,14	9	$0,32\cdot10^{-3}$	1,087	26	1825,21	$2,1\cdot10^{-2}$	15	1982,47	$7,2\cdot10^{-3}$

TABLE 7.2

Calculated characteristics of inversion zone for various detonation modes [Ref. 54]

Mode	Mixture CS_2/O_2	D, m/s	T, K	$v \to v-1$	$J \to J-1$	$\alpha_{\max}$, см$^{-1}$	τ_i, μs	Δx_i, см
1	0,05/0,95	1700	1700	8—7	20—21	$6,1\cdot10^{-3}$	3,7	0,9
2	0,10/0,90	1700	1800	8—7	19—21	$9,2\cdot10^{-3}$	4,2	1,0
3	0,20/0,80	2000	2495	8—7	22—23	$3,8\cdot10^{-3}$	6,9	1,7
4	0,10/0,90	—	2495	8—7	22—23	$5,0\cdot10^{-3}$	3,5	—

The following conclusions are drawn in Ref. 54 from the results of such a numerical analysis of the possibilities for achieving stimulated emission on the CO molecule behind an overdriven detonation wave front in a mixture of $CS_2 + O_2$:

A change in pressure causes an inversely proportional change in all characteristic times of chemical and relaxation processes, including τ_i;

the maximum gain does not change as long as the impact approximation remains valid in calculation of the linewidth;

the inversion duration increases as the composition approaches stoichiometric proportions; increasing the temperature from 1800 to 2495 K for the same composition (modes 2 and 4) reduces both gain and inversion duration;

calculations done for an idealized one-dimensional model yield relatively high values of the gain.

Processes of population inversion in the case of adiabatic cooling of the detonation products. The chemical energy of detonation of the initial fuel mixture may also serve simply as a source of thermal energy for heating the mixture of products that are formed with added gases before they are cooled in the process of subsequent adiabatic expansion. Detonation lasers that utilize such processes are quite similar to shock-wave and chemical-gasdynamic lasers (described in chapter 6) and to gasdynamic shock-tube lasers [Ref. 61]. However, what distinguishes them is that in detonation lasers thermal pumping is realized in conditions of more intense heat release in the detonation wave than that accompanying ordinary combustion, and the components required for forming the active medium, as well as the proportions of concentrations of these components necessary for stimulated emission are produced immediately during the chemical reaction in the detonation wave. Otherwise, the process of population inversion in such lasers is analogous to the method of obtaining negative temperatures by cooling the medium that was first outlined in Ref. 62, and then in Ref. 63 and 64. In accordance with this method, a three-level system is considered that has different relaxation times between subsystems -- the levels 1, 2, 3 situated in sequence one above the other. If the relaxation time between subsystems is considerably greater than the relaxation time within each subsystem, and if radiative transitions between them are possible, then with a sufficiently rapid change in thermodynamic state, equilibrium will be established fairly rapidly within each subsystem, but there will be no equilibrium between them. Then a state is possible with negative temperature with respect to transitions from the energy levels of one subsystem to those of another.

Based on such a method of getting inverse population by an abrupt change in temperature of the medium, it was demonstrated in Ref. 65 that a state of inverse population can exist for some time with respect to vibrational levels in the case of adiabatic expansion of mixtures containing molecules that have appreciably different vibrational relaxation times and that are capable of exchanging energy of vibrational excitation. This kind of exchange is effective if the energies of the vibrational levels are close to one another, or the energy deficit is

$$|\Delta E| \ll kT. \tag{7.77}$$

Mixtures of N_2/CO_2 and N_2/NO_2 were considered in Ref. 65 as media that satisfy the resonant condition (7.77) of exchange of vibrational excitation. In these

mixtures the process takes place without chemical transformations, and hence is characteristic only for purely gasdynamic lasers. However, in chemical detonation lasers with adiabatic expansion the mixtures N_2/CO_2 and N_2/NO_2 may be either added gases, or may be part of the components formed during reaction of detonation products, and therefore it is of interest here to outline the analysis of Ref. 65.

The probability of energy transfer in the mixture of N_2/CO_2 during a single collission of a molecule at room temperature is $\beta \sim 10^{-5}$ [Ref. 66]. The exchange process is considered in the assumption of a surplus concentration of molecules that are carriers of vibrational excitation as compared with the concentration of working molecules with levels that involve inversion, $n_{N_2^*} \gg n_{CO_2}$, i. e. concentration $n_{N_2^*}$ is taken as constant in time. On the other hand the time change of the number

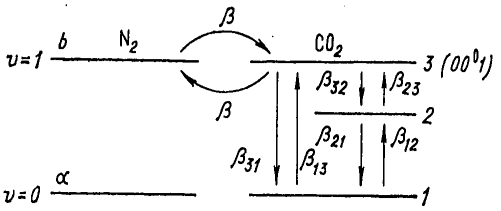

Fig. 7.17. Time change in number of CO_2 molecules on three vibrational levels

of molecules of the working gas CO_2 on three vibrational levels (Fig. 7.17) of which level 00^01 may exchange molecules of N_2^* with level v = 1, can be written as

$$\left.\begin{aligned} dn_3/dt &= -P_{ab}n_3 + P_{ba}n_1 - P_{31}n_3 + P_{13}n - P_{32}n_3 + P_{23}n_2; \\ dn_2/dt &= P_{32}n_3 + P_{12}n_1 - P_{23}n_2 - P_{21}n_2. \end{aligned}\right\} \qquad (7.78)$$

Here $n_1 + n_2 + n_3 = n$ is the concentration of working molecules; P_{ba}, P_{ab} are respectively the probabilities of forward and reverse transfer of excitation between the working molecule CO_2 and the carrier molecule N_2^*; P_{31}, P_{13}, P_{32} and so on are the probabilities of thermal relaxation of a working molecule between the corresponding vibrational levels.

Let the rate of adiabatic expansion of the gas mixture be such that its cooling time from initial temperature T_1 to final temperature T_2 is much less than the inherent vibrational relaxation time of the carrier gas. After completion of expansion of the gas mixture, steady-state distribution of the working molecules is established with respect to vibrational levels. Hence by setting the right-hand members of equations (7.78) equal to zero and denoting the probabilities of relaxations during one collision by β_{21}, β_{32}, β_{31}, we can determine the population inversion between levels 3 and 2:

$$\frac{n_3 - n_2}{n_1} = \frac{\beta(\beta_{21} - \beta_{32})}{\beta_{21}(\beta + \beta_{32} + \beta_{31})} \exp\left(-\frac{E_b - E_a}{kT_1}\right). \qquad (7.79)$$

In the derivation of (7.79), thermal perturbation of the molecule was disregarded, i. e. no consideration was taken of probabilities P_{13}, P_{23}, P_{12}, but account was

taken of deactivating collisions and condition (7.77) for temperature T_2. Expression (7.79) implies that there is no inversion when $\beta_{32} > \beta_{21}$, and inversion is maximum when $\beta_{21} \gg \beta_{32}$ and under the condition where the probability of transfer of vibrational excitation β is much greater than the probability of deactivation of level 3 of the working molecule. In this case inversion is equal to the relative concentration of excited molecules of the carrier gas with initial temperature T_2.

Ref. 65 gives a specific computational example of population inversion by using a supersonic nozzle with continuous mode of adiabatic expansion of the working mixture. For example under conditions of inverse population between levels (00^01) and (10^00) of the CO_2 molecule at $T_1 = 1000$ and $T_2 = 300$ K, it is found that $(n_3 - n_2)/n_1 \sim$ ~ 1-3.5%.

Following Ref. 62-65, a number of papers were published dealing with the process of rapid expansion of a preheated mixture of molecular gases as they are discharged through nozzles or slits, thus bringing about conditions of inverse population of vibrational states of molecules [Ref. 67-74].

Such an effect can also be produced in a strongly exothermic reaction during detonation with free dispersal of the reaction products [Ref. 6] without using gasdynamic devices like nozzles and slits.

As was already pointed out above, in this case the composition of the detonation products should correspond to a relaxation scheme analogous to that used in gasdynamic lasers of the type described in Ref. 67, 75 and 76. Many gaseous and condensed explosive media have such a composition of detonation products [Ref. 77, 78]. The rate of dispersal of detonation products heated to 2000-5000 K depending on the type of explosive is comparable to or greater than the flow velocity in gasdynamic lasers -- 10^5-10^6 cm/s. The process for an acetylene-air mixture is described by the exothermic chemical reaction [Ref. 79]

$$0.081C_2H_2 + 0.202(O_2 + 3.76N_2) = 0.162CO_2 + 0.081H_2O + 0.757N_2 + 108.9 \text{ kJ/mole}. \quad (7.80)$$

This process is analyzed in Ref. 6. Thus it is known from Ref. 79 that at a pressure of more than 0.05 MPa in an initial mixture with volumetric concentration of 8-14% C_2H_2 detonation is excited from a spark in tubes of diameter $d \geqslant 18$ mm. The detonation rate in this case is $1.8 \cdot 10^3$ m/s. For the conditions of reaction (7.80) the temperature of the reaction products is 2000-2400 K. It is assumed that the walls of the detonation tube are rapidly destroyed by pressure in the detonation wave. This destruction is accompanied by adiabatic expansion and cooling of the reaction products, the calculated rate of expansion being about $0.9 \cdot 10^5$ cm/s. Dispersal into vacuum will change the parameters of state of the reaction products with formation of population inversion of states *2* (00^01) and *1* (10^00) of the CO_2 molecule.

In this case, relaxation of the excited CO_2 molecules corresponds to the kinetic equation

$$\frac{dn_\alpha}{dt} = P_{N^*-C} N^* n_0 \delta_{2\alpha} - [n_\alpha / \tau_\alpha(t)], \quad (7.81)$$

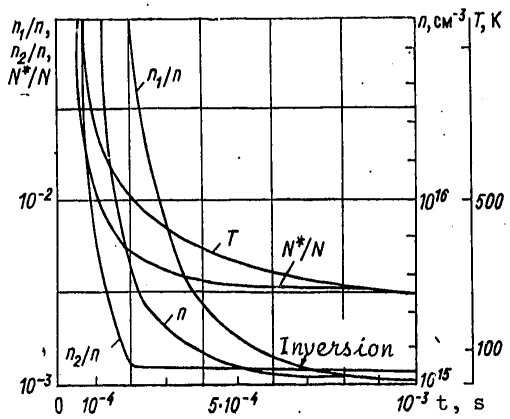

Fig. 7.18. Time dependences of gas temperature and molecule concentration in the case of cylindrical dispersal of the detonation products of an acetylene-air mixture: T--temperature of detonation products; n--concentration of CO_2 molecules; n_1/n, n_2/n and N^*/N--relative populations of excited states of molecules of CO_2 and nitrogen respectively

where $\alpha = 1.2$; $\delta_{2\alpha}$ is the Kronecker delta; N^*, n_0, n_α are the concentration of excited molecules of N_2, CO_2 in the ground and α-states; $P_{N^*\_C}$ is the probability of transfer of excitation from N_2 to CO_2; $\tau_\alpha(t)$ is the time of collisional relaxation.

The time dependence of gas temperature and molecule concentration have been calculated for cylindrical dispersal geometry [Ref. 6] (Fig. 7.18).

With consideration of data on the temperature dependence of the probability of collisional relaxation of CO_2 molecules [Ref. 80], the time $\tau_\alpha(t)$ has also been determined. The initial conditions here are selected from the following considerations. At a temperature below 1000 K the relaxation of excited molecules of CO_2 depends on collisions with molecules of H_2O and is most probable for the lower level. Due to the relatively large concentration of water in the reaction products the relaxation times are short and at pressures of the initial mixture higher than 0.1 MPa relaxation occurs faster than cooling of the gas. And at pressures of the initial medium below 0.05 MPa, as already stated, the process of detonation excitation is hampered in an acetylene-air mixture. Therefore the selected conditions corresponded to the following: pressure 0.05-0.1 MPa, tube diameter $d \approx 2$ cm.

Integration of kinetic equation (7.81) yields the time dependence of the population of excited states. In this connection we can disregard the transfer of energy from N_2 to CO_2 and approximate $\tau_\alpha(t)$ by power functions. It is found that relaxation of level *1* takes place more rapidly than depopulation of the level due to cooling of the gas, i. e. its population is determined by the Boltzmann factor. On the other hand, beginning with a certain instant the relaxation of level *2* takes place more slowly, and the vibrational temperature is separated from the temperature of random motion in the gas. It can be seen from the results of calculation on Fig. 7.18 that separation of the vibrational temperature of level *2* takes place at $t = 200$ μs, and population inversion arises 650 μs after the beginning of dispersal. The time

dependence of the population density of the excited level of the nitrogen atom N* is determined mainly by relaxation upon collision with CO_2 molecules. It is pointed out in Ref. 6 that accounting for the energy transfer from nitrogen to CO_2 should lead to an increase in inversion and to a reduction in time before onset of inversion, and moreover that inversion should occur at higher pressures in the initial mixture. Increased inversion is also possible when an explosive medium is used with a lower relative concentration of water in the products of explosion.

§7.5. Experimental Stimulation of Emission in Chemical Detonation Lasers

Lasing in an overdriven detonation wave. Realization of the possibility of lasing in detonation just as in a thermal explosion is so far a complex problem. The pertinent experimental results include the use of overdriven detonation for direct stimulation of emission and normal Chapman-Jouguet detonation and explosion for thermal pumping of an active medium.

Induced emission was first obtained directly from a detonation wave in a mixture of $F_2O/H_2/Ar = 1/1/20$ [Ref. 5, 81]. Before this, emission of vibrationally excited HF had been produced in the course of a chain reaction initiated by flash photolysis [Ref. 82]:

$$\left.\begin{array}{l} F + H_2 = HF + H \quad (-134\ \text{kJ/mole}); \\ OF + H_2 = HOF + H; \\ H + F_2O = HF + OF; \\ H + HOF = HF + OH; \\ H + OF = FH + O \text{ or } OH + F. \end{array}\right\} \qquad (7.82)$$

In carrying out reaction (7.82) in a detonation wave, the process was initiated at a wave propagation rate exceeding the Chapman-Jouguet velocity, i. e. in the overdriven detonation mode. Despite heavy dilution of the mixture with argon and relatively low initial pressure (about 0.66 kPa) the wave velocity was 1.8–2 km/s with temperature on the wave front above 2000 K. In the opinion of the authors of Ref. 5, 81, under these conditions the reaction zone is apparently quite narrow, and therefore diffraction losses in the optical cavity are high, i. e. the working conditions of such a chemical laser with respect to temperature and pressure are near critical.

In Ref. 5, 81, a detonation tube was used of the type shown in Fig. 7.19a, 16.7 cm in diameter with a special nearly confocal resonator mounted flush with the walls of the tube. The output of coherent emission from the cavity was recorded by an InSb photoelectric detector using a narrow-band filter for spectral resolution. A typical record of the emission is shown in Fig. 7.19b as a two-beam oscillogram. Here the upper curve is the radiation of gas heated by the detonation wave as observed through a CaF_2 window installed upstream relative to the resonator. The lower curve is a recording of emission from the optical cavity by the InSb photoelectric detector with aperture of 1.5 mm. Comparison of these curves shows that the amplitude of the curve characterizing the coherent radiation is 10^5 times as great. This is convincing proof of reliable observation of the effect of stimulated coherent emission.

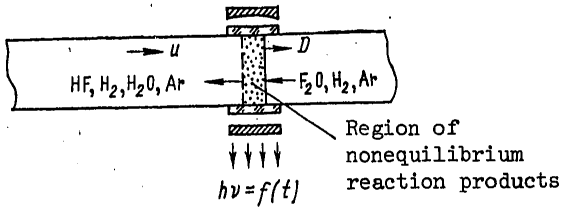

a

E, relative units

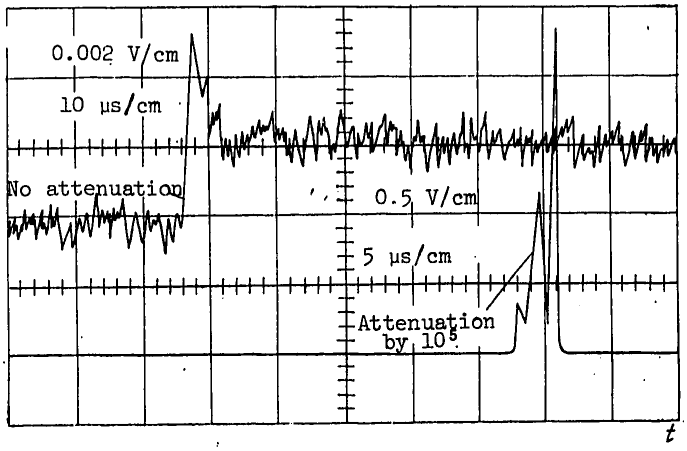

b

Fig. 7.19. Diagram of chemical detonation laser (a) and record of its output (b)

A brief report is given in Ref. 83 on theoretical analysis of processes in the chemical detonation laser described above in the form of a numerical calculation for the most realistic chemical model of the reaction. In this calculation some chemical reactions were ruled out, and the complexity of accounting for processes in the resonator was eliminated by considering the process of nonequilibrium radiation only for "zero" amplification, i. e. for the process characterized by the upper curve in Fig. 7.19. It is pointed out that the calculation utilized the results of experiments with mixtures of $F_2O/H_2/Ar$ in corresponding concentration limits from 1/1/10 to 1/1/200 with heating in the wave from 2200 to 3500 K. It is found from the calculations that during the chemical reaction the concentrations of HOF, F_2O and OF decrease rapidly to an insignificant level, so that reactions involving these components can be disregarded. Thus there remains only the first of reactions (7.83) that yields excited HF. Besides, it turned out that for the given reaction deactivation is controlled by processes of V-V transfer of energy, while V-T processes are unimportant.

Using detonation and explosion for production and thermal pumping of active laser media. Selection of the initial composition of the mixture for detonation lasers that work on the principle of adiabatic expansion of the detonation products through

a nozzle involves the relaxation scheme described in §7.4. This results in a variety of reagents that can be used, and a number of design peculiarities of the chemical detonation lasers that operate on these reagents.

We describe herewith the designs and working principles of the most typical of these lasers.

One of the first experimental lasers in which detonation was used to produce a high-temperature gas mixture at the inlet to a slit nozzle was a detonation laser based on the exothermic explosive reaction of dissociation of a hydrazoic acid molecule in a mixture of carbon dioxide and xenon [Ref. 7]. The mechanism of this reaction is determined mainly by the following processes [Ref. 84]:

$$\left.\begin{aligned} &HN_3^* \to NH + N_2 \quad (-41{,}9\ \text{kJ/mole});\\ &NH + HN_3 \to H_2 + N_2 + N_2^*\ (+635\ \text{kJ/mole});\\ &N_2^* + \varkappa HN_3 \to \varkappa HN_3^* + N_2;\\ &N_2^* + M \to N_2 + M^*;\\ &M + HN_3^* \to HN_3 + M^*. \end{aligned}\right\} \qquad (7.83)$$

When carbon dioxide is used as the diluent M, the excited nitrogen transfers its energy to the CO_2 molecule due to quasi-resonance between the vibrational levels of nitrogen and the vibrational mode (00^01) of carbon dioxide. The process of obtaining population inversion during such a chemical reaction was analyzed in detail in Ref. 85, and was investigated in Ref. 86.

A diagram [Ref. 7] of the experimental hydrazoic acid detonation laser is shown in Fig. 7.20.

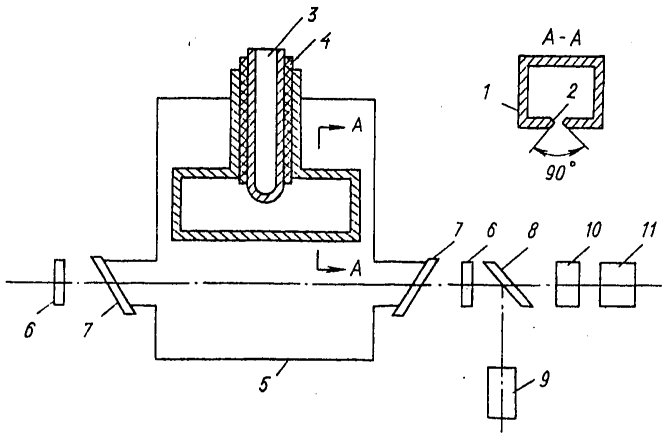

Fig. 7.20. Detonation laser based on hydrazoic acid: 1--0.3-liter high-pressure chamber; 2--200 x 0.4 mm slit; 3--metal rod with cavity; 4--heat insulation; 5--ballast tank with volume of 0.012 cu. m; 6--gold-coated mirrors 25 mm in diameter, one of which has an output aperture 2.5 mm in diameter; 7--Brewster windows of NaCl; 8--plane-parallel germanium plate; 9--calorimeter; 10--photocell; 11--oscilloscope

The gaseous mixture is admitted to tank 5 and then frozen out on hollow metal rod 3 with cavity 4 filled with liquid nitrogen. Detonation was initiated by an electric spark. The pressure and temperature in the high-pressure chamber after dispersal of the detonation products were about 1-2 MPa and 2000-3000 K depending on the amount and composition of the gas mixture. The time of discharge of the detonation products and diluents through the slit was evaluated as the ratio of the volume of the high-pressure chamber to the product of the slit area multiplied by the speed of sound in the critical cross section, and was about a millisecond. The distance from the slit to the axis of the cavity was adjusted in the experiment. The optimum distance was about 3 cm. The duration of the stimulated pulse at the optimum composition of the mixture was close to the time of discharge of the gas through the slit.

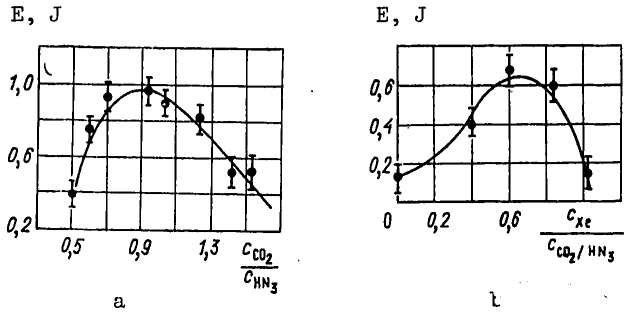

Fig. Fig. 7.21. Energy characteristics of HN_3 laser with a change in the content of CO_2 (a) and Xe (b) in the mixture

Shown in Fig. 7.21 are experimental curves for the output energy as a function of: a--the content of CO_2 in the HN_3/CO_2 mixture for a predetermined content of HN_3 (0.5 g); b--the content of Xe in the mixture $HN_3/CO_2/Xe$ for the same amount of HN_3 and CO_2 (0.33 g). The maximum energy (about 1 J) was attained at a relative content of components corresponding to initial temperatures of detonation products of about 2500 K, which is much greater than the temperatures given as optimum by Ref. 69 for mixtures of $N_2/CO_2/He$. In Ref. 7 the cause of this was discovered in the difference of gasdynamic parameters of the experimental facilities, and in the way that temperature of the mixture depends on change in composition.

Thermodynamic calculation and analysis of the detonation products showed that nearly all the hydrogen (about 90%) was oxidized to water, reducing part of the carbon dioxide to carbon monoxide. In this process, the water content in the mixture reached 15-20%. The addition of chlorine to the mixture in an amount close to the stoichiometric value for reaction with hydrogen led to a sharp (approximately triple) increase in the radiated energy. There was a concomitant reduction of water content in the products to 2-4%.

The H_2O molecules deactivate symmetric and deformation vibrational modes of the CO_2 molecule, and therefore small amounts of water in the detonation products improve the emission characteristics of the active medium. However, most explosive lasers use hydrocarbon fuels that yield so much water in the reaction products that it leads to deactivation of both the antisymmetric mode of CO_2 and the vibrationally excited N_2 molecules, i. e. to losses of vibrational energy. To reduce such losses,

additives that interact with hydrogen are introduced that form compounds for which losses of vibrational energy from the antisymmetric mode of CO_2 and the vibrational mode of N_2 are lower than for water molecules.

Research results given in Ref. 87 deal with the question of the influence that chlorine additives have on gain of a laser working on products of explosion of a hydrocarbon fuel, and specifically methane-oxygen mixtures. This paper points out that under the conditions of Ref. 7 the explanation of a nearly triple increase in lasing power as due to a reduction of water content when chlorine is added is not completely unambiguous. Actually, when hydrogen was bound by chlorine there was an increase in CO_2 content as compared with preceding experiments. It is also possible that the conditions (fairly high water vapor content) were close to the lasing threshold, and here even a slight increase in gain due to an increase in CO_2 content could significantly increase the lasing power.

In Ref. 87, in order to study the influence of additives, an explosive laser was used that consisted of an explosive chamber (volume 500 cc), a wedge-shaped nozzle (height of the critical cross section 1 mm, half-angle of the vertex 15°) and a receiver. Width of the gas stream was 400 mm. At a degree of expansion equal to 18, the wedge-shaped profile of the nozzle was changed to a plane-parallel section. The gain (absorption) of the medium was measured by a CO_2 electric-discharge laser at a distance of 80 mm from the critical cross section of the nozzle. The mixture was made up of methane, oxygen and nitrogen in partial pressures of: CH_4--30.6, O_2--61.3 and N_2--288 kPa. Chlorine additives were introduced in amounts of 25, 50, 75 and 100% of the stoichiometric content of chlorine with respect to hydrogen, and a comparison was made between the resultant gains and the gains without chlorine added. The results of thermodynamic calculation of the composition of the products of explosion as a function of the content of chlorine additive are shown in Fig. 7.22. The experimental dependence of the maximum gain on the chlorine content in

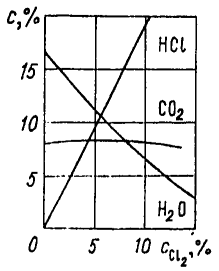

Fig. 7.22. Thermodynamic calculation of concentrations of CO_2, H_2O and HCl in the products of explosion of mixtures of $CH_4/O_2/N_2/Cl_2$ as a function of chlorine content in the initial mixture

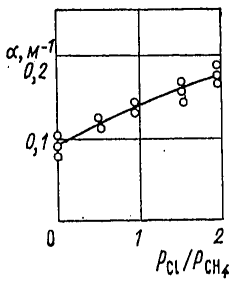

Fig. 7.23. Maximum gain in the products of explosion of a mixture of $CH_4/O_2/N_2/Cl_2$ as a function of the ratio of chlorine and methane pressures (p_{CH_4} = 30 kPa)

the initial mixture is shown in Fig. 7.23. The pressure in the prechamber in front of the nozzle that corresponds to maximum gain increases with an increase in the chlorine content in the initial mixture, and changes from 0.15 MPa in mixtures without chlorine added, to 0.25 MPa with the stoichiometric amount of Cl_2 with respect to hydrogen. At equal pressures in the prechamber the gain increases

monotonically with increasing content of Cl_2 in the initial mixture up to the stoichiometric level with respect to hydrogen. It is concluded from the research of Ref. 87 that adding chlorine to the hydrocarbon fuel reduces losses of vibrational energy from the upper energy level of stimulated emission in a laser that operates on the products of explosion of these fuels, and consequently improves the energy characteristics of these lasers.

Also operating on hydrocarbon fuel is a detonation laser proposed in Ref. 88. Experiments on achieving lasing in products of gas detonation were done on the following explosive chemical reactions:

$$\left.\begin{aligned} &1)\ C_2H_2+2{,}5\,O_2+\varkappa N_2\rightarrow 2\,CO_2+H_2O+\varkappa N_2+Q_\varkappa;\\ &2)\ CO+N_2O+\varphi He\rightarrow CO_2+N_2+\varphi He+Q_\varphi, \end{aligned}\right\} \qquad (7.84)$$

where $Q_{\kappa,\phi}$ is energy release, κ and ϕ are the fractions of nitrogen and helium dopants respectively. The properties of the initial gas mixtures are summarized in Table 7.3.

TABLE 7.3

Characteristics of explosive mixtures [Ref. 88]

Mixture composition by partial pressure	Q, J/g	Detonation rate D, m/s
$C_2H_2/O_2/N_2$ 16,7/41,6/41,7	5650	2150
12,6/31,4/56,5	4030	1920∓20
$CO/N_2O/He/H_2$ 35/35/28/2	6340	2240∓20

The relative concentrations of initial components were selected in accordance with contradictory requirements on the composition of the final mixtures and on the detonation properties of the initial mixtures. In reaction (2) of equations (7.84) the catalyst was traces of hydrogen. The experiments were done on a detonation laser diagrammed in Fig. 7.24.

The explosive gas mixture at atmospheric pressure in tube 2 was ignited by a spark, an igniter or an electric ignition wire 15. The resultant self-accelerating combustion becomes detonation moving in the direction shown by the arrows on the diagram. The double input of the detonation wave to explosion chamber 1 is to ensure more simultaneous rupture of mylar film 14 cemented to slit 3, 40 cm in length. The gas mixture of predetermined composition heated behind the detonation wave front flows through the slit into vacuum space 6 after the film breaks and is cooled upon rapid expansion. Inversion of the population of V-R levels 00^01 and 10^00 of the CO_2 molecules takes place in the gas stream. The jet of active medium shown by the broken line on Fig. 7.24 disperses through a transverse optical cavity 1.5 m long formed by two copper or gold-coated mirrors -- one flat (11) and the other spherical (4) with radius of curvature of 5 m. The distance between the slit and the axis of the cavity is 4 cm. Emission is coupled out to GeAu photoresistor 9 through an annular or circular opening in flat mirror 11. Wavelengths shorter than 8 μm are cut off by InSb filter 12 in front of photoresistor 9.

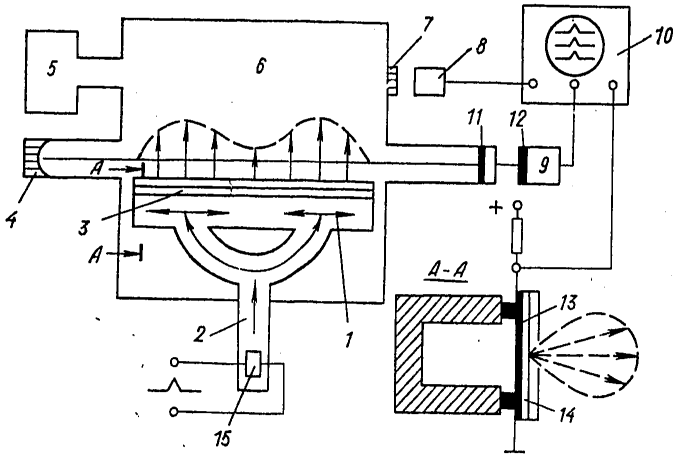

Fig. 7.24. Diagram of detonation laser with breakable film diaphragm: 1--explosion chamber; 2--tube with explosive gas mixture; 3--slit; 4--opaque mirror; 5--vacuum pump; 6--vacuum chamber; 7--NaCl window; 8, 9--Ge-Au photocells; 10--oscilloscope; 11--output mirror; 12--InSb filter; 13--contact sensor; 14--mylar film; 15--ignition

Lasing was realized on all three mixtures shown in the table as the detonation products were discharged through a slit 1 mm wide. For the $CO/N_2O/He$ mixture, lasing was also observed as the detonation products were discharged through a slit up to 4 mm in width.

It is pointed out in Ref. 88 that each lasing pulse has its own more detailed structure, apparently due to the complex gasdynamic process of unsteady discharge of the detonation products.

From the given laser designs using detonation for production and thermal pumping of active media, it can be seen that one of the peculiarities that to a great extent determines the overall design of a detonation laser is handling the problem of a *method of containment* of the initial substance in the reaction space, and cutting off this space from the evacuated optical cavity until the beginning of discharge of the products of detonation or explosion.

In Ref. 7 this problem was solved by phase transformation of the working substance to the initial condensed state. In Ref. 88 the job was handled by separating the explosion chamber from the evacuated space by a diaphragm in the form of a mylar film that was ruptured by the detonation wave.

Peculiarities of this kind are chiefly what determine the designs of other detonation lasers as well. For example Ref. 89, 90 investigated the operation of a laser (Fig. 7.25) in which the stop of gas-tight high-pressure valve 4 is released by solenoid tripper 3 at the end of the period of the explosive process in a mixture of $CO/O_2/H_2/N_2$ initiated by spark plug 1 inside chamber 2. This ensures rapid expansion of the products of explosion in two-dimensional slit nozzle 5, population inversion, and lasing in the region of optical cavity 6 with subsequent exhaust of these products into vacuum chamber 7.

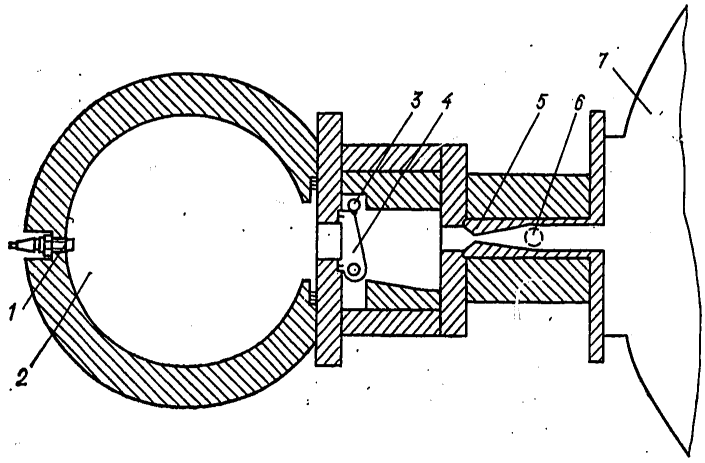

Fig. 7.25. Diagram of detonation laser with electric-release valve: 1--ignition; 2--explosion chamber; 3--solenoid release; 4--valve; 5--nozzle; 6--cavity; 7--vacuum chamber

The most typical conditions in such experiments were: composition of products of explosion $CO_2/N_2/H_2O = 15/83.5/1.5$; stagnation temperature and pressure 1500 K and 1 MPa respectively. Temperature and pressure in the cavity region 300 K and about 13 kPa respectively, Mach number $M = 4.5$. Periodicity of operation about 3 minutes.

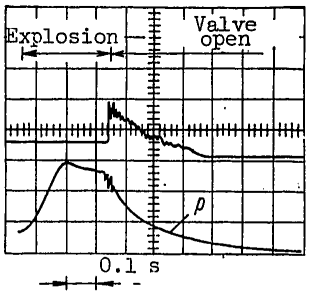

Fig. 7.26. Change of gas pressure and power of stimulated emission in a detonation laser

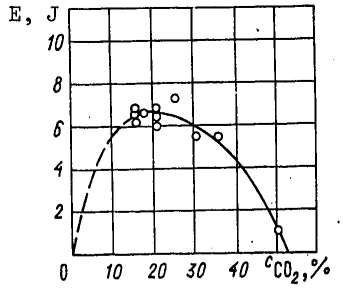

Fig. 7.27. Energy output as a function of CO_2 concentration

The changes of pressure in explosion chamber 2 and variation of stimulated emission in cavity 6 are illustrated by the synchronous oscilloscope record on Fig. 7.26. It can be seen that from the instant the valve opens, lasing begins (upper curve), whereas the pressure p in the explosion chamber falls comparatively slowly (lower curve) as the explosion products are discharged and cooled.

Of some interest are measurements made in Ref. 89 of the way that energy output depends on CO_2 concentration (Fig. 7.27). In experiments using the three types of nozzle sets shown in Fig. 7.28 -- wedge-shaped (a), profiled (b) and a block of

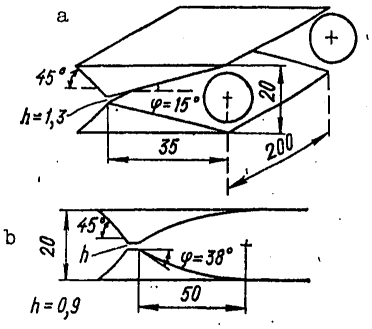

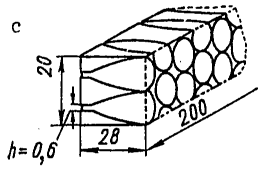

Fig. 7.28. Types of nozzle sets: a--wedge-shaped; b--profiled; c--block of axisymmetric nozzles

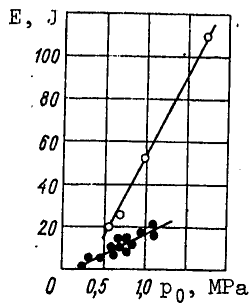

Fig. 7.29. Comparison of the energy output of a laser with different types of nozzles: o--profiled; •--wedge-shaped

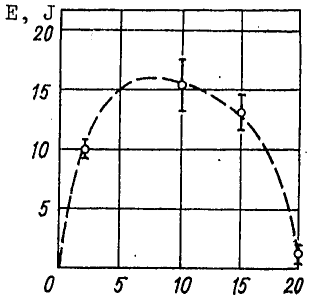

Fig. 7.30. Output energy as a function of transparency of the mirror of the optical cavity

axisymmetric nozzles (c), it was found that the energy output for the profiled nozzle is approximately 2.5 times the value for the wedge-shaped nozzle (Fig. 7.29). On this graph the blackened circles correspond to lasing processes with gas expansion in a wedge-shaped nozzle, while the unblackened circles correspond to lasing with gas expansion in the profiled nozzle. The stagnation temperature was equal to 1400 K. This difference in output energies is partly due to a reduction in the relaxation rates of molecules with more intense expansion of the flow in the profiled nozzle.

The output energy is a function of the transparency of the mirror in the optical cavity. An experimental curve for this function in the case of a profiled nozzle set is shown in Fig. 7.30 for stagnation pressure and temperature of 0.54 MPa and 1100 K respectively. The gain determined from these data was approximately 0.7 m^{-1}, whereas this parameter was about 0.4 m^{-1} for the wedge-shaped nozzle set, although the stagnation temperature is considerably higher -- 1400 K. This indicates that better conditions for freeze-out of the upper energy level of population exist for profiled nozzles. The maximum energy obtained in the described detonation laser was 110 J for a profiled nozzle. This is 0.06% of the thermal energy contained in

the initial gas. Experiments with the block of axisymmetric nozzles show that shock waves and turbulent wakes in the flow from the boundaries of the nozzles cause heating of the gas and optical inhomogeneity of the medium in the cavity.

High energy losses in a laser of the described design can be attributed to the following causes:

1. Following the end of the laser pulse about 50% of the gas remains in the explosion chamber. This is due to pressure elevation in the vacuum space -- an effect that can be reduced by using a diffuser.

2. Heat is lost to the walls as the gas expands.

3. Losses to relaxation in the nozzle.

4. The small dimensions of the cavity in the direction of flow (about 1 cm) prevent complete utilization of the energy contained in the N_2 due to slow energy transfer from $N_2(v)$ to $CO_2(00v)$, and the lower energy level cannot completely transfer its energy to the vibrational mode because of the rapid transit of gas through the cavity. Estimates show that these factors account for a loss of about 50% of the energy entering the optical cavity.

5. Flow losses in the cavity due to nonoptimality.

It is suggested in Ref. 90 that by minimizing these losses or some of them an overall efficiency of about 0.5% can be achieved, and this value can be increased still further by increasing the stagnation temperature.

In contrast to the described laser design, the problem of containment of the initial substance in the reaction zone and cutting off this space from the evacuated volume of the optical cavity is handled by using an electromagnetic valve of periodic action in Ref. 91, enabling operation of the device in periodically repeated cycles (twice a minute). A schematic diagram of such a laser with explosive pumping is shown in Fig. 7.31.

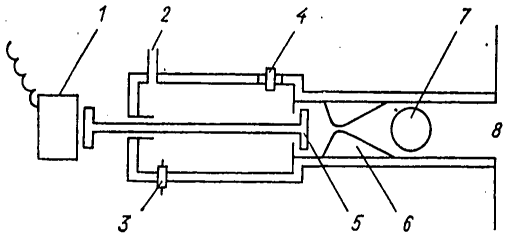

Fig. 7.31. Detonation laser with periodically acting electromagnetic valve: 1--electromagnet; 2--input of mixture; 3--spark plug; 4--pressure sensor; 5--valve; 6--nozzle; 7--optical cavity; 8--reservoir for removal of the used gas mixture

After the explosion chamber has been filled with the gas mixture to the necessary pressure, electromagnet 1 is disengaged and ignition takes place. When the maximum temperature has been attained and the burning gas has reached the maximum pressure,

valve 5 is opened and the gas rushes through nozzle 6. The pressure in front of the nozzle is recorded by sensor 4, and the temperature in this zone is calculated from the pressure increase in the chamber. Direct measurements of the temperature in this zone have shown good agreement between the results of measurements and calculated values.

After exit through the electromagnetic valve, the products of explosion expand in the nozzle, and then are removed to reservoir 8 in analogy with the design described above. Optical cavity 7, with active length of 20 cm, is placed across the gas stream at the nozzle outlet. Both mirrors of the cavity are 76 mm from the gas stream to prevent contamination during operation of the laser.

For a nozzle with $h = 1.5$ mm, ratio of cross sectional areas $S/S^* = 15$, and half-angle of the vertex $\phi = 15°$, the gas flow leaves the nozzle with $M \approx 4$, and at $h = 0.75$ mm, $S/S^* = 30$ and $\phi = 15°$, we have $M \approx 5$.

It has been established that the beginning of amplification coincides with the instant of opening of the valve in a system that uses an explosive mixture of CO/H_2 and a mixture of $CO_2/N_2/H_2O = 1.5/8.3/0.2$. For an area ratio $S/S^* = 15$, the pressure in the explosion chamber increased from 0.2 to 0.5 MPa within the first 0.15 s after initiating the explosion, and after the valve was opened fell to zero within the next 0.15 s and again slowly rose to the initial value of 0.2 MPa. At the instant of opening of the valve, optical amplification increased and there was a simultaneous increase in the power of the stimulated output radiation to 60 W with a pulse duration of this emission of 0.8 s.

After the pressure in the combustion chamber had fallen to zero, a rapid increase in optical absorption was observed in the active medium. Moreover it can be noted that the process of amplification of the active medium and generation of stimulated emission were accompanied by fluctuations in the gain of the active medium and the power of the output radiation, which were due to a change in conditions during expansion of the gas through the nozzle, and apparently to certain gasdynamic instabilities inherent in the given design.

It would be a good idea in the described lasers to consider the feasibility of using ordinary hydrocarbons as the fuel. However, the large amounts of water vapor that are liberated upon combustion of such fuel may to a considerable extent inhibit processes of stimulated emission since the cross section of processes of relaxation of antisymmetric modes of the CO_2 molecules under the action of H_2O molecules is large [Ref. 80]. To determine the influence of water vapor on the characteristics of the described lasers, a study was done in Ref. 91 on several types of CO/H_2 mixtures that yield different amounts of water vapor upon ignition. Fig. 7.32 gives the results of these studies in the form of curves for the gain as a function of the percent content of water vapor.

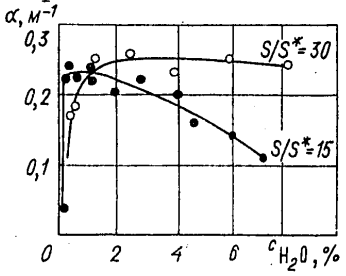

Fig. 7.32. Gain α as a function of water vapor content c_{H_2O} in the active medium

It can be seen that for a nozzle with $h = 1.5$ mm ($S/S^* = 15$) the gain reaches the maximum value at a water vapor content of ~1%, and falls to about one-half at a water vapor content of ~8%. With more rapid expansion of the gas, i. e. for $h = 0.75$ mm ($S/S^* = 30$) amplification decreases

with increasing water vapor content in the active mixture much more slowly than in the first case. The laser design with h = 0.75 mm was less sensitive to water vapor content, and therefore several types of hydrocarbon fuels were used in this design to check the extent to which the additional combustion products that are inevitably present in such fuel affect the characteristics of the system. The use of three types of such fuels -- acetylene, propane and natural gas -- was characterized by generation of an intense pulse of stimulated emission regardless of whether there was an excess or insufficiency of oxygen in this case. For example when natural gas was used as the fuel, and the active medium was $CO_2/N_2/H_2O$ = 0.66/8.0/1.34, the power of the output radiation reached 60 W with duration of the pulses of this radiation of the order of 0.03 s. On the other hand when the fuel was acetylene and the active medium was $CO_2/N_2/H_2O$ = 1.2/8.2/0.6, the power of the output radiation was 70-75 W at a pulse duration of about 0.08 s. If propane was used as the fuel, and the active medium was a mixture of $CO_2/N_2/H_2O$ = 0.85/8.0/1.15, the output radiation had a pronounced series of very short beams with power of some of them being greater than 100 W.

Further research in the area of developing the described lasers is possible in the direction of increasing the working pressure and temperature. At high temperatures there is a strong increase in the percentage of energy associated with vibrational states of the molecules, and this should mean a considerable increase in the power and energy of the stimulated coherent radiation. The use of large pressures is necessary in turn for getting higher temperatures and higher gas flow rates. Then the increased energy of coherent emission will be released in shorter periods of time, and consequently there will be a considerable increase in the peak power of the output radiation.

REFERENCES

1. B. B. Dunne, "Shock Wave Optically Pumped Laser," U. S. Patent 3451008, 1969.

2. "Problems of Electrophysics of Combustion," No 36, Moscow, "Nauchnyye issledovaniya energeticheskogo instituta imeni G. M. Krzhizhanovskogo" [Scientific Research of the Power Engineering Institute imeni G. M. Krzhizhanovskiy], 1975; REFERATIVNYY ZHURNAL: MEKHANIKA, No 11, 1976, p 101.

3. V. K. Ablekov, Yu. N. Denisov, F. N. Lyubchenko et al., "A Laser," USSR Patent 589841, 2 Nov 76, Patent Bulletin No 4, 1979, p 251.

4. V. K. Ablekov, "A Method of Producing a Medium with Negative Absorption Factor," USSR Patent No 475964, 27 Nov 64, Patent Bulletin No 4, 1979, p 251.

5. R. W. F. Gross, R. R. Giedt, T. A. Jacobs, "Stimulated Emission Behind Overdriven Detonation Waves in F_2O-H_2 Mixtures," J. CHEM. PHYS., Vol 51, No 3, 1969, p 1250.

6. V. M. Marchenko, A. M. Prokhorov, "On the Feasibility of Producing an Inverse Medium for Lasers by Explosion," PIS'MA V ZHURNAL EKSPERIMENTAL'NOY I TEORETICHESKOY FIZIKI, Vol 14, No 2, 1971, pp 116-120.

7. M. S. Dzhidzhoyev, V. V. Korolev, V. N. Markov et al., "The Gasdynamic Detonation Laser," PIS'MA V ZHURNAL EKSPERIMENTAL'NOY I TEORETICHESKOY FIZIKI, Vol 13, 1971, pp 73-76.

8. F. A. Williams, "Theory of Combustion," translation from English by S. S. Novikova and Yu. S. Ryazantseva, Moscow, Nauka, 1971, 615 pages.

9. D. L. Chapman, "On the Rate of Explosion in Gases," PHIL. MAG. J. SCI., 1899, Vol 47, series 5, No 284, pp 90-104.

10. Ya. B. Zel'dovich, "On the Theory of Propagation of Detonation in Gaseous Systems," ZHURNAL EKSPERIMENTAL'NOY I TEORETICHESKOY FIZIKI, Vol 10, No 5, 1940, pp 542-568; "On Distribution of Pressure and Velocity in Detonation Explosion Products, in Particular in the Case of Spherical Propagation of a Detonation Wave," ZHURNAL EKSPERIMENTAL'NOY I TEORETICHESKOY FIZIKI, Vol 12, No 9, 1942, pp 389-406; "Teoriya goreniya i detonatsiya gazov" [Theory of Combustion and Detonation of Gases," Moscow-Leningrad, USSR Academy of Sciences, 1944, 72 pages.

11. J. Neuman, "Theory of Detonation Waves," Office of Scientific Research and Development Report No 549, 1942; W. Döring, "Über den Detonationsvorgang in Gasen," ANN. PHYSIK, Vol 43, 1943, pp 421-436.

12. C. Campbell, D. W. Woodhead, "The Ignition of Gases by an Explosion Wave. I. Carbon Monoxide and Hydrogen Mixtures," J. CHEM. SOC., Vol 129, 1926, pp 3010-3012; "Striated Photographic Records of Explosion Waves," J. CHEM. SOC., Vol 130, pp 1572-1578.

13. Yu. N. Denisov, B. V. Voytsekhovskiy et al., "The Phenomenon of Wave Splitting (Fine Structure) of Spin Detonation," Certificate of Discovery No 134, Priority 12 Feb 57, 24 Feb 58, BYULLETEN' IZOBRETENIY i OTKRYTIY, No 48, 1973, pp 4, 5.

14. M. A. Rivin, A. S. Sokolik, "Explosive Limits of Gas Mixtures, 3. Limits in Mixtures of Carbon Monoxide and Methane," ZHURNAL FIZICHESKOY KHIMII, Vol 8, 1936, pp 767-773; Ya. K. Troshin, K. I. Shchelkin, "On Spin at the Limits of Gas Detonation," IZVESTIYA AKADEMII NAUK SSSR: OTDELENIYE TEKHNICHESKIKH NAUK, No 8, 1957, pp 142-143.

15. Yu. N. Denisov et al., "The Phenomenon of Instability of a Detonation Wave in Gases," Certificate of Discovery, No 111, Priority 5 Nov 57, BYULLETEN' IZOBRETENIY I OTKRYTIY, No 24, 1972, pp 4, 5; Yu. N. Denisov, Ya. K. Troshin, "Pulsating and Spin Detonation of Gas Mixtures in Tubes," DOKLADY AKADEMII NAUK SSSR, Vol 125, No 1, 1959, pp 110-113.

16. Yu. N. Denisov, Ya. K. Troshin, "Structure of Gas Detonation in Tubes," ZHURNAL TEKHNICHESKOY FIZIKI, Vol 30, No 4, 1960, pp 450-459.

17. B. V. Voytsekhovskiy, V. V. Mitrofanov, M. Ye. Topchiyan, "Struktura Detonatsii v gazakh" [Structure of Detonation in Gases], Novosibirsk, Izdatel'stvo SO AN SSSR [Siberian Department, USSR Academy of Sciences], 1963, p 168.

18. V. I. Manzhaley, V. V. Mitrofanov, V. A. Subbotin, "Measurement of Inhomogeneities of a Detonation Front in Gas Mixtures at Elevated Pressures," FIZIKA GORENIYA I VZRYVA, No 1, 1974, pp 102-110.

19. R. A. Strehlow, C. D. Engel, "Transverse Waves in Detonations: II. Structure and Spacing in H_2-O_2, C_2H_2-O_2, C_2H_4-O_2 and CH_4-O_2 Systems," AIAA JOURN., Vol 7, No 3, 1969, pp 492-496.

20. A. Schmidt, "Über den Nachweis der Gültigkeit der hydrodynamisch-thermodynamischen Theorie der Detonation für feste und flüssige Sprengstoffe," Z. PHYS. CHEM., Vol A189, 1941, pp 88-94.

21. B. F. Volin et al., "On the Kinetic-Reaction Nature of Inhomogeneities in a Shock Front, and Their Role in the Process of Propagation of a Gas Detonation," ZHURNAL PRIKLADNOY MEKHANIKI I TEKHNICHESKOY FIZIKI, No 2, 1960, pp 78-89.

22. Yu. N. Denisov, Ya. K. Troshin, "Concerning the Discrete Nature of Change in Structure of a Gas Detonation," ZHURNAL PRIKLADNOY MEKHANIKI I TEKHNICHESKOY FIZIKI, No 2, 1967, pp 90-92.

23. K. I. Shchelkin, "Bystroye goreniye i spinovaya detonatsiya gazov" [Rapid Combustion and Spin Detonation of Gases], Moscow, Voyenizdat, 1949, 195 pages.

24. Yu. N. Denisov, Ya. K. Troshin, "Mechanism of Detonation Burning," ZHURNAL PRIKLADNOY MEKHANIKI I TEKHNICHESKOY FIZIKI, No 1, 1960, pp 21-34.

25. V. V. Mitrofanov, "Structure of a Detonation Wave in a Flat Channel," ZHURNAL PRIKLADNOY MEKHANIKI I TEKHNICHESKOY FIZIKI, No 4, 1962, pp 100-105.

26. A. N. Voinov, "On the Mechanism of Arisal of Detonation Spin," DOKLADY AKADEMII NAUK SSSR, Vol 73, No 1, 1950, pp 125-128.

27. B. V. Voytsekhovskiy, "On Spin Detonation," DOKLADY AKADEMII NAUK SSSR, Vol 11,, 1957, pp 717-720.

28. B. V. Voytsekhovskiy, "Investigation of the Structure of a Spin Detonation Front" in: "Trudy MFTI" [Transactions of Moscow Physicotechnical Institute], Moscow, Oborongiz, 1958, pp 81-91.

29. B. V. Voytsekhovskiy, "Optical Studies of a Spin Detonation Wave Front," IZVESTIYA SIBIRSKOGO OTDELENIYA AKADEMII NAUK SSSR, No 4, 1958, pp 74-80.

30. B. V. Voytsekhovskiy, V. V. Mitrofanov, M. Ye. Topchiyan, "On Flow Structure in a Spin Detonation Wave," ZHURNAL PRIKLADNOY MEKHANIKI I TEKHNICHESKOY FIZIKI, No 3, 1962, pp 27-30.

31. M. Ye. Topchiyan, "Experimental Studies of Spin Detonation by Pressure Sensors," ZHURNAL PRIKLADNOY MEKHANIKI I TEKHNICHESKOY FIZIKI, No 4, 1962, pp 94-99.

32. V. V. Mitrofanov, V. A. Subbotin, M. Ye. Topchiyan, "On Pressure Measurement in a Transverse Spin Wave," ZHURNAL PRIKLADNOY MEKHANIKI I TEKHNICHESKOY FIZIKI, No 3, 1963, pp 45-48.

33. Yu. N. Denisov, Ya. K. Troshin, "Thermogasdynamic Model of Pulsating Detonation" in: "Tret'ye Vsesoyuznoye soveshchaniye po teorii goreniya" [Third All-Union Conference on Combustion Theory], Vol 1, Moscow, Izdatel'stvo Akademii Nauk SSSR, 1960, pp 200-207.

34. Yu. N. Denisov, Ya. K. Troshin, "On the Mechanism of Detonative Combustion" in: "Eighth Symp. on Combustion," Baltimore, 1962, pp 600-610.

35. Yu. N. Denisov, "Influence of the Volume Effect on the Structure of the Detonation Front," DOKLADY AKADEMII NAUK SSSR, Vol 187, No 2, 1969, pp 358-361.

36. V. Ye. Gordeyev, "The Reason for Multiplication of Kinks of a Detonation Front," DOKLADY AKADEMII NAUK SSSR, Vol 226, No 2, 1976, pp 288-291.

37. A. V. Dremin, "Current Problems of Studying Detonation in Condensed Media," in: "Nauchnyye trudy Instituta mekhaniki Moskovskogo universiteta" [Scientific Papers of the Institute of Mechanics, Moscow University], No 21, Moscow, Moscow State University, 1973, pp 150-157.

38. Yu. N. Denisov, "High-Frequency Processes in the Core of a Spin Detonation," FIZIKA GORENIYA I VZRYVA, No 3, 1974, pp 386-392.

39. Yu. N. Denisov, I. I. Podtiynkov, "Components of the High-Frequency Process in Detonation Waves" in: "Chetvertyy Vsesoyuznyy simpozium po goreniyu i vzryvu. Annotatsiya dokladov" [Fourth All-Union Symposium on Combustion and Explosion. Abstracts of the Papers], Chernogolovka, Institute of Chemical Physics, Academy of Sciences of the USSR, 1974, p 45; in: "Goreniye i vzryv" [Combustion and Explosion], Moscow, Nauka, 1977, pp 454-460.

40. M. Busco, "Optical Properties of Detonation Waves (Optics of Explosives)" in: "Proc. Fifth Symp. (Int.) on Detonation, 1970, Pasadena, Calif.," Arlington, pp 513-522; W. B. Benedick, "Detonation Wave Shaping" in: "Behav. and Util. Explos. Eng. Des. and Biomech. Princip. Appl. Clin. Med. Proc. 12th Annu. Symp., Albuquerque, New Mexico, 1972," Albuquerque, N. M., pp 47-56.

41. T. V. Bazhenova, L. V. Gvozdeva, Yu. S. Lobastov et al., "Udarnyye volny v real'nykh gazakh" [Shock Waves in Real Gases], Moscow, Nauka, 1968, 198 pages.

42. I. A. Kunin, "Teoriya uprugikh sred s mikrostrukturoy" [Theory of Elastic Media with Microstructure], Moscow, Nauka, 1975, 416 pages.

43. A. A. Borisov, "Long-Wave Perturbations in Reacting Media" in: "Issledovaniya po gidrodinamike i teploobmenu" edited by S. S. Kutateladze, Novosibirsk, Izdatel'stvo SO AN SSSR, 1976, pp 94-95.

44. V. I. Aref'yev, Yu. N. Denisov, "On the Phase Theory of Propagation of Detonation Waves in Plasma-Like Media" in: "Elektromagnitnyye protsessy v neodnorodnykh sredakh" [Electromagnetic Processes in Inhomogeneous Media], Vladivostok, Izdatel'stvo DVNTs [Far Eastern Science Center], 1977, p 48.

45. Ya. B. Zel'dovich, Yu. P. Rayzer, "Fizika udarnykh voln i vysokotemperaturnykh gidrodinamicheskikh yavleniy" [Physics of Shock Waves and High-Temperature Hydrodynamic Phenomena], Moscow Fizmatgiz, 1963, 632 pages.

46. S. K. Aslanov, "On Periodic Instability as a Theoretical Basis of Pulsation Structure of Detonation," DOKLADY AKADEMII NAUK UKRAINSKOY SSR, SER. A, No 4, 1977, pp 318-321.

47. Yu. N. Denisov, "Investigation of Detailed Detonation Mechanism" in: "Dvenadtsataya Vsesoyuznaya konferentsiya po voprosam ispareniya, goreniya i gazovoy dinamiki dispersnykh sistem. Tezisy dokladov" [Twelfth All-Union Conference on

Problems of Vaporization, Combustion and Gas Dynamics of Dispersed Systems. Abstracts of the Papers], Odessa, 1976, p 41; "Detailed Mechanism of Detonation," DOKLADY AKADEMII NAUK SSSR, Vol 251, No 3, 1980, pp 628-632.

48. F. A. Baum, S. A. Kaplan, K. P. Stanyukovich, "Vvedeniye v kosmicheskuyu gazodinamiku" [Introduction to Space Gasdynamics], Moscow, Fizmatgiz, 1958, 424 pages.

49. Y. H. Lee, R. Knystautas, C. M. Guirao, "Critical Power Density for Direct Initiation of Unconfined Gaseous Detonation" in: "15th Symp. (Intern.) Combust., Tokyo, 1974," Pittsburgh, Pasadena, 1974, pp 53-66.

50. Yu. N. Denisov, P. I. Kopeyka, S. K. Aslanov, "Arisal of Spin Detonation" in: "Fizika aerodispersnykh sistem" [Physics of Aerodispersed Systems], No 11, Kiev, Vysha shkola, 1974, pp 66-71.

51. V. Ye. Gordeyev, "Maximum Overdriven Detonation Rate and Stability of Discontinuities in a Detonation Spin," DOKLADY AKADEMII NAUK SSSR, Vol 226, No 3, 1976, pp 619-622.

52. V. I. Manzheley, V. A. Subbotin, "Experimental Investigation of Stability of an Overdriven Detonation in a Gas," FIZIKA GORENIYA I VZRYVA, Vol 12, No 6, pp 935-942.

53. J. H. S. Lee, "Recent Advances in Gaseous Detonation," AIAA Paper, 1979, No 0287.

54. V. M. Akulintsev, A. S. Bashkin, N. N. Gorshunov et al., "Concerning the Feasibility of Lasing on the CO Molecule Behind an Overdriven Detonation Wave Front in a $Cs_2 + O_2$ Mixture," FIZIKA GORENIYA I VZRYVA, Vol 12, No 5, 1976, pp 739-744.

55. V. N. Kondrat'yev, "Konstanty skorostey gazofaznykh reaktsiy. Spravochnik" [Rate Constants of Gas-Phase Reactions. A Reference], Moscow, Nauka, 1971, 351 pages.

56. R. D. Stuart, P. H. Dawson, G. H. Kimbell "CS_2/O_2 Chemical Lasers: Chemical and Performance Characteristics," J. APPL. PHYS., Vol 43, No 3, 1972, pp 1022-1032.

57. K. H. von Homann, G. Krome, H. G. Wagner, "Schwefelkohlenstoff-Oxydation, I. Geschwindigkeit von Elementarreaktionen," BERICHTE DER BUNSEN-GESELLSCHAFT FÜR PHYSIKALISCHE CHEMIE, Vol 78, 1968, pp 998-1004; II. "Zur Oxydation von Carbonylsulfid," Ibid., Vol 73, No 10, 1969, p 967; III. "Die Isotherme-oxydation von Schwefelkohlenstoff," Ibid., Vol 74, No 7, pp 654-659.

58. D. W. Howgate, T. A. Barr, Jr., "Dynamics of the CS_2-O_2 Flame," J. CHEM. PHYS., Vol 59, No 6, 1973, pp 2815-2829.

59. G. Hancock, C. Morley, W. M. Smith, "Vibrational Excitation of CO in the Reaction: $O + CS \rightarrow CO + S$," CHEM. PHYS. LETT., Vol 12, No 1, 1971, pp 193-196.

60. B. F. Gordiyets, A. I. Osipov et al., "Vibrational Relaxation in Gases, and the Molecular Laser," USPEKHI FIZICHESKIKH NAUK, Vol 108, No 4, 1972, pp 655-699.

61. J. D. Anderson, M. T. Madden, "Population Inversions Behind Normal Shock Waves," AIAA JOURN., Vol 9, No 8, 1971, pp 1630-1632.

62. N. G. Basov, A. N. Orayevskiy, "Getting Negative Temperatures by the Method of Heating and Cooling a System," ZHURNAL EKSPERIMENTAL'NOY I TEORETICHESKOY FIZIKI, Vol 44, No 5, 1963, pp 1742-1745.

63. I. R. Hurle, A. Hertzberg, "On the Possible Production of Population Inversions by Gas Dynamic Techniques," Minutes of the 1963 Annual Meeting of the Division of Fluid Dynamics, Cambridge Massachusetts, 25-27 Nov 1963, BULL. AMER. PHYS. SOC., Vol 9, No 5, 1964, pp 582-595.

64. I. R. Hurle, A. Hertzberg, "Electronic Population Inversion by Fluid-Mechanical Techniques," PHYS. FLUIDS, Vol 8, No 9, 1965, pp 1601-1607.

65. V. K. Konyukhov, A. M. Prokhorov, "Inverse Population with Adiabatic Expansion of a Gas Mixture," PIS'MA V ZHURNAL EKSPERIMENTAL'NOY I TEORETICHESKOY FIZIKI, Vol 3, No 11, 1966, pp 436-439.

66. J. E. Morgan, H. I. Schiff, "The Study of Vibrationally Excited N_2 Molecules with the Aid of an Isothermal Calorimeter," CANAD. JOURN. CHEMISTRY, Vol 41, No 4, 1963, pp 903-912.

67. V. K. Konyukhov, I. V. Matrosov, A. M. Prokhorov et al., "A Gasdynamic cw Laser Based on a Mixture of Carbon Dioxide, Nitrogen and Water," PIS'MA V ZHURNAL EKSPERIMENTAL'NOY I TEORETICHESKOY FIZIKI, Vol 12, No 10, 1970, pp 461-464.

68. N. G. Basov, A. N. Orayevskiy, V. A. Shcheglov, "Thermal Methods of Laser Excitation," ZHURNAL TEKHNICHESKOY FIZIKI, Vol 37, No 2, 1967, pp 339-348.

69. D. M. Kuehn, D. J. Monson, "Experiments with a CO_2 Gas-Dynamic Laser," APPL. PHYS. LETT., Vol 16, No 1, 1970, pp 48-51.

70. A. P. Dronov et al., "A Gas-Dynamic CO_2 Laser with Discharge of a Mixture Heated in a Shock Tube Through a Slit," PIS'MA V ZHURNAL EKSPERIMENTAL'NOY I TEORETICHESKOY FIZIKI, Vol 11, No 11, 1970, pp 516-519.

71. B. R. Bronfin, L. R. Boedecker, J. P. Cheyer, "Thermal Laser Excitation by Mixing in a Highly Convective Flow," APPL. PHYS. LETT., Vol 16, No 5, 1970, pp 214-216.

72. A. S. Biryukov, B. F. Gordiyets, L. A. Shelepin, "Nestatsionarnyye sposoby sozdaniya inversnoy zaselennosti kolebatel'nykh urovney molekuly CO_2" [Unsteady Methods of Setting up Population Inversion of Vibrational Levels of the CO_2 Molecule], Preprint No 41, Physics Institute imeni Lebedev, 1969, p 51.

73. A. S. Biryukov, L. A. Shelepin, "A Chemical-Mechanical Molecular Laser," ZHURNAL TEKHNICHESKOY FIZIKI Vol 40, No 12, 1970, pp 2575-2577.

74. N. G. Basov et al., "Population Inversion of Molecules in a Supersonic Binary Gas Flow in a Laval Nozzle," ZHURNAL TEKHNICHESKOY FIZIKI, Vol 38, No 12, 1968, pp 2031-2041.

75. "Avco Describes Gas-Dynamic System that Attains 60-Kilowatt Pulses," LASER FOCUS, Vol 6, No 7, 1970, pp 16-18.

76. E. Gerry, "The Gas-Dynamic Laser," LASER FOCUS, Vol 6, No 12, 1970, pp 27-31.

77. F. A. Baum, K. P. Stanyukovich, B. I. Shekhter, "Fizika vzryva" [Physics of Explosion], Moscow, Fizmatgiz, 1959, p 800.

78. K. K. Andreyev, A. F. Belyayev, "Teoriya vzryvchatykh veshchestv" [Theory of Explosives], Moscow, Oborongiz, 1960, 595 pages.

79. B. A. Ivanov, "Fizika vzryva atsetilena" [Physics of Explosion of Acetylene], Moscow, Khimiya, 1969.

80. R. I. Taylor, S. Bitterman, "Survey of Vibrational Relaxation Data for Processes Important in the CO_2-N_2 Laser System," REV. MOD. PHYS., Vol 41, 1969, pp 26-47.

81. R. W. F. Gross, R. R. Giedt, T. A. Jacobs, "Stimulated Emission Behind Overdriven Detonation Waves in F_2O-H_2 Mixtures," IEEE J. QUANT. ELECTRON., Vol QE-6, 1970, p 168.

82. R. W. F. Gross, N. Cohen, T. A. Jacobs, "Chemical Laser Produced by Flash Photolysis of F_2O-H_2 Mixtures," J. CHEM. PHYS. Vol. 48, No 8, 1968, pp 3821-3822.

83. N. Cohen, R. Wilkins, T. A. Jacobs, "Theoretical Calculations of Detonation Initiated Chemical Lasers," IEEE J. QUANT. ELECTRON., Vol QE-6, 1970, pp 168-169.

84. V. G. Voronkov, A. S. Rozenberg, "Explosive Properties of Mixtures of Gaseous Hydrazoic Acid with Inorganic Diluents," DOKLADY AKADEMII NAUK SSSR, Vol 177, No 4, 1967, pp 835-838.

85. M. S. Dzhidzhoyev, M. I. Pimenov, V. G. Platonenko et al., "On Producing Population Inversion in Polyatomic Molecules Through the Energy of a Chemical Reaction," ZHURNAL EKXPERIMENTAL'NOY I TEORETICHESKOY FIZIKI, Vol 57, No 2, 1969, pp 411-420.

86. N. G. Basov, V. V. Gromov, Ye. L. Koshelev et al., "Induced Radiation in Explosion of HN_3 and CO_2," PIS'MA V ZHURNAL EKSPERIMENTAL'NOY I TEORETICHESKOY FIZIKI, Vol 10, No 1, 1969, pp 5-8.

87. N. Ya. Vasilik, V. M. Shmelev, A. D. Margolin, "Influence of Chlorine on the Gain of a CO_2 Gasdynamic Laser Based on Products of Combustion of Methane Mixtures," KVANTOVAYA ELEKTRONIKA, Vol 3, No 10, 1976, pp 2171-2175.

88. Yu. A. Bokhon, I. I. Davletchin, V. M. Marchenko et al., "Observation of Stimulated Emission in a Gas-Dynamic Laser Based on Products of Gas Detonation," KRATKIYE SOOBSHCHENIYA PO FIZIKE, No 11, 1972, pp 52-56.

89. S. Jatsiv, E. Greenfield, F. Dothan-Deutsch et al., "Pulsed CO_2 Gas-Dynamic Laser," APPL. PHYS. LETT., Vol 19, No 3, 1971, pp 65-68.

90. S. Jatsiv et al., "Experiments with a Pulsed CO_2 Gas-Dynamic Laser IEEE J. QUANT. ELECTRON. Vol QE-8, No 2, 1972, pp 161-163.

91. J. Tulip, H. Seguin, "Explosion-Pumped Gas-Dynamic CO_2 Laser," APPL. PHYS. LETT., Vol 19, No 8, 1971, pp 263-265.

Contents

[76-6610]

6610
CSO: 1862

UDC 621.373.8

THE ELECTRON-BEAM METHOD OF PUMPING GAS LASERS, AND ITS APPLICATIONS

Moscow TRUDY ORDENA LENINA FIZICHESKOGO INSTITUTA IMENI P. N. LEBEDEVA AKADEMII NAUK SSSR: ELEKTROIONIZATSIONNYY METOD NAKACHKI GAZOVYKH LAZEROV I YEGO PRILOZHENIYA in Russian Vol 116, 1980 (signed to press 26 Aug 80) pp 2, 210-211

[Annotation and abstracts from book "Proceedings of Lebedev Physics Institute, USSR Academy of Sciences: The Electron-Beam Method of Pumping Gas Lasers, and Its Applications", edited by Academician N. G. Basov, Izdatel'stvo "Nauka", 1350 copies, 211 pages]

[Text] This collection covers research done in the Quantum Physics Laboratory of Lebedev Physics Institute on making and studying high-pressure molecular lasers stimulated by the electron-beam method, as well as research on using electron-beam excitation to stimulate fusion reactions.

The book is written for a wide range of scientists and engineers working in the field of quantum radiophysics, the physics of high-power electric discharges, and chemical kinetics.

UDC 621.375.8

THE PRESENT STATE OF RESEARCH ON THE ELECTRON-BEAM METHOD OF EXCITATION

[Abstract of article by N. G. Basov, V. A. Danilychev and I. B. Kovsh]

[Text] The article briefly examines the current state of research on electron-beam-controlled [EBC] lasers and points out major trends in studies in this field. A condensed survey is given of the latest developments in pulsed and cw high-power carbon dioxide EBC lasers, design improvements and optimization of pumping conditions of such lasers, development of a theory of EBC lasers, research and development in EBC lasers based on new active media, investigation of the stability of a semi-self-maintained discharge excited by the electron-beam method, and the use of an EBC discharge for stimulating chemical reactions. References 22.

UDC 621.378.33

THEORETICAL STUDY OF KINETICS AND ENERGY CHARACTERISTICS OF ELECTRON-BEAM LASERS

[Abstract of article by N. Ye. Vtorova, V. I. Dolinina, A. N. Lobanov, A. F. Suchkov and B. M. Urin]

[Text] Mathematical modeling of physical processes in an active medium is used in detailed theoretical investigations of the kinetics and lasing characteristics of electron-beam controlled lasers based on vibrational-rotational transitions of CO_2, CO, H_2 and HD molecules. Relations are found for the power, energy, efficiency and lasing spectrum as functions of the composition of the active medium and the

pumping conditions (the quantity E/N, power and duration, spatial homogeneity). An investigation is made of the influence that the isotopic makeup of carbon monoxide has on the lasing characteristics of a CO laser. Limitations are examined that are due to breakdown of the active medium by self-radiation for lasers based on molecules of CO_2, H_2 and HD. Figures 39, tables 10, references 113.

UDC 621. 375.85; 621.378.33

EXPERIMENTAL INVESTIGATION OF PULSED ELECTRON-BEAM CONTROLLED CARBON MONOXIDE LASERS

[Abstract of article by N. G. Basov, V. A. Danilychev, A. A. Ionin and I. B. Kovsh]

[Text] The paper describes experimental facilities and investigations of the energy, time and spectral characteristics of emission of high-pressure pulsed CO lasers excited by the electron-beam method with emission energy of up to 400 J, and efficiency up to 35% when the excitation volume is 5 liters. An investigation is made of the way that the output parameters of such lasers depend on the power and duration of excitation, as well as the makeup and density of the working gas mixture. It is shown that the results of numerical calculations of the parameters of pulsed electron-beam controlled CO lasers agree qualitatively with experimental data. The greatest divergence is observed for lasers that operate without cooling of the gas mixture, and for a cooled laser based on pure carbon monoxide. Figures 33, table 1, references 73.

UDC 621.378.33

OPTIMIZING THE WORKING CONDITIONS OF PULSED ELECTRON-BEAM CONTROLLED CO_2 LASERS

[Article by V. A. Danilychev, I. B. Kovsh and V. A. Sobolev]

[Text] An examination is made of the relations between the emission characteristics of a pulsed electron-beam controlled carbon dioxide laser and the conditions of excitation. An analysis is made of the way that laser efficiency, emission pulse duration and specific power output depend on pumping duration and intensity, composition of the gas mixture and cavity parameters. It is shown that the optimum pumping pulse duration for attaining high specific power output and efficiency is 10-40 μs. The best working mixtures with such durations are those containing CO_2 and N_2 in proportions of (1:2)-(1:4). Doping the CO_2:N_2 mixture with a small amount of H_2 increases the efficiency by 15-20% over the same mixtures without H_2. When a CO_2:N_2:He mixture is replaced by CO_2:N_2:H_2, the maximum efficiency realized in the experiment remains practically unchanged, but the specific power output rises due to the attainment of greater specific pumping energy. Figures 17, tables 6, references 41.

UDC 621.378.33

AN ELECTRON-BEAM CONTROLLED CO_2 LASER WITH PLASMA MIRROR

[Abstract of article by I. V. Kholin]

[Text] A detailed analysis is made of a new design for a powerful electron-beam controlled CO_2 laser based on using the modulating properties of a high-temperature

laser plasma (plasma mirror) formed by the action of laser radiation on the surface of a solid target, and acting as one of the mirrors of the laser cavity. This design produces laser emission pulses of nanosecond duration with power of several tens of GW at an efficiency of about 6-10%, yielding a laser plasma with temperature of several millions of degrees. The author demonstrates the feasibility of practical utilization of a plasma mirror for applications as a powerful source of soft x-rays. Figures 26, tables 5, references 84.

UDC 539.196

THEORETICAL AND EXPERIMENTAL STUDY OF ELECTRON-BEAM CONTROLLED SYNTHESIS OF NITROGEN-CONTAINING COMPOUNDS

[Abstract of article by N. G. Basov, V. A. Danilychev, V. I. Dolinina, A. N. Lobanov, A. N. Orayevskiy, V. I. Panteleyev, A. F. Suchkov, B. M. Urin, F. S. Fayzullov, Yu. N. Shebeko, E. V. Gorozhankin, V. V. Kurenkov and V. N. Men'shov]

[Text] A theoretical and experimental investigation is made of an electron-beam controlled method of synthesizing nitrogen-containing compounds. It is shown that the principal chemically active form of nitrogen in an electron-beam controlled discharge is vibrationally excited N_2 molecules. The experimental technique is outlined, and results are given on synthesis of nitrogen oxides, hydrogen cyanide and nitrides of phosphorus. The isotopic content of vibrationally excited molecules of nitrogen and carbon monoxide is calculated. Figures 23, table 1, references 71.

UDC 621.375.8

CALCULATION OF DIVERGENCE OF RADIATION OF PULSED ELECTRON-BEAM CONTROLLED LASERS

[Abstract of paper by Ye. P. Glotov, V. A. Danilychev, V. V. Pustovalov and A. M. Soroka]

[Text] In electron-beam controlled lasers the angular divergence is determined by refraction of emission on gradients of electronic and gas density. At short pumping pulse durations (of the order of 1 μs or less) and consequently high densities of charged particles (n_e of the order of 10^{14} cm^{-3}) divergence is caused by nonuniformity of ionization of the active medium. At longer durations (greater than 10 μs) divergence is determined by the refraction of radiation on gradients of gas density caused by hydrodynamic motion of the active medium during the pumping pulse. A considerable increase in the energy of radiation with divergence due to diffraction can be attained by using unstable telescopic cavities with dimensions smaller than the region of energy input. Figures 5, references 7.

UDC 621.375.85; 621.378.33

STICKING AND RECOMBINATION IN A PLASMA DISCHARGE EXCITED BY THE ELECTRON-BEAM METHOD

[Abstract of article by Ye. P. Glotov, V. A. Danilychev and I. V. Kholin]

[Text] An experimental study is done on the laws of deionization of a discharge plasma stimulated by the electron-beam method. The balance of charged particles is calculated. Measurements are made of the "effective" rate constants of sticking and

recombination that are needed for selecting the optimum pumping conditions for electron-beam controlled lasers operating in the pulse-recurrence mode. An investigation is made of the influence that oxygen impurities have on the characteristics of an electron-beam controlled discharge. Figures 7, table 1, references 17.

UDC 621.375.85; 621.378.33

INVESTIGATION OF MECHANISMS OF DESTRUCTION AND METHODS OF PROTECTION OF THE SEPARATIVE FOIL OF ELECTRON GUNS DURING STREAMER BREAKDOWN OF THE DISCHARGE GAP

[Article by Ye. P. Glotov, V. A. Danilychev and V. D. Zvorykin]

[Text] In practical utilization of electron-beam controlled lasers, a very important problem is working reliability. The weakest link of the EBC laser is the separative foil of the electron guns, breakdown of the discharge gap being the principal cause of failure of this foil. In this article an investigation is made of the mechanisms of destruction of the foil and a method is proposed for protection that considerably improves the working reliability of EBC lasers. Figures 5, references 7.

6610
CSO: 1862

UDC 621.373.826.038.823

THEORETICAL STUDY OF A REPETITIVELY PULSED COPPER-VAPOR LASER

Moscow KVANTOVAYA ELEKTRONIKA in Russian Vol 7, No 11, Nov 80 pp 2319-2325

[Article by S. V. Arlantsev, V. V. Buchanov, L. A. Vasil'yev, E. I. Molodykh, V. V. Tykotskiy and N. I. Yurchenko; submitted 22 Feb 80]

[Text] A procedure is proposed for the numerical design of a copper-vapor laser. The results obtained for lasers with high buffer gas pressure and transverse discharge are consistent with the experimental data. The optimal transverse dimension of the active zone is determined under effective gas heating conditions. A procedure is presented for estimating the concentration, the electron temperature and population of metastable levels in the periodic pulse mode confirmed by numerical calculation.

1. Introduction

At the present time the study of pulsed metal-vapor lasers is attracting a great deal of attention from experimental scientists. Nevertheless, the expected high values of the efficiency and average lasing power [1] have not been realized up to now. There is also no united opinion on the role of the various physical processes in the limitation of these output characteristics or the repetition frequency of the pulses although many proposals have been made in this regard [2, 3]. In the present paper a theoretical model and the results of numerical experiments are presented for a neon and copper vapor mixture laser (LPM) operating in the periodically pulsed mode (PPM) at pulse repetition frequencies on the order of several kilohertz. Primary attention is given to the LPM with transverse discharge and neon pressure on the order of atmospheric [4].

2. Theoretical Model

The presence of two characteristic stages in the LPM plasma kinetics during periodic repetition of the pumping pulses permits the calculation to be divided into two parts: the intensive excitation of the atoms and development of lasing (the pulse mode) and the predominant recombination phase [5] during which joint relaxation of the electron concentration, their temperature and the population of the metastable states of the copper atoms (the relaxation mode) occurs.

In the first phase a number of kinetic processes in the copper atom during electron-atom collisions (Figure 1) and direct ionization of the neon by electron impact are taken into account. High electron densities (10^{13} to 10^{15} cm^{-3}) characteristic of PPM permit consideration that the setup time for equilibrium distribution between the upper levels of the copper atoms (above resonance) and the free electrons is small and amounts to 10^{-7} to 10^{-9} seconds. Therefore an approximation of the instantaneous ionization of all the upper levels is made in the given model. The consideration of the finite ionization time of these levels is reflected insignificantly in the calculation results in the investigated range. The high electron densities and significant capture of the radiation also permit elimination of the consideration of spontaneous transitions which are completed at the ground and operating levels. All of the indicated inelastic processes and also the elastic collisions of the electrons with neon and copper atoms and cooling of them during the process of ambipolar diffusion determine the electron temperature. In order to save computer calculation time, the development of lasing is calculated only for the 510.6-nm line. The populations of the working levels of the 578.2-nm line are considered indirectly: they are taken with accuracy to the statistical weight to be equal to the corresponding populations for the 510.6-nm line. The field intensity in the plasma is determined considering the electric feed circuit and the variable discharge resistance. The cathode potential drop is not considered.

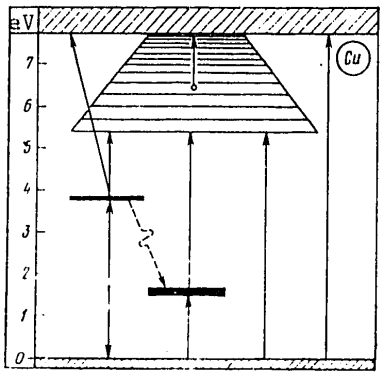

Figure 1. Pulse mode. Transition is taken into account during electron-atom collisions.

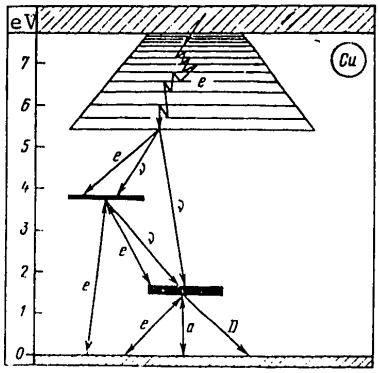

Figure 2. Relaxation mode. Transition is taken into account as a result of electron (e) and atomic (a) collisions, spontaneous radiation (ν) and diffusion (D).

In the relaxation mode it is proposed that the recombination flux formed during the process of impact recombination diffuses with respect to the upper states of the copper atom to levels of $5p^2P^0$ and $4d^2P$ (6.12-6.19 eV) as a result of electron-atom collisions. Then it is divided into the spontaneous and "electron" (as a result of electron impact) fluxes to the resonance levels and spontaneous flux to the metastable levels. The spontaneous times are defined considering the possible capture of the radiation, and Doppler line broadening is assumed

Further movement of the recombination flux and relaxation of the metastable states are calculated in detail considering all of the direct and inverse transitions under the effect of electron collision between the ground, metastable and resonance levels. Spontaneous transition from resonance to metastable level with correction for capture of the radiation and deactivation of the metastable states by neon atom impact are also taken into account.

The described calculation of the distribution of the recombination flux (Figure 2) is based on a qualitative comparison of the characteristic relaxation process times for standard LPM conditions. It permits not only more precise definition of the effectiveness of the population of metastable states from above, but also calculation of the proportion of the discharge energy going to heating the gas.

In the relaxation mode, the impact and dissociative recombinations of the neon atoms are also taken into account. The electron temperature is determined by heating by the above-described inelastic processes and cooling, both elastic and diffusion, during the process of ambipolar diffusion. The diffusion processes--cooling of the electrons, drift of the electrons, ions and metastable atoms--are taken into account in the null-dimensional approximation (that is, with the help of the introduction of characteristic diffusion times). They play a role primarily for low neon pressures and small transverse dimensions of the active zone. The choice of the considered processes ensures a smooth transition from the pulse mode to the relaxation mode.

The used cross sections of all the electron-atom collision processes were averaged with respect to Maxwell distribution function. From the experiment the following cross sections are known: excitation of the working levels [6], ionization of copper [7, 8] and neon [9], elastic collisions with copper [6] and neon [9], deactivation of the metastable states by the inert gases (in addition to neon) [10], and dissociative recombination of the neon [11]. The remaining excitation cross sections are taken from the calculation tables in the Born approximation [12] or they are estimated from oscillator strengths. The Born cross sections are doubled with respect to amplitude, and they are shifted with respect to the position of the peak in accordance with the experimental data [6, 13, 14]. The diffusion coefficients in the mixture, depending on the gas temperature, were estimated by the approximate data on the interatomic potentials Ne^+-Ne, Cu^+-Cu, Cu^+-Ne by the procedure discussed in [15]. The diffusion cooling rate of the electrons was calculated by [16].

The system of kinetic equations realizing the described model of the LPM, was solved numerically on the BESM-6 computer jointly with the nonsteady equation for the electron temperature and the discharge circuit equation. The most significant assumptions about the model are the following: Maxwell form of the electron distribution function with respect to velocities, absence of the cathode potential drop, null-dimensionality of the description of the diffusion processes, the process of penetration of the field into the plasma and the process of development of radiation. The latter assumption leads to the fact that the calculated value of the power output corresponds more to radiation from the active zone in all directions than in the fixed laser beam (the difference in standard conditions can be 1.5-2 times). For this reason the dependence of the power output on the resonator

parameters turned out to be very weak in the calculation, and it will not be discussed further.

3. Results

The shape of the active zone (AZ) was considered to be a rectangular parallelepiped, the pair of opposite sides of which served as electrodes. The set of initial parameters of the active zone and the excitation pulse was limited to the following: ℓ--length, b--width; d--height of the active zone (electrode spacing with transverse discharge); L--total inductance of the discharge circuit; n_{Cu}, n_{Ne}--component concentrations; U_0--voltage of the storage element (or $E_0 = U_0/d$); W_0--specific pulse energy of the storage element; f--pulse repetition frequency. The duration and the shape of the electric excitation pulse at the entrance to the circuit or the switch characteristic were also given. When using a circuit with discharge through the cable line by U_0 we mean the pulse amplitude at the entrance to the cable line, and by W_0, the specific energy of this pulse (that is, per unit volume of the active zone).

The characteristics of the PPM were determined by the method of establishment, that is, the train of pulses to arrival at the steady PPM was calculated. Inasmuch as the establishment of the average atom temperature takes place in hundreds or thousands of pulses, it was considered constant for each pulse repetition period. The steady-state heating of the gas with respect to the cell walls was determined by the repetition frequency and the energy contribution to heat in each period, and it was more precisely defined in the process of establishment.

For the first series of calculations the parameters were used for a laser with transverse excitation, relatively large active zone volume and high neon pressure. This made it possible to estimate the fitness of the program in this region, for which it was primarily designed and also discovery of the causes limiting the output characteristics of the given laser in the PPM. The excitation pulse was fed to the cell through a long cable line so that the equivalent circuit was the wave impedance R of the line, inductance L and discharge resistance R_d connected in series. The initial pulse usually was given as triangular in shape with 50-nanosecond front and a total duration of 200 nanoseconds.

The variation of the parameters n_{Cu}, n_{Ne}, E_0, W_0 and f led to the maximum average power, the position of which turned out to be close to experimental, and the value (28 milliwatts/cm^3) exceeded the experimental value by approximately 1.7 times. The calculated time relations for some of the plasma parameters in the pulse mode near the optimal point are shown in Figure 3 (n_e, n_2, n_3 are the electron and atom concentrations in metastable and resonance states, respectively; T_e is the electron temperature; E is the field intensity in the discharge; J is the current density; P_{ex} is the output power of the radiation). Here the output energy was 13.3 microjoules/cm^3 and the total efficiency was 2 percent. Variation of the inductance near the selected point (5 nanohenries) had little effect on the output energy, although the discharge current-voltage curves changed significantly in this case. It turned out that for the adopted configuration of the active zone and shape of the pumping pulse, the increase in repetition frequency or pulse energy is limited to gas heating. With heating to 3,000-3,500 K the degree of relaxation of the metastable states was insufficient, and the increase in power ceased.

For large neon pressures the electron temperature after the pulse relaxes to the atomic temperature (T_a). Large electron densities characteristic of the PPM and the ratio of the electron and atomic degradation of the metastable states (on the order of 10^6) lead to the fact that the distribution temperature of the metastable states follows the electron temperature. Therefore the prepulse value of the mestable concentration can be estimated by T_e. The difference arises either for insufficiently high n_e or if T_e in front of the pulse is appreciably higher than T_a, and therefore the equilibrium value of n_2 with respect to T_e decreases quickly. From what has been stated it follows that with an increase in the repetition frequency the relaxation of the metastable states can be successful if, first of all, the prepulse T_e is below the critical value from the point of view of pumping possibilities (usually corresponding to n_2 on the order of 1-3 percent of n_{Cu}) and, secondly, the prepulse value of n_e increases proportionately to the repetition frequency. These conditions contradict each other, for the density and the electron temperature increase simultaneously as a result of the heat balance ratio (1) (see below). The described mechanism imposes a fundamental restriction on the growth of the repetition frequency even in the absence of gas heating. It is also maintained in the case where the diffusion cooling of the electrons predominates over elastic cooling, although there may be deviations from this rule near the walls.

The electron temperature and concentration before the pulse can be estimated from the following system of equations:

$$\begin{aligned} T_e\,(\nu^T + \nu_W^T) &= {}^2/_3\, E_{Cu}^*\, \beta\,(T_e)\, n_e^2, \\ \beta\,(T_e)\, n_e^2 &\approx k_1 f, \end{aligned} \tag{1}$$

where ν^T and ν_W^T are the cooling frequencies as a result of the elastic and diffusion mechanisms; E_{Cu}^* is the effective recombination potential of the copper; $\beta(T_e)$ is the impact recombination constant; k_1 is a factor close to unity.
The first equation reflects the heat balance of the electrons in the quasisteady mode, and the second equation compares the pulse repetition frequency and the collision recombination frequency. The use of the second equation is based on the quadratic dependence of the latter on n_e. On substitution of $E_{Cu}^* = 6$ eV, $k_1 = 1.5$, $\nu_W^T = 0$ and the known ν^T, we obtain the prepulse values of n_e^{st} and T_e^{st}:

$$\begin{cases} T_e^{st} = \dfrac{T_a}{2}\left(1 + \sqrt{1 + \dfrac{4\cdot 10^{18}}{n_{Ne}}\dfrac{f}{(10\cdot T_a)^2}}\right); \\ n_e^{st} = \sqrt{1{,}5\cdot 10^9 f/\beta(T_e^{st})}, \end{cases} \tag{2}$$

where f is in kilohertz; T_e, T_a are in electron-volts; n_e, n_{Ne} are in cm^{-3}; β is in cm^6/sec. The accuracy of these formulas was checked out in different modes, and it turned out to be entirely acceptable. The value obtained for T_e^{st} offers the possibility of a rough estimate also of the degree of relaxation of the metastable states.

If the basic cause preventing an increase in the volume of the high pressure LPM is heating the gas, this limits one of the transverse dimensions of the active zone. For a laser with transverse excitation, it is natural to take the electrode width (in our case this is the width of the active zone) as this dimension, from

the point of view of influence of the discharge inductance and cathode drop. Here the electrode gap and the length of the zone can be limited by other effects, for example, the divergence of the radiation. Joint optimization of the initial parameters, including the width of the active zone with respect to the average lasing power from the entire volume is of interest. It is easy to show that for this purpose it is first possible to optimize $X = P\eta/\eta_T$ (P is the specific average lasing power; $\eta = W/W_d$ is the kinetic efficiency; $\eta_T = W_T/W_d$ is the gas heating efficiency; W, W_d, W_T are the specific energy contributions to the useful lasing, to the discharge and heating of the gas, respectively) with a constant active zone width and without consideration of heating, and then to find the optimal width of the active zone considering the latter.

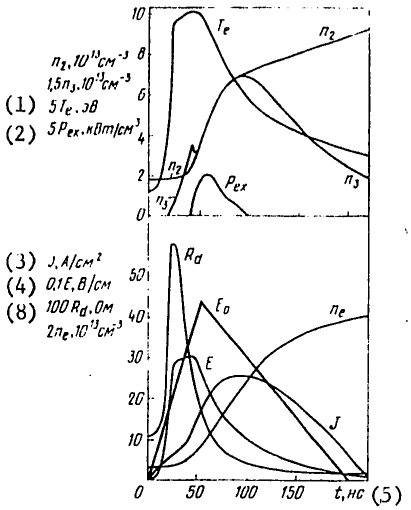

Figure 3. Time characteristics of a pulse mode for E_0 = 0.43 kv/cm, W_0 = 0.65 millijoules/cm^3, n_{Cu} = 2 x 10^{15} cm^{-3}, n_{Ne} = 8 · 10^{18} cm^{-3} and f = 2 kilohertz.

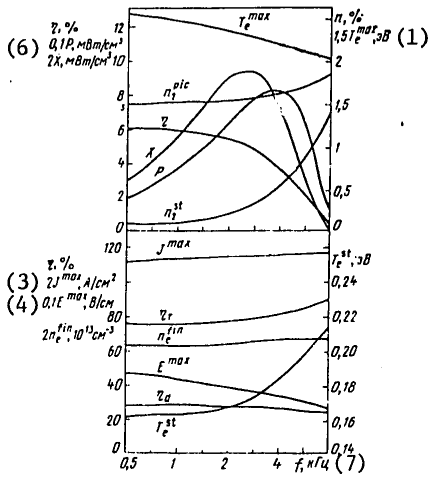

Figure 4. Variation of the repetition frequency f for T_a = 0.16 eV, n_{Ne} = 8 x 10^{18} cm^{-3}, n_{Cu} = 10^{16} cm^{-3}, E_0 = 1 kv/cm and W_0 = 2.2 millijoules/cm^3.

Key to Figures 3 and 4:

1. ... eV
2. ... kilowatts/cm^3
3. ... amps/cm^2
4. ... volts/cm
5. ... nanoseconds
6. ... milliwatts/cm^3
7. ... kilohertz
8. ... ohms

We carried out this optimization using the Gauss-Seidel method for fixed neon concentrations of 4 · 10^{18} and 8 · 10^{18} cm^{-3} and for fixed shape of the pulse described above. The values of n_{Cu}, E_0, f, $R(W_0)$ were optimized with respect to the

maximum X and b with respect to the maximum average power from the entire volume of the active zone. During the process of such optimization the relations not distorted by the heating of the gas were obtained simultaneously for the output, characteristics of the LPM as a function of all of the variable parameters which is of independent interest. Some of them are shown in Figures 4-6. Here the index max corresponds to the maximum of the given parameter during the time of the pulse. The indices st, fin, pic refer to the times of the beginning and end of the pulse mode and the end of the lasing pulse. At the end of the lasing pulse the population of the resonance level is close to its maximum value for the entire calculation period. At this time usually the amplification coefficient is saturated, that is, $n_2 = 1.5\ n_3$. Therefore n^{pic}_2 characterizes the pumping intensity in the given mode, just as n^{st}_2 characterizes the degree of relaxation of the metastable states.

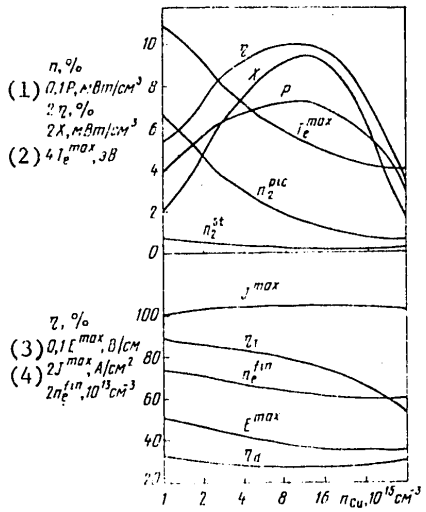

Figure 5. Variation of copper concentration for T_a = 0.16 eV, $n_{Ne} = 8 \cdot 10^{18}$ cm^{-3}, f = 2.5 kilohertz, E_0 = 1 kv/cm and W_0 = 2.2 millijoules/cm^3.

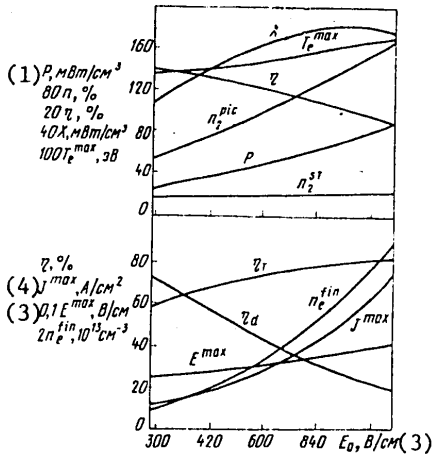

Figure 6. Variation of the voltage of the storage element for T_a = 0.16 eV, n_{Ne} = 8 x 10^{18} cm^{-3}, n_{Cu} = 8 · 10^{15} cm^{-4}, f = 2.5 kilohertz ($W_0 = E_0^2$ millijoules/cm-kv^2).

Key to Figures 5 and 6:

1. ... milliwatts/cm^3
2. ... eV
3. ... volts/cm
4. ... amps/cm^2

From the graph of the output characteristics of the function of the repetition frequency (Figure 4) it is obvious that the pumping efficiency n_{pic}^2 does not diminish with an increase in frequency although T_e^{max} decreases. The drop in the output energy occurs as a result of impairment of the relaxation of metastable states n_2^{st} caused by an increase in the T_e^{st}, where n_2^{st} is the second above the equilibrium

value with respect to T_e^{st}. This can be explained by the fact that for high frequencies T_e does not reach T_a in the relaxation time, and the equilibrium value of n_2 with respect to T_e before the pulse decreases too rapidly. The variation in copper density by comparison with the optimal value (Figure 5) leads to redistribution of the discharge energy in favor of either excitation of the copper metastable states or ionization of the neon by comparison with excitation of the resonance levels. With an increase in E_0 (and W_0, respectively), the efficiency of the energy contribution to the discharge decreases ($\eta_d = W_d/W_0$). In addition, the increase in ionization leads the increase in pumping intensity; therefore slow growth of the output energy is accompanied by a decrease in the kinetic efficiency (Figure 6).

Among the characteristic results of the calculations it is necessary to note the following: the proportion of the copper ions in the total volume of ions to the end of the pulse mode was no less than 70 percent, and on the average, 90-100 percent; 50 to 90 percent of the discharge power went to heating the gas; the electron concentration before the pulse was 10^{12} to 10^{13} cm^{-3}, copper ionization by stages predominated over simple ionization. The kinetic efficiency for sufficiently deep relaxation of the metastable states was quite stable, and it amounted to 3-5 percent. The basic process limiting it obviously is a sharp departure from the resonance level upward with subsequent ionization.

The optimization required performance of calculations of several hundreds of different PPM. The optimal values of the parameters for both neon concentrations ($4 \cdot 10^{18}$ and $8 \cdot 10^{18}$ cm^{-3}) turned out to be similar and amounted to the following: b = 4.5-3.5 cm, $n_{Cu} \approx (0.5\text{-}1) \cdot 10^{16}$ cm^{-3}, $E_0 \approx 1$ kv/cm, $W_0 \approx 2$ millijoules/cm^3, f $\approx$ 2.5 kilohertz. Here the specific average powers reached 36 and 55 milliwatts/cm^3, that is, 160 and 200 milliwatts/cm^3 of the side heat-removing surface under the indicated neon pressures, respectively. It must be noted that the optimal modes obtained are related to the adopted shape of the excitation pulse, and on variation of the latter they can also vary. The preliminary calculations demonstrated that with a decrease in the pulse duration the output characteristics of the LPM can be improved significantly.

We have performed a number of calculations at low neon pressures and for small transverse dimensions of the active zone. The excitation circuit with a cable line or with capacitance discharge was used. It turned out that the relaxation of the metastable states under these conditions is determined as before by the electron temperature relaxation, but the elastic mechanism of cooling of electrons is replaced by diffusion. Therefore the gas temperature has no noticeable effect on the relaxation processes. The output energy in the monopulse mode turned out to be weakly dependent on the neon concentration. Its dependence on the copper concentration had the form of a blunt peak. The optimal copper concentration increased with an increase in the pumping pulse amplitude, reaching 10^{16} to 10^{17} cm^{-3} at E_0 to 10-20 kv/cm.

BIBLIOGRAPHY

1. A. A. Isayev, G. G. Petrash, TRUDY FIAN, No 81, 1975, p 3.

2. V. M. Batenin, P. A. Vokhmin, I. I. Klimovskiy, G. A. Kobzev, TVT, No 14, 1976, p 1316.

3. P. A. Bokhan, V. A. Gerasimov, V. I. Solomonov, V. B. Shcheglov, KVANTOVAYA ELEKTRONIKA, No 5, 1978, p 2162.

4. I. S. Aleksandrov, Yu. A. Babeyko, A. A. Babayev, et al., KVANTOVAYA ELEKTRONIKA, No 2, 1975, p 2077.

5. L. G. D'yachkov, G. A. Kobzev, ZhTF, No 48, 1978, p 2343.

6. S. Trajmar, W. Williams, J. PHYS. B, No 10, 1977, p 3332.

7. S. I. Pavlov, V. I. Rakhovskiy, G. M. Fedorova, ZhETF, No 52, 1967, p 21.

8. I. M. Schrour et al., J. CHEM. PHYS., No 58, 1973, p 5135.

9. E. D. Lozanskiy, O. B. Firsov, "Teoriya iskry" [Spark Theory], Moscow, Atomizdat, 1975.

10. D. W. Trainor, J. CHEM. PHYS., No 64, 1976, p 4131.

11. B. M. Smirnov, "Iony i vozbuzhdennyye atomy v plazme" [Ions and Excited Atoms in a Plasma], Moscow, Atomizdat, 1974.

12. L. A. Vaynshteyn, I. I. Sobel'man, Ye. A. Yukov, "Secheniye vozbuzhdeniya atomov i ionov elektronami" [Excitation Cross Section of Atoms and Ions by Electrons], Moscow, Nauka, 1973.

13. I. S. Aleksakhin et al., ZhPS, No 30, 1979, p 351.

14. V. S. Borozdin, Yu. M. Smirnov, Yu. D. Sharonov, OPTIKA I SPEKTROSKOPIYA, No 43, 1977, p 384.

15. J. MacDaniel, A. Mason, "Podvizhnost' i diffuziya ionov v gazakh" [Ion Mobility and Diffusion in Gases], Moscow, Mir, 1978.

16. V. Ye. Golant, A. P. Zhilinskiy, S. A. Sakharov, "Osnovy fiziki plazmy" [Fundamentals of Plasma Physics], Moscow, Atomizdat, 1977.

10845
CSO: 1862

UDC 533.951

NUMERICAL STUDY OF THE INTERACTION OF LASER RADIATION WITH A TARGET IN A VACUUM CONSIDERING THE SPECTRAL COMPOSITION OF THE RADIATION EMITTED BY THE RESULTANT PLASMA

Moscow KVANTOVAYA ELEKTRONIKA in Russian Vol 7, No 11, Nov 80 pp 2356-2361

[Article by V. I. Bergel'son and I. V. Nemchinov, Earth Physics Institute imeni O. Yu. Shmidt, Moscow; submitted 12 Mar 80]

[Text] Numerical calculations were made of the one-dimensional planar, nonsteady-state radiation gas dynamics problem of the interaction of the radiation pulse of a neodymium laser with an aluminum target in a vacuum. Detailed tables of absorption coefficients of aluminum plasma (containing 10^3 intervals with respect to quantum energies) constructed considering the bound-bound transitions were used. For acceleration of the calculations, the method of averaging the radiation transport equations was used, which permits detailed consideration of the spectral and angular composition of the radiation. The laws of variation of the basic parameters on variation of the laser power are defined. A comparison is made between the obtained results and the results of previously performed calculations of the analogous multigroup problem for absorption coefficients without considering lines. The conclusion of high effectiveness of the radiation of a low-temperature laser plasma reaching tens of percentages of the laser intensity is confirmed. It is demonstrated that the spectra of the radiation emitted by a plasma into a vacuum are characterized by a complex line structure.

In the theoretical studies of the process of the interaction of a laser pulse with a target in a vacuum [1, 2] attention was paid to the fact that under defined conditions the erosion plasma occurring at the target itself radiates intensely in the infrared, visible and especially the ultraviolet sections of the spectrum. The power of the luminescence into a vacuum reaches 30-40 percent of the laser power. The natural thermal radiation of the plasma influences not only the energy balance, but also the nature of variation of the parameters with time (due to deexcitation, the maximum temperature is limited) and in space (in particular, a comparatively cold layer of vapor forms at the target connected with its evaporation

that the disintegration of the plasma layer takes place in practice two-dimensionally. The laser radiation flux density q is constant in time.

In Figure 1a the distributions of the pressure p and temperature T with respect to the mass of the vapor layer at the time t = 6.5 microseconds from the beginning of operation of the laser are presented for q = 50 Mwatts/cm^2 (the maximum pressure 65 bars, maximum temperature 8.5 eV, vapor mass $m_w \approx 0.32$ mg/cm^2), and the variation of the laser radiation flux densities q_l and the natural plasma radiation q_r with respect to mass is also demonstrated. It is possible to note that at the target the plasma radiation absorption is predominant. The radiation losses by the plasma into the vacuum are approximately 15 Mwatts/cm^2, that is, 30 percent of the laser power.

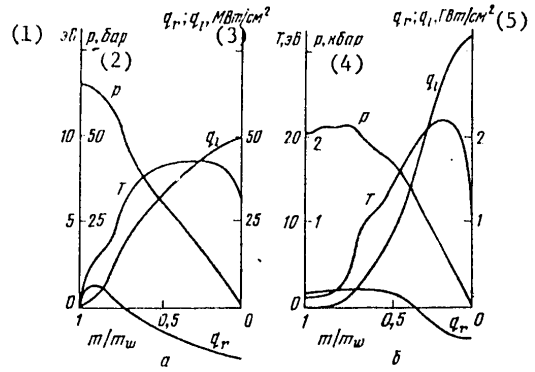

Figure 1

Key: 1. ... eV
2. ... bars
3. ... megawatts/cm^2
4. ... kilobars
5. ... gigawatts/cm^2

If we introduce the distance from the target as the characteristic size of the layer where half of the mass of the vapor is concentrated, for the given point in time this dimension will be 2.5 cm. The picture will be approximately planar for approximately the same radius of the irradiation spot. This corresponds to a quite large value of the supplied energy of 6-7 kilojoules. However, even for small times and, consequently, for small values of the total energy the deexcitation can be significant. For example by time $t \approx 1.5$ μs, when an energy of 75 J/cm^2 is being delivered to a unit of area and the conditions of planar configuration are observed for a spot with radius of 0.6 cm, i. e. the total energy flux is about 85 J, the deexcitation reaches ~10%, i. e. it becomes quite peceptible.

With an increase in q, the plasma temperature increases more rapidly, and the reemission effects are manifested at earlier points in time. In Figure 1b, for q = 3.2 gigawatts/cm^2, the distributions of the parameters with respect to the plasma mass are constructed for t = 27 nanoseconds, when $m_w = 0.041$ mg/cm^2.

under the effect of the radiation fluxes from the hot regions of the plasma). These results were obtained not only by estimates, but also by direct numerical solution of the corresponding one-dimensional (planar) nonstationary radiation gas dynamic problem. However, in these calculations the absorption coefficients were used which take into account only the photo effect from the ground and excited states and the braking absorption, and the absorption and emission in the lines was not considered. In connection with the fact that under such assumptions the radiation spectrum is quite simple, the transport equation was solved in the multigroup approximation. The natural question arose of how a detailed consideration of the spectral composition of the plasma radiation (absorption and emission in lines) will quantitatively influence the energy budget, the plasma parameters and also the development of the phenomenon as a whole, and what the emitted radiation spectrum is? This problem is considered below.

The problem of the interaction of laser radiation with an aluminum target in a vacuum was solved under the conditions of plane geometry of the vapor layer considering the natural radiation. For the calculations tables were used for the spectral absorption coefficients of an aluminum plasma compiled considering not only the free-free and bound-free, but also bound-bound transitions [3]. These tables contain information about the absorption coefficients at 1,000 points with respect to the spectrum arranged nonuniformly in accordance with the nature of variation of the absorption coefficients with respect to frequency, in a wide range of plasma densities and plasma temperatures. All of this information was used in our calculations, and the transport equation was solved for 1,000 spectral intervals.

The method of averaging the radiation transport equations with respect to frequency [4] was used to accelerate the calculations. The essence of this method follows. The solution of the spectral transport equation is found only at defined points in time. For the given temperature and density profile at each calculated point in space, the radiation spectrum is found, and the absorption coefficient average with respect to this "true" spectrum was determined by integration with respect to the frequency. The averaging is carried out within the limits of a small number of quite broad spectral intervals--groups--the number of which in the given case was 8-12, depending on the maximum attainable temperature. In the intervals between averagings, multigroup transport equations averaged over several groups are solved, in which the "true" mean absorption coefficients and mean cosines of the angle between the direction of propagation of the radiation and the direction of motion interpolated in a defined way with respect to space and time, are used. The method turned out to be quite effective: with an increase (by comparison with the multigroup calculation) in the number of intervals with respect to spectrum from 10 to 1,000, that is, by 100 times, the volume of the expended machine time increased by only 4-5 times so that the problem remained solvable on the BESM-6 computer. For the characteristic number of calculation layers with respect to time $\sim 10^4$, 20 to 30 averagings were entirely sufficient.

Let us consider some of the results of calculating the spectral problem. Let the radiation of a neodymium laser (with quantum energy of 1.16 eV) be incident on an aluminum target in a vacuum. The illumination of the target is assumed to be uniform, and the time of the effect and size of the spot are considered to be such

The qualitative picture of the parameter distribution is close to that which is found in Figure 1a for lower flux density. The maximum pressure is much higher than in the preceding example: about 2 kilobars, but still lower than the critical vapor pressure of aluminum (in the sense of van der Waals); therefore the application of the concepts of the evaporation wave with defined phase transition temperature is admissible. The evaporation of the target takes place primarily under the effect of quite hard quanta emitted by the plasma: with energies from 50 to 300 eV. The appearance of such hard radiation arises from the fact that the maximum temperature is about 22 eV. The radiation flux density to the vacuum (350 Mwatts/cm^2) will be about 11 percent of the laser emission flux. Thus, with an increase in the laser radiation intensity by 64 times the time of reaching the relative luminescence (10 percent) was reduced from 1.5 microseconds to 27 nanoseconds, that is, by approximately 50-fold.

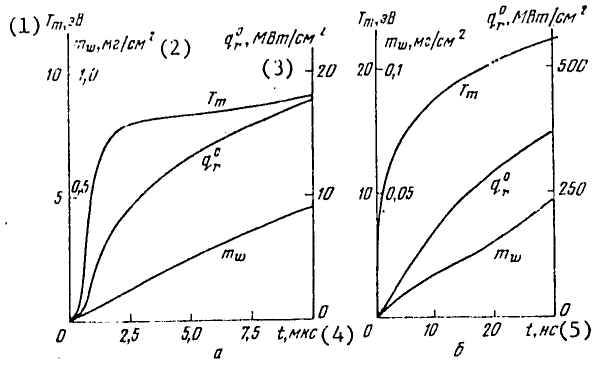

Figure 2

Key: 1. ... eV
2. ... mg/cm^2
3. ... megawatts/cm^2
4. ... microseconds
5. ... nanoseconds

At the time t = 27 nanoseconds the maximum height to which the plasma rises will be a total of only 2 mm. Therefore for observation of the conditions of plane geometry of the disintegration and heating of the plasma a spot diameter of about 5 mm or an area of about 0.2 cm^2 is entirely sufficient. At a specific energy of about 85 J/cm delivered to a unit of area for 27 ns, the total energy will be only about 17 J, i. e., it will be entirely accessible for experiments at the present time. Figure 2 shows the variation with time of the maximum temperature T_m of the plasma, the vapor mass m_w and the flux density q_r^0 of the radiation emitted into the vacuum. In the case of q = 50 Mwatts/cm^2 (Figure 2a), beginning with a time of approximately 3-4 microseconds, the "maximum" temperature limited by the reemission is almost reached. For q = 3.2 Gwatts/cm^2 (Figure 2b) by 30 nanoseconds the deexcitation still has not halted the temperature growth; the magnitude of the flux q_r^0 also increases rapidly. Qualitatively, the nature of variation with time of the basic parameters is the same as in [1, 2] when solving the multigroup problem without considering the lines.

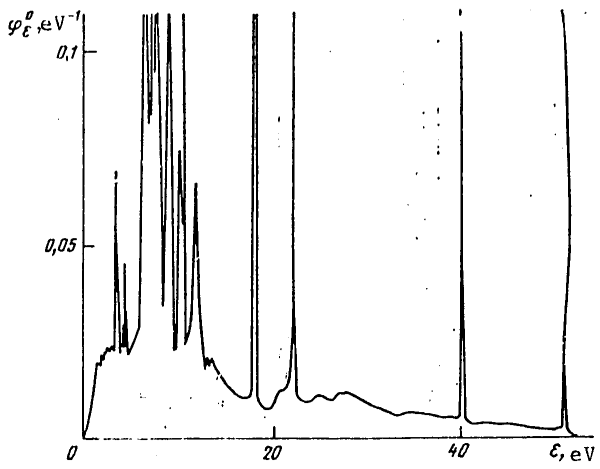

Figure 3

Now let us make a quantitative comparison of the results of solving the spectral and multigroup [2] problems. For q = 50 Mwatts/cm^2 the difference in the deexcitation and the evaporated mass is approximately 20-30 percent. This error caused by the application of multigroup approximation can turn out to be entirely acceptable for approximate calculations not requiring high accuracy. The difference in the maximum temperatures is still less. This type of comparison of the parameters of the multigroup problem without considering the lines and the spectral problem considering the lines was made also for several other versions, for example, for q = 400 MW/cm^2. Such comparisons of separate variants lead us to conclude that lines can be disregarded and the multigroup approximation can be used for estimates of the major parameters in problems of this class with accuracy of 20-30%. While this conclusion is to some extent provisional, it is nevertheless rather important. In reality, the geometry of the phenomenon is not always near one-dimensional (plane, cylindrical or spherically symmetric), i. e. of the type for which difference algorithms have already been worked out and programmed for solving problems with detailed consideration of the spectral and angular makeup of emission. Under conditions of more complicated two-dimensional geometry, it is presently quite difficult to carry out calculations in appreciably unsteady spectral problems. Let us point out that the multigroup approximation using Planck-averaged coefficients with consideration of lines is rigorous only for the case of volumetric deexcitation. However, in our case, such an approach would lead to considerable errors both in the magnitude of deexcitation and in major plasma parameters. Here we have used a less rigorous approach, totally disregarding the lines, and have obtained good results. Thus multigroup methods can be used, although this will require some

caution and a special preliminary analysis, for example, by comparison of the exact solution of the spectral problem and different approximations.

The solution of the spectral problem permits determination of the true spectrum of the plasma radiation along with finding the plasma parameters, which can be important both for different possible applications of the reemission effect and for plasma diagnostics. Figure 3 shows the radiation spectrum for q = 50 Mwatts/cm^2 and t = 6.5 microseconds. As is obvious, it is essentially determined by the broadened and overlapping lines, especially in the vicinity of the maximum of the spectrum occurring in the quantum energy interval of 5-12 eV (or for wavelength of 100-250 nm), that is, the HUV range.

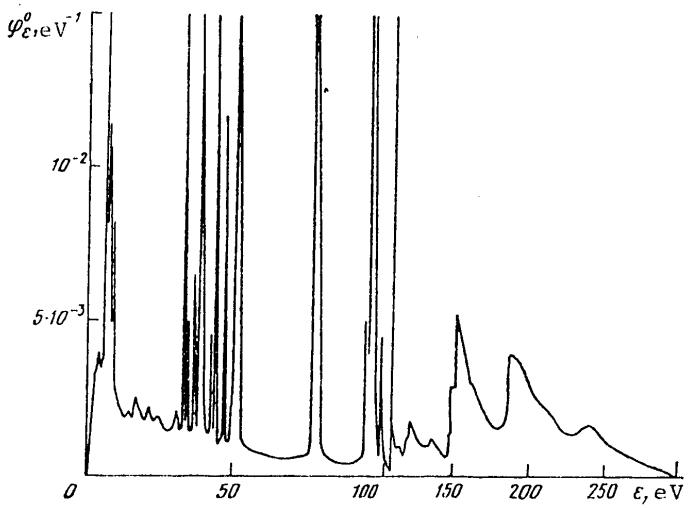

Figure 4

The spectral composition of the radiation emitted into the vacuum at the time t = 27 nanoseconds for q = 3.2 Gwatts/cm^2 is presented in Figure 4. Numerous lines are obvious which are located in several sections of the spectrum (5-10, 35-55, 75-100 eV), obviously connected with the fact that the radiation in these ranges is emitted by layers of plasma heated to various temperatures. The recombination continuums for quanta with energies greater than 100 eV are also clearly observed. The spectrum extends to 300 eV or to wavelength of 4 nm, that is, it reaches the ultrasoft X-radiation region.

Thus, the solution we found for the spectral radiation gas dynamic problem of the interaction of laser radiation with a target in a vacuum confirmed the previously drawn conclusion that the proportion of the energy lost to radiation can be tens of percentages of the laser pulse energy, and it permitted determination of the form of the radiation spectrum.

BIBLIOGRAPHY

1. V. I. Bergel'son, I. V. Nemchinov, "Tezisy dokl. III Vsesoyuz. konf. 'Dinamika izluchayushchego gaza'" [Theses on Papers of the Third All-Union Conference on Dynamics of a Radiating Gas], Moscow, 1977, p 42.

2. V. I. Bergel'son, I. V. Nemchinov, KVANTOVAYA ELEKTRONIKA, No 5, 1978, p 2123.

3. V. P. Buzdin, A. V. Dobkin, I. B. Kosarev, "Absorption Coefficients, Spectral and Integral Characteristics of Aluminum Plasma Radiation in the Temperature Range of 8-240 kK and Relative Densities of $3.16 \cdot 10^{-3}$ to 100," deposited at the VINITI, No 370-79 Dep., 1979.

4. I. V. Nemchinov, ZHURN. PRIKL. MEKH. I MATEMATIKI, No 34, 1970, p 706.

10845
CSO: 1862

UDC 621.375.826+533.6.011

CO_2 GAS DYNAMIC LASER UTILIZING CO-CONTAINING MIXTURES

Moscow KVANTOVAYA ELEKTRONIKA in Russian Vol 7, No 11, Nov 80 pp 2385-2392

[Article by P. V. Belkov, V. V. Val'ko, A. S. D'yakov, N. N. Ostroukhov and B. K. Tkachenko, Moscow Physicotechnical Institute; submitted 25 Mar 80]

[Text] A study was made of a CO_2 gas dynamic laser utilizing mixtures of nitrogen and carbon monoxide as a vibrational energy reservoir. The CO_2 was injected into the main flow in the cross section with Mach number M = 2.5-3. It was established that for significant amounts of carbon monoxide the inverse characteristics depend more on the injection point than in the case of pure nitrogen. With optimal choice of the injection point the total replacement of the nitrogen by carbon dioxide no more than cuts the gain in half, which is appreciably better than the published experimental results. A specific energy output of 15 joules/g is achieved in this lasing mode with a vibrational energy reserve of 42 joules/g without considering the CO_2 flow rate.

1. Introduction

The study of a CO_2 gas dynamic laser with mixing performed in [1-3] demonstrated that this system of creating an inverse population has a number of advantages over the ordinary gas dynamic lasers (GDL). The absence of active molecules in the receiver permits the gas to be heated to higher temperatures without fear of CO_2 dissociation and also avoidance of the energy losses as a result of relaxation in the region of the critical cross section of the nozzle. The practical realization of the given system is connected with selection of an appropriate method of heating the gas, primarily nitrogen, to a temperature of 3 kK. It appears convenient to use fuel, the combustion products of which could play a role analogous to nitrogen. The nitrogen can be replaced by carbon monoxide. However, the efficiency of the GDL decreases. This has been demonstrated in [4]. On the other hand, there are a number of fuels, the combustion products of which basically contain N_2 and CO with a temperature to 3 kK. Therefore the study of the characteristics of CO_2-GDL with mixing where nitrogen is used in a mixture with carbon monoxide as the pumping gas, is of interest.

[5-7] report some of the results of studying CO_2-GDL with mixing where the nitrogen is either partially or completely replaced by carbon monoxide. The data from [5] indicate that 50-100-percent replacement of the nitrogen by carbon monoxide leads to twofold to fivefold reduction in the gain, respectively. These results are explained by lower effective energy exchange rate between the $CO^*(v)$ and $CO_2(v_3)$ by comparison with N_2 and also the higher VT relaxation rate of CO. The partial dissociation of the CO which the authors of [5] considered to be a possible cause of a decrease in gain on replacement of the N_2 by CO, does not, in our opinion, play a role. If this assumption were satisfied, then with an increase in temperature in the receiver the losses would increase and lead to a reduction in gain. However, according to the results of [5] this was not observed. The results obtained in [6] where on injection of CO_2 into the combustion products of the nitro compound the gain reached 2.6 percent/cm and also the results of [7] permit an optimistic attitude toward the problem of replacing nitrogen by carbon monoxide. In both of these papers the injection and mixing of the CO_2 with the main flow were realized not in the critical cross section, but in the cross section with Mach number M > 1. Therefore, in our opinion, the choice of the point of injection of the CO_2 acquires great significance in improving the characteristics of the CO_2-GDL utilizing CO-N_2 mixture. In the given paper a report is presented on the results of the numerical analysis and experiments confirming the possibility of the effective use of the products of fuels containing carbon monoxide in CO_2-GDL with mixing.

2. Numerical Analysis

The scheme for analysis of the relaxation processes occurring in a supersonic flow is analogous to that used in [4]. The variations pertained only to the probabilities for the relaxation processes

$$CO\ (1)+CO_2\ (00^00)\rightleftarrows CO\ (0)+CO_2\ (00^01)+\Delta E; \quad (1)$$

$$N_2\ (1)+CO_2(00^00)\rightleftarrows N_2\ (0)+CO_2\ (00^01)+\Delta E. \quad (2)$$

In accordance with the results of [8] the probabilities for the processes (1), (2) were calculated by the process rate constants given by the expression

$$K=\sum_{n=0}^{5} A_n\,(T/T_0)^n,$$

where T_0 = 300 K, and A_n are presented in the table.

The relations found in the temperature range of 300-800 K were extrapolated to T = 1.1 kK.

Consideration of the variation of the gas dynamic parameters in the scheme with mixing in the supersonic flow is a highly complex problem. For small relative flow rates of the injected gas, judging by the measurements of the gain [11], satisfactory agreement of the parameters averaged with respect to cross section with those calculated by the model of instantaneous mixing in the injection cross section occurs. In accordance with this uniform model under the conditions of the

performed experiments on injection of more than 30-40 percent of the CO_2 blocking of the flow should occur, that is, conversion of it to subsonic. However, smooth variation of the gain was observed experimentally without conversion to absorption for injections exceeding the flow rate of the hot gas by 3-4 times. Here the optimal ratio of the mass flow rates was close to unity.

An analysis of the gain measurements (no other diagnosis of the flow was performed in the given experiment) demonstrated that satisfactory agreement of the measured and calculated values in the case of high injections is obtained in the roughest approximation, that is, where variation of the gas dynamic parameters during injection does not occur, and the processes of vibrational relaxation connected with the CO_2 begin in the injection cross section. This scheme was also selected for calculating the inverse characteristics.

Figure 1 shows the results of calculating the gain in the cross section with M = 5 as a function of the Mach number in the CO_2 injection cross section for three compositions of the mixture in the receiver. On injection of the CO_2 into a pure nitrogen flow with M = 1, the calculation gives 1.3 percent/cm for the gain. With an increase in the Mach number, an insignificant increase in the gain is observed. This growth is caused by a decrease in the intensity of the VT relaxation processes as a result of transfer of the mixing zone to the flow region with lower translational temperature. For the mixture N_2:CO = 1:1 and pure carbon monoxide the calculated value of the gain on injection of the CO_2 in the critical cross section (M = 1) is 2-3 times less. This result compares qualitatively with the data of [5] and can be explained by an increase in the intensity of the relaxation processes as a result of the presence of carbon monoxide in the main flow. On displacement of the injection coordinates from the critical cross section downstream (M > 1) the calculation predicts a more significant increase in the gain for mixtures with carbon monoxide than for pure nitrogen. The difference between the results for pure nitrogen and carbon monoxide is reduced, and for the optimal case (M = 2.5) the results do not differ by more than a third. This behavior of the gain as a function of the Mach number of the main flow is explained by the following facts.

Mixture	A_0	A_1	A_2	A_3	A_4	A_5
CO_2—N_2	61,786	−111,052	96,254	−41,997	9,188	−0,793
CO_2—CO	16,735	−41,768	53,481	−31,692	8,997	−0,961

The shifting of the injection point downstream means transfer of the entire zone of mixing of the injected CO_2 to the region of lower pressures and translational temperatures, that is, to the region where the velocities of all of the relaxation processes decrease. It must be noted that the rate constant for the VV exchange between N_2 and CO_2 increases with a decrease in temperature, but this increase does not compensate for the decrease in the VV exchange rate as the result of a decrease in pressure. Decreasing the relaxation process rate on the one hand retards the transmission rate of the vibrational energy from N_2 and CO to CO_2, and on the other hand, it decreases the relaxation losses as the result of the VT processes.

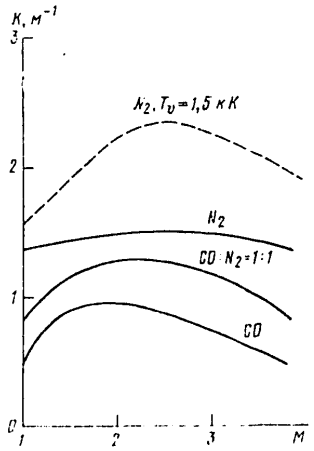

Figure 1. Gain as a function of M of the main flow in the injection cross section T_0 = 1.5 kK, p_0 = 4 atm.

The calculation shows that for all the investigated mixtures the exchange rate is quite high for excitation of all of the injected CO_2 in the measurement cross section on transfer of the injection to the cross section with M = 3. This conclusion agrees well with the results of [11] where for the investigated nozzle even on injection in the cross section with M = 3.5 the excitation efficiency was no less than 0.7-0.9. Therefore all the variations of the gain on variation of the injection point must be explained by variation of the relaxation losses connected with the VT processes. In the mixtures based on nitrogen, the relaxation losses are low, and the gain on transfer of the injection downstream increases insignificantly. In the presence of CO, the losses become significant; therefore decreasing them on transfer of the injection leads to a greater increase in the gain. Thus, the performed analysis predicted the increase in the efficiency of the CO_2-GDL with mixing in CO-N_2 with an increase in the Mach number of the main flow in the injection cross section to M = 2.5-3. The results of this analysis were used to perform the experimental study.

3. Experimental Setup

The diagram of the experimental setup is indicated in Figure 2. The setup consists of the gas heating chamber, nozzle unit and the systems for supplying the components, CO_2 injection and measurements. The heated mixture of gases consisting of CO and N_2 was obtained by two methods. In the first method the mixture was formed by the combustion products of the nitro compounds; in this case the combustion chamber analogous to that described in [6] was used.

For the second procedure, the previously prepared mixture was heated by electric discharge of the capacitor bank. Here the chamber was a steel cylindrical tube, the inside surface of which (d = 50 mm) was covered with ceramic. For initiation of the discharge between the ends of the chamber, nichrome wire 0.09 mm in diameter was installed. In the preliminary experiments it was established that for

discharge in a blind chamber the initial pressure of the mixture in which was 1 atm, the increment of the internal energy of the gas was ~50 percent of the energy stored in the capacitors. This result coincides with the data of [9].

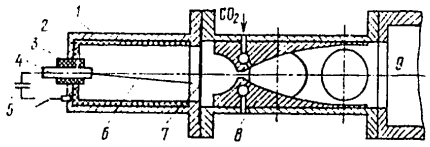

Figure 2. Diagram of the experimental setup: 1--housing; 2, 3--insulators; 4--electrode; 5--capacitor; 6--wire; 7--diaphragm; 8--nozzle; 9--vacuum tank.

In this paper a plane-shaped nozzle 200 mm wide was used. In the sidewalls of the nozzle there were openings for installing windows and mirrors. In the experiments with the nitro compounds the height of the critical cross section was 0.3 mm; in all of the rest it was 0.6 mm. The gain was measured in the cross section with M = 5.0.

The CO_2 was injected through a series of openings 1.0 mm in diameter drilled at spacings of 10 mm from each other along the normal to the generatrix of the nozzle. The rows of holes on the opposite sides of the nozzle were shifted by 5 mm relative to each other.

The system for measuring the gain was analogous to that used in [4, 11]. To investigate stimulated emission, two types of resonators were used: single-pass and triple-pass. The single-pass was mounted in the same cross section as the gain was measured. One optical axis of the three-pass resonator was located in the cross section where the gain was measured and a second, 7 cm downstream. All of the blind mirrors of the resonators were copper, bent with a radius of curvature of 1.5 m and a reflection coefficient no worse than 0.97. The yield of the radiation from the single-pass resonator was realized through an opening 2 mm in diameter in the mirror which was also copper. Here the hole was covered with an NaCl plate. For removal of the radiation from the triple-pass resonator, a germanium mirror was used, the surface of which, turned inward, was coated with aluminum with the exception of the central zone 10 mm in diameter. The lasing pulse energy was measured by the IMO-2 device.

The working mixtures were prepared in a 2-liter tank 24 hours before the experiments. After feeding the mixture to the chamber the CO_2 injection valve was opened, then the voltage was fed to the chamber electrodes. In all of the experiments the pressure in the chamber was measured by the LKh-412 gauge. Typical oscillograms for amplification, lasing and pressure are shown in Figure 3.

4. Gain as a Function of Injection Point

It was calculated that the injection coordinate essentially influences the degree of excitation and the magnitude of the gain. The process of cross injection of the cold gas into the supersonic flow is accompanied by flow deceleration and,

consequently, an increase in its temperature and density in the mixing zone. The degree of variation of the parameters is basically determined by the amount of injected gas and the injection coordinate. On the other hand, the presence in the mixture of carbon dioxide increases the relaxation losses, the intensity of which is directly connected with the amount of CO_2 in the flow. Therefore a study was made of the gain as a function of the amount of injected gas and the Mach number of the flow in the injection cross section. The results were obtained when working with the nitro compound combustion products. In these experiments the temperature of the mixture reached 2.6 kK, and the pressure reached 6 atm. The composition of the combustion products (the composition of the main flow) was the following: 40 percent CO, 37.5 percent N_2, 15 percent H_2, 6.5 percent H_2O, and 1 percent CO_2.

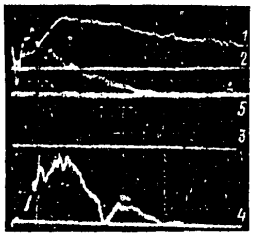

Figure 3. Oscillograms of amplification, lasing and pressure in the chamber: 1--signal of the probe laser with gain; 2--signal of the probe laser without gain; 3--zero level of the probe laser signal; 4--lasing; 5--pressure.

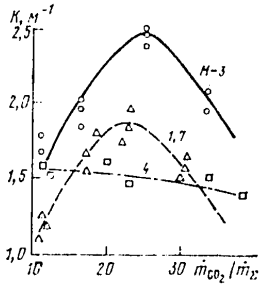

Figure 4. Gain as a function of the flow rate of the injected CO_2 when working with nitro compounds.

The results of the experiments are presented in Figure 4. They qualitatively confirm the presence of the optimum of the gain with respect to the injection point although the experiments were performed for conditions differing from those for which the calculation was made. The maximum gain is achieved for injection in the cross section with M = 3.

5. Replacement of Nitrogen With Carbon Monoxide

The study of the effect of the replacement of N_2 by CO was made for fixed values of the parameters of the mixture in the receiver. The heating was realized by electric discharge. The stagnation temperature of the main flow I_0 was equal to 1.5 kK, the pressure p_0 = 4 atm, and the water concentration in the mixture X_{H_2O} = 0.01. The CO_2 injection was to the cross section of the main flow with M = 2.5. The gain was measured in the plane 30 mm from the critical cross section where M = 5. The results of the experiment and the numerical analysis of the gain as a function of the amount of injected gas are presented in Figure 5.

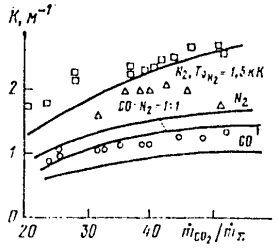

Figure 5. The same as Figure 4 on replacement of N_2 by CO (see the text).

Attention is attracted by the fact that for qualitative comparison of the calculation with the experimental data the calculated curve for N_2 lies below the experimental points, whereas in accordance with the selected theoretical analysis system in the Lorentz region of broadening of the lines the calculation should give the upper bound of the gain. The cause for this divergence between the calculation and the experimental data can be the fact that the gas heated by electric discharge is thermally nonuniform. The occurrence and existence of such nonuniformity connected with sharp variation of the plasma parameters during electric arc heating of the nitrogen was indicated in [10]. The measurements made in [10] demonstrated that with this method of heating the nitrogen, an excess of the vibrational temperature over the translational temperature by 1-3 kK is possible. We made a correction to the gain calculation considering the possible nonuniformity. Under the assumption that in the discharge the vibrational temperature reaches 4.5 kK, and the time of beginning of recording of the gain lags behind the end of discharge by 3 milliseconds, the excess of the vibrational temperature over the translational was estimated. This difference (not exceeding 150 K) was taken into account on giving the initial conditions for the calculation. The results of the calculation performed under these conditions demonstrate quantitative agreement with the experimental data.

6. Effect of Hydrogen and Water Vapor

The products of combustion of the fuels can contain a significant amount of H_2 and H_2O. The problem arises of the effect of these additives on the laser characteristics. The study of the effect was made for the flow consisting of CO, H_2O, H_2 and N_2. The results are presented in Figure 6. Let us note the increase in gain with an increase in hydrogen concentration from 0 to 5 percent for mixtures based

on CO. In the experiments with nitrogen no noticeable variation of the gain was recorded. It is also necessary to note the quite large gain of 1 percent/cm for the investigated mixtures containing a significant (to 12 percent) amount of water vapor.

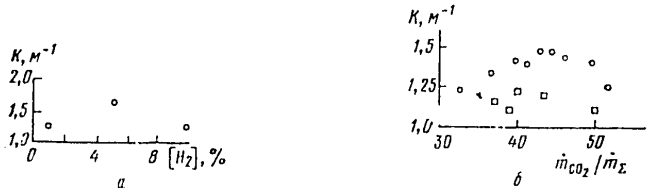

Figure 6. Effect of H_2 and H_2O admixtures on the gain: mixtures of $CO:N_2:H_2O$ = 97:2:1 (a), $CO:N_2$ = 1:1 in the presence of 5-percent H_2 and 3 percent H_2O (b, o), 2.4 percent H_2 and 12.2 percent H_2O (b, □).

7. Gain Profile With Respect to the Nozzle Cross Section

In all of the investigated experiments the gain was measured on the nozzle axis which, as was noted in [11], does not give a complete idea about the inverse characteristics of the flow. Accordingly, for two mixtures with relative flow rate of the injected CO_2 ~ 40 percent, experiments were performed to determine the gain profile with respect to the nozzle cross section. The results are presented in Figure 7.

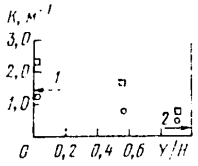

Figure 7. Gain profile with respect to the nozzle cross section: o--mixture 97 percent CO + 2 percent N_2 + 1 percent H_2O; □--mixture 99 percent N_2 + 1 percent H_2O; the arrows indicate the plane of symmetry of the nozzle (1) and the nozzle wall (2).

The basic reasons causing nonuniformity of the gain with respect to cross section are the following: nonuniformity of the main flow in the nozzle, nonuniformity of the concentration of the injected CO_2 and the effect of the turbulent boundary layer, the significant influence of which was noted in [7].

It is obvious that the nonuniformity of the gain with respect to the nozzle cross section is a deficiency of the investigated CO_2-GDL system. However, this nonuniformity can be decreased by taking special measures. In particular, the concentration profile can be equalized by varying the injection angle, arranging injection through two rows of holes or a combination of these procedures. It is necessary also to note the fact that even for very high (>50 percent) concentration of the injected CO_2 in the central zone of the flow the gain retains a high value, which indicates smallness of the relaxation losses for such CO_2 concentrations.

8. Lasing Power and Power Output

Lasing was observed both for a single-pass resonator and a triple-pass resonator. On measurement of the energy of the laser pulse the entrance opening of the measuring head of the IMO-2 was butted against the exit mirror of the resonator. Since the reproducibility of the results in the series of experiments was good, simultaneous recording of the energy and the shape of the pulse was not used in the experiment. The shape of the lasing pulse was recorded in individual experiments by the method of photoreceiver recording of the laser pulse scattered by powdered metal. The transmission coefficient of the germanium mirror was 40 percent. An energy of 2.2 joules was recorded for operation with a mixture of 99 percent N_2 + 1 percent H_2O and a relative mass CO_2 flow rate of 40 percent. The lasing pulse had a duration of 12.1 milliseconds and a shape close to triangular. The maximum power corresponded to the conditions for which the maximum gain was observed; in this case the flow rate of the basic mixture was 24 g/sec. Thus, the specific power output at the time of reaching the maximum power is 15 joules per gram of basic flow. The specific energy stored in the nitrogen before the mixing zone was estimated by the calculated vibrational temperature and considering the quantum efficiency it was E_{eff} = 42 joules/g.

For a mixture of 97 percent CO + 2 percent N_2 + 1 percent H_2O the lasing pulse energy did not exceed 0.74 joule, that is, it was three times less than for the mixture based on nitrogen. Since the experimental conditions were the same, the stored energy was estimated at 19 joules/g; this sharp decrease in the power output, in our opinion, was connected with a decrease in the value of K_0L (L is the resonator length) determining the effectiveness of the resonator. It can be expected that with an increase in the length, the power output from such mixtures will be increased.

When working with nitro compounds, in the combustion products of which, as was indicated, there is up to 40 percent CO, a power of 0.98 kilowatt was reached, which corresponds to a specific energy output of 42 joules per gram of main flow. This value is only insignificantly inferior to the results of [12] obtained for nitrogen-based mixtures; E_{eff} was ~100 joules/g in these experiments.

9. Conclusion

The results obtained in this paper prove the possibility of effective operation of CO_2-GDL with mixing utilizing mixtures containing carbon monoxide. The performed numerical analysis demonstrated that when working with mixtures based on carbon monoxide the optimal laser characteristics are reached on injection of CO_2 in the flow cross section with M = 2.5. The performed experiments confirmed the correctness of this conclusion and proved high effectiveness of mixtures with carbon monoxide. For a mixture of 40 percent CO + 37 percent N_2 + 15 percent H_2 + 1 percent CO_2 + 6.5 percent H_2O for T_0 = 2.6 kK and p_0 = 6 atm, a gain of 2.6 percent/cm and specific energy output of 42 joules/g were achieved for a stored power of ~100 joules/g. The high inverse characteristics are maintained with a significant content of H_2 (to 10 percent) and water vapor (to 12 percent) in the basic mixture. The high effectiveness of the vibrational excitation of CO_2 is maintained for high relative injections of it. The application of the electric arc method of heating

the nitrogen possibly will lead to additional improvement of the characteristics as a result of the creation of vibrational nonuniformity in the gas mixture.

BIBLIOGRAPHY

1. V. N. Kroshko, R. I. Soloukhin, DAN SSSR, No 211, 1973, p 829.

2. V. N. Kroshko, R. I. Soloukhin, N. A. Fomin, FIZIKA GORENIYA I VZRYVA, No 10, 1974, p 473.

3. J.-P. E. Taran, M. Charpenel, B. Borghi, AIAA Paper No 73-662, 1973.

4. A. S. D'yakov, A. K. Piskunov, Ye. N. Cherkasov, KVANTOVAYA ELEKTRONIKA, No 2, 1975, p 1419.

5. R. Baily, M. Pelat, J.-P. E. Taran, REVUE DE PHYSIQUE APPLIQUEE, No 12, 1977, p 1705.

6. A. S. D'yakov, A. I. Didyukov, B. K. Tkachenko, Ye. M. Cherkasov, KVANTOVAYA ELEKTRONIKA, No 5, 1978, p 1166.

7. P. Cassady, J. Newton, P. Rose, AIAA J., No 16, 1978, p 305.

8. A. I. Vargin, V. V. Gogokhiya, V. K. Konyukhov, A. M. Pasynkova, KVANTOVAYA ELEKTRONIKA, No 3, 1976, p 216.

9. A. I. Odintsov, A. I. Fedoseyev, D. G. Bakanov, PIS'MA V ZhTF, No 2, 1976, p 145.

10. B. V. Abakumov, Yu. V. Kurochkin, A. V. Pustogarov, N. N. Smagin, B. A. Tikhonov, V. V. Ukolov, KVANTOVAYA ELEKTRONIKA, No 6, 1979, p 1903.

11. N. N. Ostroukhov, B. K. Tkachenko, KVANTOVAYA ELEKTRONIKA, No 5, 1978, p 924.

12. B. A. Vyskubenko, Ye. T. Demenyuk, G. A. Kirillov, Yu. V. Kolobyanin, S. B. Kormer, N. A. Nitochkin, DAN SSSR, No 248, 1979, p 81.

10845
CSO: 1862

UDC 535.417.2

CHARACTERISTICS OF UNSTABLE RESONATORS WITH FIELD DISTORTIONS IN THEIR ELEMENTS. I. CYLINDRICAL MIRRORS

Moscow KVANTOVAYA ELEKTRONIKA in Russian Vol 7, No 11, Nov 80 pp 2416-2421

[Article by S. B. Bunkin and Yu. B. Konev, High Temperatures Institute of the USSR Academy of Sciences, Moscow; submitted 7 Apr 80]

[Text] By numerical solution of the integral equations of an unstable confocal resonator with cylindrical mirrors by the method of fast Fourier transformations, a study was made of the effect of the field distortions in the resonator elements on its characteristics. The field distortions characteristic of the operation of the resonator filled with a high-speed flow of active medium were considered: asymmetric distortion of the mirror surface simulating thermal deformation and small-scale random phase nonuniformities of the active medium. Lasing in the supersonic flow of mixtures of carbon dioxide, nitrogen and water vapor was calculated for various gains.

Unstable resonators are of practical interest for the generation of high-power, bright light [1, 2]. Their properties have been the subject of intense research by both analytical and numerical methods. It is most important to study how the disturbances of various types influence the operation of the resonator. In the cases of practical importance this study must be performed by numerical methods. For this purpose, approximation of the geometric optics [3], numerical solution of the parabolic wave equations [4, 5] and calculations using the Fresnel-Kirchhoff integrals were used (see, for example, [6-8]). Now the effects of the misalignment of the resonator [9, 10], nonuniformity of the wedge or lens type [2], and small-scale periodic nonuniformities [11] have been well investigated. The main advantage of the numerical methods is the fact that they permit investigation of the effect of arbitrary specific disturbances of the resonator, it is true, at the price of very labor-consuming and prolonged calculations and frequently to the loss of generality of the results. Only a few papers are known which study the characteristics of resonators filled with a nonuniform medium or with deformed mirrors. In this paper numerical methods were used to investigate the distribution of the intensity and phase of the field at the output mirror and the intensity distribution in the far zone of the confocal resonator with this type of distortions, the mirrors of which have cylindrical shape.

The calculations were performed using the fast Fourier transformation algorithm for the solution of the integral equations of the resonator in the Fresnel-Kirchhoff approximation. It has been proposed that the concave mirror of the resonator is so large that its edges have no influence on the field distribution, and the nonuniform medium is concentrated in the thin layers near the mirror surface [7, 8]. These layers are, therefore, the phase-amplitude shields with complex characteristic

$$\Phi(x)=2\pi w(x)+i(g(x)-\beta)/2, \tag{1}$$

where w(x) are the phase nonuniformities measured in wavelengths, positive with an increase in the optical path between the mirrors; g(x) and β are the gains and losses; all of the values correspond to passage through the layer in one direction. Then the relation between the complex amplitudes of the waves $E_n^+(x)$ and $E_n^-(x)$ propagated to the convex and concave mirrors will have the following form on the n-th passage through the resonator:

$$E_n^{(+)}(\xi)=\sqrt{iN}\int_{-1/M}^{1/M}d\xi_1 E_n^-(\xi_1)\exp\left[-i\pi N(\xi-\xi_1)^2\right]\times \tag{2}$$
$$\times\exp[-i\Phi_1(\xi_1)-i\Phi_2(\xi)];$$

$$E_n(\xi)=\sqrt{iN}\int_{-\infty}^{\infty}d\xi_1 E_{n-1}^+(\xi_1)\exp\left[-i\pi NM(\xi_1-\xi/M)^2\right]\times \tag{3}$$
$$\times\exp[-i\Phi_1(\xi)-i\Phi_2(\xi_1)],$$

where ξ = x/a (a is the half-width of the region occupied by the field on the concave mirror in the geometric approximation); L is the spacing between mirrors; M is the magnification; $N = a^2/(\lambda L)$ is the Fresnel number; the phase is reckoned from the surface of equal phase of the corresponding waves in the undisturbed resonator in the geometric approximation; the subscripts 1, 2 correspond to layers near the convex and concave mirrors. Initially uniform distribution of the complex amplitude on one of the mirrors was given. Then after each complete passage through the resonator in the linear mode, the field amplitude distribution was normalized on the mirror so that $|E_n|_{max} = 1$; iterations were continued until the complex amplitude distribution after the following iteration agreed with the preceding one with the given accuracy. Normalization was not done for lasing.

In cases where the active medium is prepared in advance, and then travels across the resonator at high speed, the radiation intensity distribution turns out to be nonuniform and is concentrated in the upstream half of the resonator (see, for example, [5-7]). Under these conditions the thermal swelling of the mirror surface will also take place more sharply in this half. The complete solution of the problem of the effect of thermal deformations on the operation of the resonator is very complicated. Therefore it is of interest to give the distribution w(x) which on the average resembles the thermal deformation and to see how the intensity and phase distribution on the exit mirror of the resonator and the field pattern in the far zone vary.

Figure 1a indicates the corresponding distributions for the undisturbed resonator with Fresnel number N = 30 and M = 1.5. The two upper curves are the intensity and phase at the exit mirror and the third is the intensity in the far zone. The intensity distributions are normalized so that the maximum values will be 1. Figure 1b indicates analogous data for the resonator, the exit mirror of which has additional convexity

$$w(x) = -^{27}/_{32}\, w_m\ (1-(Mx/a)^2)(1+Mx/a)$$

with the maximum $w_m = 0.1$ for $x_m = a/(3M)$. In this case the tendency toward an increase in the field is noted in the half of the resonator where the convexity of the mirror is less. The maximum radiation in the far zone is shifted in the same direction. These circumstances may relax somewhat the nonuniformity of the intensity distribution caused by the active medium. Such calculations have demonstrated that with an increase in w_m the trend toward the field concentration is intensified, and phase variation with respect to the exit mirror exceeds 3π for $w_m > 0.3$. As a result the divergence of the radiation becomes sharply worse.

When using the high-speed gas flows as the active medium, small-scale nonuniformities are possible. Their effect on the operation of the resonator has been very slightly studied. In the example of periodic nonuniformities [11] it was demonstrated that very weak nonuniformities with a phase lead not exceeding several hundredths of a wavelength can already noticeably change the resonator properties. In [12] the point of view was stated that as a result of the small-scale nonuniformities in the far zone, the diffraction pattern characteristic of the unstable resonators will be located on the diffuse background. We performed a number of calculations in which the value w(x) at the nodes of the grid, the spacing of which was such that there were 64 nodes per mirror, were given in the form of uncorrelated random numbers distributed according to a normal law with zero mean value and dispersion σ. Figure 2 shows examples of the field distributions for the resonator with the parameters N = 30, M = 1.5. In the case of $\sigma = 0.01$ all of the distributions are close to those which are depicted in Figure 1a for the undisturbed resonator. For $\sigma = 0.03$ the intensity at the exit mirror differs significantly from that which occurred in the undisturbed resonator. Apparently, for the given realization w(x) a local stable resonator was formed near the optical axis. Such cases were noted in [11] with periodic nonuniformity. In the far zone, a noticeable diffuse background appeared. Increasing σ to 0.1 leads to a sharp broadening of the radiation pattern which acquires the nature of individual random diffraction peaks on a broad diffuse background.

For calculation of lasing in the active medium of a high-speed flow of carbon dioxide, nitrogen and water vapor mixture, the kinetic equations for the level populations presented in [13] were used. The rate constants of the relaxation processes with participation of the carbon dioxide and nitrogen molecules are presented there. The relaxation rate constants of the levels (00^01) and (01^10) of carbon dioxide for collisions with water molecules are taken from [14, 15]. The calculations were performed for a mixture of $CO_2:N_2:H_2O = 0.1:0.86:0.04$ at a pressure p = 0.04 atm, a temperature T = 280 K, and a velocity u = 1,750 m/sec. The vibrational temperatures of the deformation and antisymmetric types of vibrations of carbon dioxide T_2 = 320 K, T_3 = 1,400 K and nitrogen T_4 = 1,400 K were given at

the input to the resonator. These conditions are characteristic of the second-generation gas dynamic lasers.

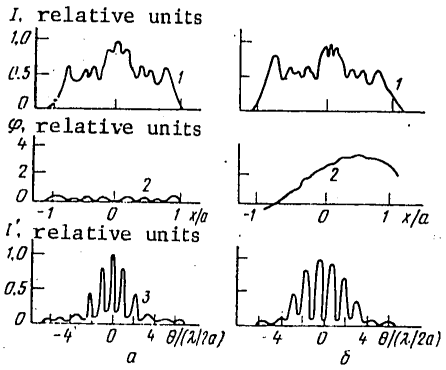

Figure 1. Intensity distribution (1, 3) and phase distribution (2) on the exit mirror of the resonator (1, 2) and in the far zone (3) for N = 30 and M = 1.5 (see the text).

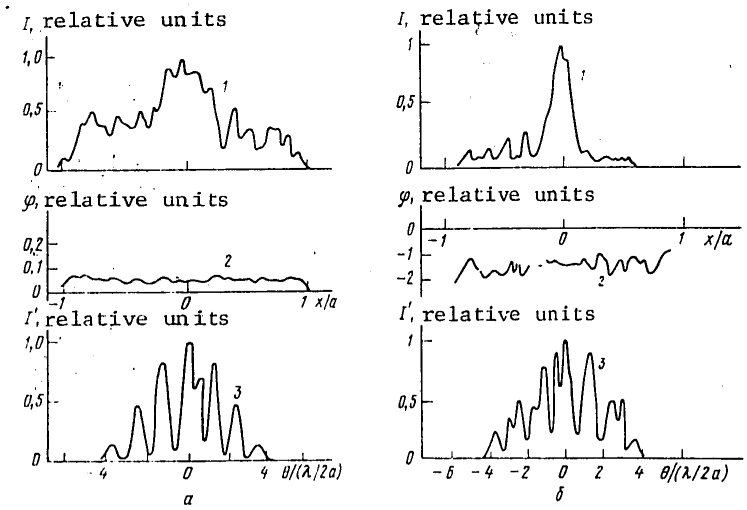

Figure 2. The same as Figure 1 for σ = 0.01 (a), 0.03 (b).

In Figure 3 it is possible to see the field distributions in the plane of the exit mirror and in the far zone. The field concentration in the upstream half of the resonator is appreciably more strongly expressed for small magnification. In the same case the departure of the intensity in the far zone from the direction of the optical axis of the resonator noted earlier is highly noticeable [4]. As the magnification increases, this effect in practice completely disappears, and the radiation pattern becomes noticeably more narrow.

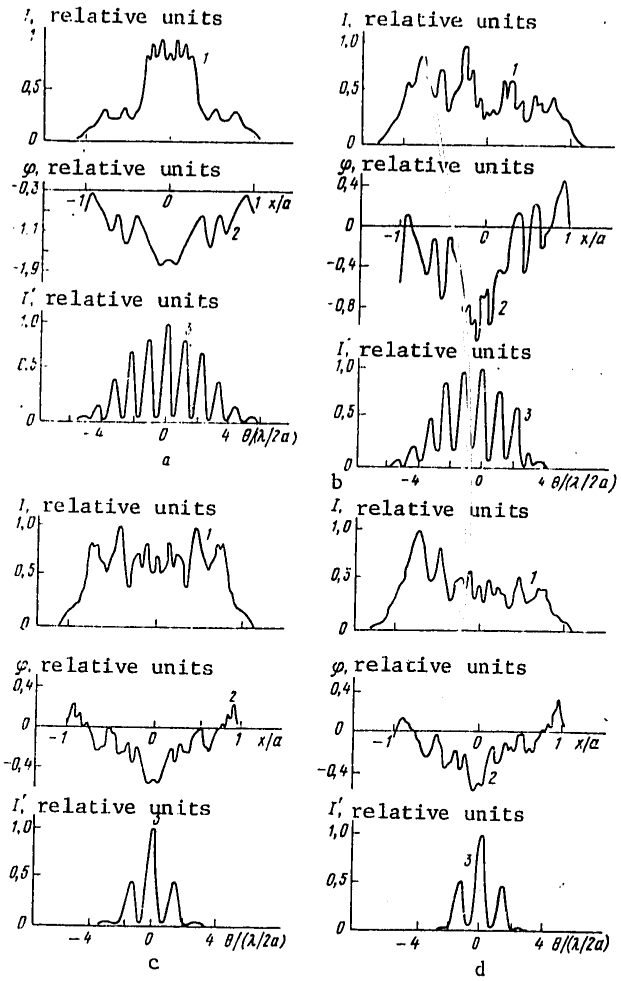

Figure 3. Field distributions in an undisturbed resonator (a, c) and in the lasing mode (b, d) for N = 30, M = 1.3 (a, b) and 2.5 (c, d). The notation is the same as in Figures 1, 2.

M	$P_{1/2}/P$	K_{coupl}	K^0_{coupl}
1.3	0,74	0,31	0,11
1.5	0,73	0,44	0,25
1,7	0,72	0,51	0,43
2	0,69	0,63	0,54
2,5	0,69	0,69	0,62

Figure 4 shows how the radiation power in the plane in front of the exit mirror (1), the power leaving the resonator (2) and the brightness in the far zone (3) vary as a function of the magnification in the range from 1.3 to 2.5. The brightness in the far zone is defined as the ratio of the power with respect to the 0.7 level of the total to the angle at which this power is emitted. All the values are normalized to their maximum values. In these calculations it was assumed that amplification per pass at the entrance to the resonator is $q_0 = 0.9$, the Fresnel number $N = 30$, the index of losses per pass $\beta = 0.03$. The output power for the indicated parameters depends little on the magnification, whereas with respect to brightness of the radiation the optimum magnification is expressed strongly. In the table the relative magnitude of the power emitted by the upstream half of the resonator and the coupling coefficients of the resonator in the lasing mode K_{coupl} and the empty resonator K^0_{coupl} are presented for several values of the magnification. With small magnification the coupling coefficient in the lasing mode increases appreciably more sharply than for high magnification. Frequently this explains the weak dependence of the output power on the magnification of the resonator.

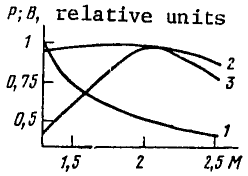

Figure 4. Power P and brightness B of radiation as a function of the magnification (see the text).

The results of the calculations permit a defined representation to be compiled of how the properties of the radiation of unstable resonators depend on the characteristic features of the high-speed gas flows as the active medium. In particular, it is possible to conclude from them that the problem of optimizing the power and brightness of the radiation requires comprehensive consideration of the optical and kinetic characteristics of the active medium and the properties of the resonator mirrors.

BIBLIOGRAPHY

1. A. E. Siegman, PROC. IEEE, No 53, 1965, p 277.

2. Yu. A. Anan'yev, KVANTOVAYA ELEKTRONIKA, No 6, 1971, p 3.

3. A. F. Mamzer, V. S. Rogov, A. S. Rumyantsev, KVANTOVAYA ELEKTRONIKA, No 4, 1977, p 142.

4. Yu. N. Karamzin, Yu. B. Konev, KVANTOVAYA ELEKTRONIKA, No 2, 1975, p 256.

5. D. B. Rensch, APPL. OPTICS, No 13, 1974, p 2546.

6. A. E. Siegman, E. A. Sziklas, APPL. OPTICS, No 13, 1974, p 2775.

7. E. A. Sziklas, A. E. Siegman, APPL. OPTICS, No 14, 1975, p 1874.

8. A. E. Siegman, IEEE J., QU-12, 1976, p 35.

9. A. N. Chester, APPL. OPTICS, No 11, 1972, p 2584.

10. J. F. Perkins, C. Cason, APPL. PHYS. LETTS, No 31, 1977, p 198.

11. L. V. Koval'chuk, V. Ye. Sherstobitov, KVANTOVAYA ELEKTRONIKA, No 4, 1977, p 2166.

12. A. E. Siegman, IEEE J., QE-13, 1977, p 334.

13. N. V. Karlov, Yu. B. Konev, I. V. Kochetov, V. G. Pevgov, preprint of FIAN, No 183, Moscow, 1976.

14. A. N. Vargin, V. V. Gogokhiya, V. K. Konyukhov, L. M. Pasynkova, ZhTF, No 45, 1975, p 604.

15. S. A. Losev, "Gazodinamicheskiye lazery" [Gas Dynamic Lasers], Moscow, Nauka, 1977.

10845
CSO: 1862

UDC 535.417.2

CHARACTERISTICS OF UNSTABLE RESONATORS WITH FIELD DISTORTIONS IN THEIR ELEMENTS. II. SPHERICAL MIRRORS

Moscow KVANTOVAYA ELEKTRONIKA in Russian Vol 7, No 11, Nov 80 pp 2422-2426

[Article by S. B. Bunkin and Yu. B. Konev, High Temperatures Institute of the USSR Academy of Sciences, Moscow; submitted 5 Apr 80]

[Text] A numerical solution was found to the integral equations of an unstable confocal resonator with spherical mirrors by the method of fast Fourier transformation. The field distortions characteristic of the operation of the resonator filled with a high-speed flow of active medium were investigated: asymmetric distortion of the mirror surface simulating thermal deformation, small-scale random phase nonuniformities, phase nonuniformity occurring as a result of compression wave formation and expansion in a supersonic flow. Lasing was calculated in a high-speed flow of a mixture of carbon dioxide, nitrogen and water vapor.

Unstable resonators have been studied theoretically for a number of years (see, for example, [1, 2]). However, only a few papers report the results of the studies of three-dimensional resonators [3-5]. In this paper the characteristics of a three-dimensional, confocal, passive resonator with phase distortions in its elements which can arise when using high-speed flows of active media and also a resonator in the lasing mode, were investigated numerically. Analogous problems were considered in the first part of this paper for a two-dimensional resonator.

The calculations were performed using the algorithm of fast Fourier transformation for the solution of the integral equations of the resonator in the Fresnel-Kirchhoff approximation. The resonator mirrors were considered to be rectangular. It was also proposed that the dimensions of the concave mirror are so great that its edges have no influence on the field distribution, and the nonuniform medium is concentrated in thin layers near the mirrors. The complex characteristics of the transmission of these layers were represented in the form

$$\Phi_k(x, y) = 2\pi w_k(x, y) + i(g_k(x, y) - \beta_k)/2, \quad (1)$$

where $w_k(x, y)$ are the values of the phase nonuniformity measured in wavelengths, positive with an increase in the optical path between the mirrors; g_k and β_k are the gain and loss factors, all of the values correspond to passage through the k-th layer in one direction. On the n-th passage through the resonator, the following relation exists between the complex amplitudes of the waves $E_n^+(x, y)$ and $E_n^-(x, y)$ propagated to the convex and concave mirrors:

$$E_n^+(\xi, \eta) = i\sqrt{N_x N_y} \int_{-1/M}^{1/M} d\xi_1 \int_{-1/M}^{1/M} d\eta_1 E_n^-(\xi_1, \eta_1)\, G^+(\xi, \eta, \xi_1, \eta_1); \quad (2)$$

$$E_n^-(\xi, \eta) = i\sqrt{N_x N_y} \int_{-\infty}^{\infty} d\xi_1 \int_{-\infty}^{\infty} d\eta_1 E_{n-1}^+(\xi_1, \eta_1)\, G^-(\xi, \eta, \xi_1, \eta_1), \quad (3)$$

where $\xi = x/a$; $\eta = y/b$; a, b are the half-widths of the region occupied by the field in the concave mirror in the geometric approximation; M is the magnification; $N_x = a^2/(\lambda L)$; $N_y = b^2/(\lambda L)$ are the Fresnel numbers; L is the spacing between the mirrors;

$$G^+(\xi, \eta, \xi_1, \eta_1) = \exp[-i\pi N_x (\xi-\xi_1)^2 - i\pi N_y (\eta-\eta_1)^2] \exp[-i\Phi_1 \times (\xi_1, \eta_1) - i\Phi_2(\xi, \eta)]; \quad G^-(\xi, \eta, \xi_1, \eta_1) = \exp[-i\pi M N_x (\xi_1 - \xi/M)^2 - i\pi M N_y (\eta_1 - \eta/M)^2] \exp[-i\Phi_1(\xi, \eta) - i\Phi_2(\xi_1, \eta_1)];$$

the phase is reckoned from the surface of equal phase of the corresponding waves in the undisturbed resonator in the geometric approximation, 1 and 2 correspond to the layers near the convex and concave mirrors. The solution was found by the method of iterations, beginning with uniform distribution of the complex amplitude with respect to one of the mirrors. The calculations continued until the complex amplitude distribution after the next iteration coincided with the preceding one with given accuracy. The calculations were performed for a resonator with the parameters $N_x = 10$, $N_y = 5$, $M = 1.5$.

Figure 1 shows the intensity distributions before the exit mirror and in the far zone of the undisturbed resonator in the form of the contour lines of the corresponding three-dimensional surfaces.

The distortions in the resonator elements characteristic of its operation with high-speed flow of active medium include the density discontinuities which are formed on transition of the supersonic flow from the nozzle to a channel of constant cross section, deformation of the reflecting surface of the mirrors under the effect of radiation on them concentrated in the upstream half of the resonator and also small-scale fluctuations of the index of refraction of the active medium.

Density discontinuities have been experimentally studied [6]. Fig. 2 shows distributions taken from [6] for the refractive index in different planes of a channel of fixed cross section with a low ledge on the lower wall at the nozzle outlet (normalization in Fig. 2 is arbitrary, and corresponds to the phase lead along lines of sight across the flow rather than to relative change of gas density). These data

were used in the resonator calculations. Figure 3 shows the results of the calculation for the case where the maximum phase advance per pass was $w_{max} = 0.1$. By comparison with the undisturbed resonator the intensity distributions in the plane of the exit mirror and in the far zone varied significantly. The effect of the asymmetry of the index of refraction with respect to the core of the channel is very obvious. A phase advance of this size or even larger is entirely possible in supersonic flows of the active medium and it greatly worsens the divergence of the radiation.

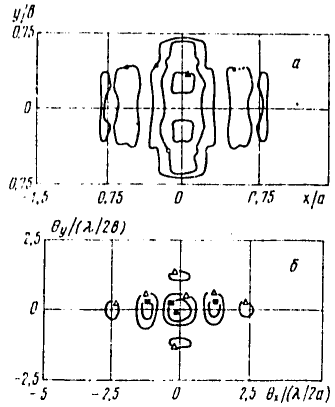

Figure 1. Radiation intensity at the exit mirror (a) and in the far zone (b) of the resonator: level lines: 30% (●), 50% (o), 90% (▲), 10% (Δ) and 20% (■) of the maximum; coupling coefficient $K_{coupl} = 0.51$.

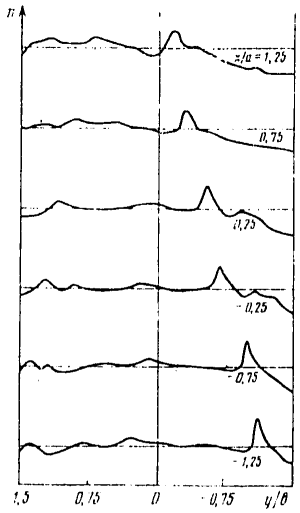

Figure 2. Distributions of the index of refraction n in a supersonic flow [5] for the indicated values of x/a.

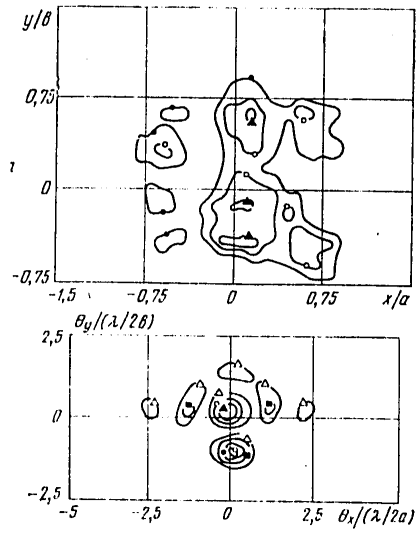

Figure 3. Radiation intensity at the exit mirror (a) and in the far zone (b) of the resonator with nonuniformity of the index of refraction. The notation is the same as in Figure 1: $K_{coupl} = 0.47$.

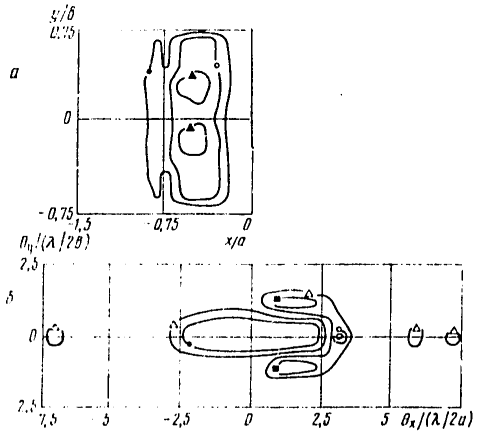

Figure 4. The same as in Figure 3 for a resonator with deformation of the exit mirror, $K_{coupl} = 0.42$.

The solution of the self-consistent problem of deformation of the reflecting surface of mirrors under the effect of radiation in a resonator is very complex. Therefore it is expedient to give the distribution w(x, y) on the average describing the deformation under the effect of radiation more strongly heating one-half

of the mirror in order to study the nature of the variations of the field pattern at the exit mirror and in the far zone. In Figure 4 it is possible to see the results of the calculation in the case where the deformation of the exit mirror is given by the expression

$$w(x, y) = -{}^{16}/_{27}\, w_m(1-(Mx/a)^2(1+Mx/a)^2(1-(My/b)^2)$$

for a value of the maximum deformation $w_m = 0.1$ at point $x_m = a/2M$, $y_m = 0$. In this case the field is more strongly localized in the half of the exit mirror where the deformation is less, and this can to some degree weaken the field concentration in the upstream half. In the greater part of the surface of the exit mirror of Figure 4a the radiation intensity does not exceed 30% of maximum. The radiation divergence with this deformation is essentially worse in the direction of the X axis, and the radiation maximum in the far zone is shifted along this axis.

We also performed calculations of resonators with small-scale phase fluctuations. For this purpose random variables w(x, y) were given at the grid nodes distributed according to a Gaussian law with zero mean and dispersion σ. The surface of the exit mirror and part of the surface of the concave mirror in which the field is concentrated in the geometric approximation has 32 x 32 nodes. For a value of $\sigma > 0.02$ the field distribution over the surface of the exit mirror became very irregular and was poorly represented by contour lines. Figure 5 shows the field pattern in the far zone for a value of $\sigma = 0.05$. It has the nature of individual irregular peaks against a quite broad diffuse background which is well visible in Figure 6 where for the series of cases investigated above, the proportion of the power emitted in the solid angle $|\theta_x| \leq \theta\lambda/2a$, $|\theta_y| \leq \theta\lambda/2b$ is demonstrated.

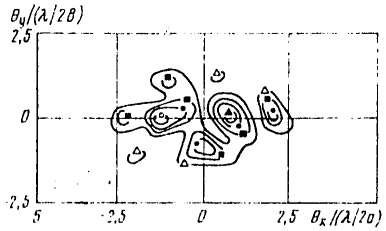

Figure 5. Radiation intensity in the far zone of the resonator with small-scale random nonuniformities of the index of refraction. The notation is the same as in Figure 1; $K_{coupl} = 0.44$.

The lasing calculations in the supersonic flow of the mixture of carbon dioxide, nitrogen and water vapor were performed the same as in [6] for the two-dimensional resonator. The conditions were the following: a mixture of $CO_2:N_2:H_2O$ = 0.1:0.86:0.04, pressure 0.04 atm, temperature 280 K, flow velocity 1,750 m/sec, vibrational temperatures of the deformation and antisymmetric types of vibrations of carbon dioxide T_2 = 320 K, T_3 = 1,400 K, nitrogen T_4 = 1,400 K, the amplification per pass at the input to the resonator $g_0 = 0.9$, loss index per pass $\beta = 0.03$.

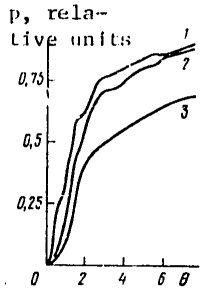

Figure 6. Relative part of the radiation power in the far zone for the levels in Figure 1 (1), Figure 4 (2) and Figure 5 (3).

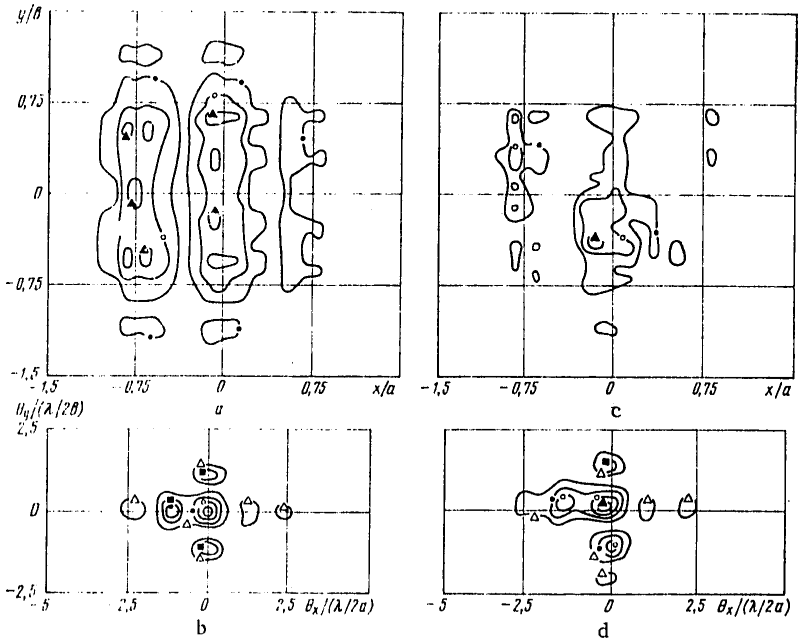

Figure 7. The same as in Figure 1 (a, b) and 3 (c, d), but in the lasing mode, $K_{coupl} = 0.61$ (a, b) and 0.55 (c, d).

In Figure 7a, b, the calculation results are presented for a resonator without phase nonuniformities; in Figure 7c, d, for the same resonator, in the active medium of which there are nonuniformities of the index of refraction depicted in Figure 2 for $w_m = 0.1$. A trend toward field concentration in the upstream half of the resonator ($x < 0$), some shift in the intensity peak in the far zone from the direction of the optical axis of the resonator and also significant worsening of

the divergence of the radiation as a result of nonuniformity of the index of refraction are clearly visible. The radiation power in the presence of nonuniformity of the index of refraction decreased somewhat and was 68 percent of the radiation power in a uniform medium.

Analyzing the above-presented data and the results of the first part of the experiment, it is possible to conclude that for response to a number of problems of practical importance such as the nature of the beam load on the mirror, the coupling coefficient of the resonator and the radiation power, the effect of the mirror deformation and nonuniformity of the index of refraction in the flows, three-dimensional calculations of the resonators are required. At the same time, for determination of the requirements on the quality of the resonator elements, beginning with the admissible worsening of the radiation divergence, in many cases it is possible to limit ourselves to two-dimensional calculations for which significantly less time is required.

BIBLIOGRAPHY

1. Yu. A. Anan'yev, KVANTOVAYA ELEKTRONIKA, No 6, 1971, p 3.

2. A. E. Siegman, IEEE J., QE-12, 1976, p 35.

3. D. B. Rensch, APPL. OPTICS, No 13, 1974, p 2546.

4. E. A. Sziklas, A. E. Siegman, APPL. OPTICS, No 14, 1975, p 1874.

5. A. T. Jones, J. PHYS. D, No 11, 1978, p 871.

6. M. N. Director, AIAA Paper 73-626.

10845
CSO: 1862

UDC 621.378.33

10-kw STATIONARY PROCESS CO_2-LASER

Moscow KVANTOVAYA ELEKTRONIKA in Russian Vol 7, No 11, Nov 80 pp 2467-2471

[Article by F. A. Abil'siitov, A. V. Artamonov, Ye. P. Velikhov, Yu. A. Yegorov, A. V. Kazhidub, F. V. Lebedev, Ye. M. Sidorenko, V. V. Sumerin and V. M. Frolov, Nuclear Power Institute imeni I. V. Kurchatov, Moscow; submitted 15 May 80]

[Text] A report is presented on the creation of a 10-kw, closed-cycle stationary process electric discharge CO_2-laser operating on a helium-free mixture. The structural design of the device is described, its operating characteristics are reported, and data are presented on the stability and divergence of the radiation, the maximum radiation density at the focal point. The prospects for the use of such a laser in industry are discussed.

1. The experimental models of the powerful CO_2-lasers appearing at the present time [1-5] have made it possible to discover serious technological and economic advantages of laser working of materials over traditional methods. There are reports on the successful use of lasers for cutting and welding metals [4-7], thermal hardening, alloying and cladding of steels [5]. The broad introduction of these prospective methods of industrial processing requires the creation of powerful process CO_2-lasers characterized by high reliability.

The power of the process lasers built in the USSR and abroad which make use of the simplest and, from the technical point of view, the most reliable pumping of the working medium by independent DC discharge does not exceed 5 kw [1, 5]. In the 10-15-kw lasers, a complex, still unreliable technology of independent discharge with ionization by an electron beam is used [3, 8]. In practice in all of the known process lasers expensive and scarce helium is used as one of the components of the working medium. As a result of absence of reliable regeneration systems for the chemical composition of the working medium, the necessity arises for continuous renewal of it in the amount of ~1 percent of the flow rate in the gas loop. The helium requirement is 30-50 mg/sec per kilowatt of laser power.

In this paper a report is made on the creation of a closed-cycle, 10-kw stationary process CO_2-laser with pumping by a transverse independent DC discharge operating on a helium-free working medium. The engineering and operating characteristics of

the laser are presented, and the possibility of using it to work materials is discussed.

2. The choice of the electro-optical system, structural execution and optimization of the operating conditions of the laser was made on the basis of experiments performed on a mockup of the device [2, 9, 10]. In these experiments the possibility of effective pumping by transverse DC discharge under the conditions of an electrode gap enlarged to 6 cm and also the advantages of using a combined electro-optical laser system by comparison with a separated one were demonstrated.

The diagram of the laser is presented in Figure 1. It consists of a lasing unit (BG), the control panel and auxiliary systems providing electric power and cooling of the BG elements and also maintenance of constant pressure and composition of the working medium. The general view of the BG appears in Figure 2. It is formed by two parallel gas loops, in each of which there is an electric compressor and two heat exchangers. The gas flows are joined in the discharge chamber. Stimulated emission takes place in an unstable confocal four-pass resonator with one amplifying pass, fully matched with the discharge chamber.

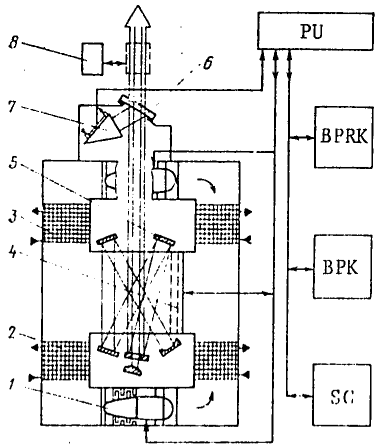

Figure 1. Diagram of the laser: 1--compressor; 2, 3--heat exchangers; 4--cathode plate electrode; 5--resonator mirror; 6--one of the KCl single crystals; 7--calorimeter; 8--through-type power pickup; PU--control panel; BPRK--discharge chamber power supply; BPK--compressor power supply; SG--gas exchange system.

The circulation of the working mixture in the BG is realized by specially developed, small-scale axial compressors. The working medium of the laser is excited by a transverse independent DC discharge. The discharge chamber is installed inside the vacuum housing of the laser and is 0.4 m long with respect to the flow, and 2 m with respect to the optical axis. It consists of a continuous shaped anode made of sheet stainless steel and a cathode plate 6 cm from it. In the given laser a collapsible design of the cathode plate with row-by-row sectioning

has been used for the first time. It consists of 17 identical sections placed one after the other along the flow, each of which combines all of the 39 channels arranged in one row across the flow and their individual ballast resistances R_0 = 5.1 kilohms. The emitting surface of the plate cathodes [9] is located on the same level with the surface of the cathode plate and has dimensions of 45 x 1.5 mm. The shaping of the discharge current along the gas flow needed for optimization of the operating conditions of the laser was realized using additional ballast resistances common to each row R_{sh} = 25-250 ohms.

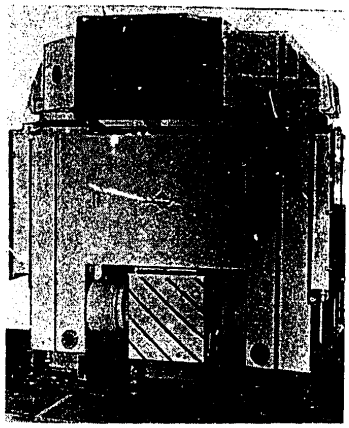

Figure 2. General view of the lasing unit (BG).

The laser radiation is taken out of the vacuum tank of the BG through the single KCl crystal installed at an angle of ~20° to the optical axis. Part of the radiation energy reflected from the crystal hits the power meter, which is a cooled absorbing cone. The speed of this continuous output power monitoring system is ~1 sec. When necessary the laser radiation exiting through the window can be directed at the target through a through-type balometric power meter with transparency of ≥98 percent and speed ~0.1 sec. The calibration of both sensors is realized by a calorimetric absolute power meter.

During the work on creating the laser, a great deal of attention was given to satisfying the requirements imposed on technological machinebuilding equipment such as stability of the operating characteristics, the endurance and operating reliability, economical use of production area, low operating costs, simplicity and reliability for servicing. The weakest elements of the laser from the point of view of endurance are the exit opening, the cathode plate and the resonator mirror. The systems for fastening the exit opening and the mirrors and also the sectional construction of the cathode plate permit rapid replacement of them. For this purpose a spare set of replaceable elements is provided. The laser is equipped with an emergency protection system permitting the basic assemblies to be kept operating on occurrence of emergencies, for example, if the loop begins to leak, the water or electric power supplies are interrupted. The modular execution of the basic functional assemblies of the laser permits the BG and the control unit

to be installed separately from the systems supporting its operation (converters, power supplies, pumps, gas ramp, and so on). The control of the operation of all of the laser elements is by one operator from a control panel. The general noise level in direct proximity to the BG does not exceed the admissible values.

3. The basic operating conditions and characteristics of the laser are presented in its engineering specifications.

Engineering Specifications

Working mixture	CO_2:(N_2 + air) = 1:19
Pressure of the mixture, mm Hg	~25
Gas velocity at the entrance to the discharge chamber, m/sec	~80
Gas flow rate in the loop, g/sec	~400
Degree of makeup of the mixture, %	~0.5
Cooling water consumption, kg/sec	~3
Overall dimensions of the BG, m:	
In plan	2.7 x 3
Height	2.8
Area for placing the laser, m^2	~100
Maximum output power, kw	10
Total intake, kw	~140
Laser efficiency, %	7

The output power of the laser is varied from 1 to 10 kw (Figure 3, curve 1) by varying the voltage of the main power supply of the discharge chamber. The maximum electric power contributed to the discharge is limited by the discharge stability and is 70 kw. The power released in the normal mode in the ballast resistances is 35 kw. Approximately 35 kw are required to power the electric compressors, the vacuum system and service systems. Thus, the total efficiency of the laser does not exceed 7 percent with an electro-optical efficiency of ~15 percent.

The experiments performed when operating the laser in the air with maximum moisture content demonstrated the theoretical possibility of using a working mixture of CO_2 and air with relative humidity of ~10 percent (at room temperature) under closed-cycle conditions. The output power of the laser in this case did not drop more than 20 percent. On replacement of the air in the working mixture by helium at a partial pressure of p_{He} ~ 25 mm Hg, the output power of the laser increased.

The study of the time characteristics of the laser emission demonstrated the presence of output power pulsations to 10-15 percent occurring with frequencies of 100-300 hertz and also slow, reversible variation of its magnitude within the limits of ~10-15 percent in the time ~10 minutes. The presence of "high-frequency" pulsations does not appear dangerous when using the given laser under process conditions, for the time of effect of the radiation on the machined part usually greatly exceeds the period of these oscillations. The "low-frequency" variations of the output power within the indicated limits are admissible for many technological processes. However, their magnitude can be easily decreased by introducing feedback into the basic power supply. The sensors in the feedback system

may have considerable lag time, and depending on the specific technological process they must follow the output power of the laser or the temperature of the machined sample. In the former case it is possible to use either of the two sensors used in the given device for continuous power monitoring. The possibility of measuring the temperature of the sample irradiated by the laser with good time resolution (≤0.1 millisecond) was reported in [11].

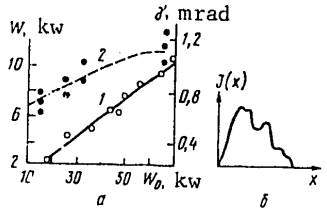

Figure 3. Output power of a laser W (1) and divergence of the radiation γ (2) as a function of the power contributed to discharge for a mixture of CO_2:(N_2 + air) = 1:19 (a) and the standard type of distribution of the radiation intensity at the focal point (b).

The divergence of the output radiation of the laser was determined experimentally by the intensity distribution

$$J(x) = \int_{-\infty}^{x} \left[\int_{-\infty}^{\infty} J(x, y)\, dy \right] dx$$

in the focal plane of the spherical mirror with a focal length F = 3 m. The standard form of this distribution for W = 10 kw obtained during scanning of a focal point with respect to the X coordinate is indicated in Figure 3b. The magnitude of the divergence of the radiation determined by the angular dimensions of the focal point at which 90 percent of the energy of the laser radiation is concentrated, increased with an increase in the output power (see Figure 3a, curve 2), and for the rated values of it, it was γ ≈ 0.8-1.2 mrads for a calculated diffraction divergence γ_{dif} ≈ 0.5 mrad.

The radiation was taken out of the BG in the form of a ring with outside diameter 50-55 mm. The minimum focal length of the optical system permitting this radiation to be focused without aberration is F_{min} ~ 30-40 cm; therefore the minimum dimensions of the focal point for the above-indicated divergences can reach 0.4 -0.4 mm. The average radiation power density at this spot with rated laser power of 10 kw is S ~ 8 megawatts/cm^2. For comparison let us note that for realization of effective welding with deep fusion and cutting of carbon and alloyed steels, a laser radiation power density of ~1-10 megawatts/cm^2 is required [6, 7]. The experiments performed with respect to surface hardening, alloying and cladding of metals [5] indicate that for such processes power density at the 10-100 kw/cm^2 level is sufficient.

4. Summing up the results, it is possible to state that the described process laser has maximum output power among the known closed-cycle stationary process lasers excited by transverse independent discharge. During creation of it the requirements imposed on the process equipment are taken into account to the maximum. Having high efficiency, it is simple and reliable to operate and does not require helium for its operation. The output characteristics and the attainable radiation power densities ($10 megawatts/cm^2) permit effective use of it in many technological operations of working metals and nonmetallic materials.

All of this makes the given laser suitable for experimental industrial operation already at the present time and is opening up broad prospects for the use of such lasers in the near future.

BIBLIOGRAPHY

1. F. K. Kosyrev, N. P. Kosyrev, Ye. I. Lunev, AVTOMATICHESKAYA SVARKA, No 9, 1976, p 174.

2. G. A. Abil'siitov et al., KVANTOVAYA ELEKTRONIKA, No 6, 1979, p 204.

3. N. G. Basov et al., KVANTOVAYA ELEKTRONIKA, No 6, 1979, p 772.

4. A. M. Belen'kiy et al., SVAROCHNOYE PROIZVODSTVO, No 11, 1977, p 23.

5. E. V. Locke, OPT. ENGGN., No 17, 1978, p 192.

6. M. J. Yessik, OPT. ENGGN., No 17, 1978, p 202.

7. R. A. Willgoss, OPT. AND LASER TECHNOL., No 11, 1979, p 73.

8. U.S. Patent No 3,970,962 of 20 July 1976.

9. A. V. Artamonov et al., KVANTOVAYA ELEKTRONIKA, No 5, 1978, p 920.

10. A. V. Artamonov et al., KVANTOVAYA ELEKTRONIKA, No 4, 1977, p 419.

11. A. V. Bondarenko et al., PIS'MA V ZhTF, No 5, 1979, p 221.

10845
CSO: 1862

MISCELLANEOUS

UDC 537.591

CHARGED PARTICLE DISTRIBUTION IN NEAR-EARTH SPACE

Moscow TRUDY ORDENA LENINA FIZICHESKOGO INSTITUTA IMENI P. N. LEBEDEVA: RASPREDELENIYE ZARYAZHENNYKH CHASTITS V OKOLOZEMNOM PROSTRANSTVE in Russian Vol 122, 1980 (signed to press 13 Aug 80) pp 2, 78-79

[Annotation and abstracts from book "Proceedings of Lebedev Physics Institute: Charged Particle Distribution in Near-Earth Space", edited by Academician N. G. Basov, Izdatel'stvo "Nauka", 1000 copies, 79 pages]

[Text] The papers published in this collection deal with experimental studies of the planetary distribution and altitude behavior of charged particles by weather balloon, probing rocket and satellite. The studies cover the behavior of charged particles in the magnetic field of the earth, the altitude behavior of cosmic ray and albedo particles, and also the influence of solar activity on particle fluxes in nearby space. An examination is made of the peculiarities of behavior of albedo particles from the earth's atmosphere, for example quasicapture of charged particles in the earth's field into closed drift shells that keep energetic particles at high intensity at altitudes of 200-500 km, and also fluxes of particles that arise upon interaction of cosmic rays with matter in the low-density medium on the closed shells. It is significant that this collection combines experimental data obtained by different methods at different altitudes, including measurements in the stratosphere by weather balloons at altitudes where we begin to see intense interaction and absorption of cosmic radiation particles overcoming the shielding action of the earth's magnetic field.

All these studies play an important part in understanding of the processes that take place near the earth. The behavior of charged particles reflects mainly the distribution and time behavior of the geomagnetic field. Of considerable importance is an estimate of dosimetric parameters on orbits where prolonged space missions are in progress.

UDC 523.125

PLANETARY DISTRIBUTION OF INTENSITY OF COSMIC RAYS FROM MEASUREMENTS IN THE STRATOSPHERE

[Abstract of article by A. Ye. Golenkov, V. P. Okhlopkov, A. V. Svirzhevskaya, N. S. Svirzhevskiy and Yu. I. Stozhkov]

[Text] The paper gives experimental data on the longitudinal and latitudinal distribution of intensity of galactic cosmic rays in the stratosphere. It is shown

that in the vicinity of the Brazilian and South African magnetic anomalies experimental data evidence the need for introducing corrections in the geomagnetic cutoff rigidities calculated by the trajectory method. The angular distribution of particles is calculated from sea level to altitudes of about 30 km in the rigidity range of 0.1-14 Bv. The latitude dependence of albedo particles is found by the method of extrapolating the data to the limit of the atmosphere. Figures 12, tables 3, references 26.

UDC 523.165

TIME CHANGES IN THE INTENSITY OF COSMIC RAYS IN THE ATMOSPHERE

[Abstract of article by A. N. Charakhch'yan, G. A. Bazilevskaya, Yu. I. Stozhkov and T. N. Charakhch'yan]

[Text] From data of more than 10,000 radiosonde probes on balloons from 1957 to 1975, new results are found on the distribution of cosmic ray intensity in the atmosphere. The authors discuss the mean annual values of cosmic ray intensity at levels of atmospheric pressure of 10, 20, 50, 90 160, 240, 320, 400, 480, 560, 720 and 800 g/cc at the latitudes of Murmansk, Mirnyy (Antarctica), Moscow and Alma-Ata. The data indicate variable anisotropy of primary cosmic rays arriving at the earth. Two-year, four-year and ten-year cycles are found in effects of anisotropy with amplitudes of up to 5-10% in the lower atmosphere and up to 1-2% in the stratosphere. Hypotheses are suggested on the modulation nature of the observed phenomena and their connection with the overall magnetic field of the sun. Figures 13, tables 2, references 4.

UDC 537.591

ALTITUDE BEHAVIOR OF THE INTENSITY OF CHARGED PARTICLES FROM 75 TO 500 km ACCORDING TO ROCKET AND SATELLITE DATA

[Abstract of article by V. V. Klimenko, L. V. Kurnosova, S. I. Prokop'yev, L. A. Razorenov, M. I. Fradkin and Yu. G. Shafer]

[Text] The paper compares results of measurement of fluxes of charged particles in rocket, satellite and stratospheric experiments. The results of analysis agree with the hypothesis of an altitude trend in the range of altitudes from stratospheric to 500 km for charged particle fluxes with energy of 10 MeV. Figures 2, tables 4, references 18.

UDC 537.591

ANALYSIS OF THE ENERGY SPECTRUM OF SECONDARY ELECTRONS FROM DATA OF THE KOSMOS-225 SATELLITE WITH CONSIDERATION OF ORIENTATION

[Abstract of article by V. S. Gorshkov, L. V. Kurnosova, L. A. Razorenov, V. G. Sinitsina, M. I. Fradkin and I. G. Khatskevich]

[Text] Data are given on the spectra of secondary electrons with energy of more than 150 MeV at altitudes of 200-500 km measured by equipment on the Kosmos-225 satellite. Orientation data are used to compare the spectra of secondary electrons going toward the earth and away from the earth. Figures 6, references 6.

UDC 537.591

INVESTIGATION OF FLUXES OF CHARGED PARTICLES ON THE KOSMOS-555 SATELLITE

[Abstract of article by L. V. Kurnosova, A. T. Matachun, L. A. Razorenov and M. I. Fradkin]

[Text] The paper gives data on fluxes of electrons with energy greater than 10 MeV and protons with energy greater than 400 MeV at altitudes of 250 km going toward the earth and away from the earth. Figures 5, tables 7, references 12.

UDC 537.591

FLUXES OF ELECTRONS WITH ENERGY GREATER THAN 150 MeV ACCORDING TO DATA OF THE KOSMOS-555 SATELLITE

[Abstract of article by L. V. Kurnosova, A. T. Matachun, L. A. Razorenov and M. I. Fradkin]

[Text] Data are given on fluxes of electrons with energy greater than 150 MeV measured by equipment on board the Kosmos-555 satellite (angle of inclination of orbit 81.3°). Major emphasis is placed on investigation of fluxes of secondary electrons. The flux of secondary electrons in the equatorial region with low pitch angles is determined by the particle drift around the globe. Up to energies of 2 GeV, electrons at high altitudes take part in drift motion, and thus are quasi-captured into part of the drift orbit. The index of the integral energy spectrum of these electrons is equal to 0.86 ± 0.02. Figures 6, tables 3, references 14.

UDC 581.521.6

LONG-PERIOD VARIATIONS OF THE NUCLEAR COMPONENT OF COSMIC RAYS

[Abstract of article by V. V. Klimenko, L. V. Kurnosova, V. I. Logachev, L. A. Razorenov, M. I. Fradkin and Yu. G. Shafer]

[Text] The paper gives the results of investigation of the time dependence of intensity of multiply charged nuclei of cosmic rays with energies in excess of 400 MeV/nucleon. The measurements were made on the Molniya-1 satellite from November 1973 to December 1974. It is shown that both the singly charged and nuclear components of cosmic rays have the same relative amplitude of modulation, which does not agree with the concept of strong dependence of the amplitude of variations on particle rigidity. Figures 3, table 1, references 2.

UDC 537.591

ON THE QUESTION OF THE PART PLAYED BY HORIZONTAL ALBEDO IN FORMATION OF SURPLUS RADIATION

[Abstract of article by L. V. Kurnosova, L. A. Razorenov and M. I. Fradkin]

[Text] The article analyzes the question of the existence of surplus radiation. New data are given on charged particle fluxes at stratospheric altitudes in the equatorial region. Figures 2, table 1, references 17.

[87-6610]

6610
CSO: 1862

UDC 551.501+551 510+535.533.34

REMOTE METHODS OF ATMOSPHERIC RESEARCH

Novosibirsk DISTANTSIONNYYE METODY ISSLEDOVANIYA ATMOSFERY in Russian 1980 (signed to press 18 Jul 80) pp 2, 161

[Annotation and abstracts from book "Remote Methods of Atmospheric Research", edited by Associate Member of the Soviet Academy of Sciences V. Ye. Zuyev, Izdatel'stvo "Nauka", 1300 copies, 161 pages]

[Text] The book presents survey papers by workers at the Institute of Optics of the Atmosphere, Siberian Department, USSR Academy of Sciences on laser probing of atmospheric aerosols and laser spectroscopy of some atmospheric gases. An examination is made of general procedural problems of separation of the molecular and aerosolic components of the atmosphere in remote determination of their characteristics. The theory of double scattering of laser beams in dense dispersed media is given as well as its applications to remote determination of characteristics of clouds; methods are outlined for solving incorrect problems of the theory of scattering by polydisperse systems of particles associated with on-the-spot remote determination of the microstructure of aerosols by multiple-frequency pulsed and bistatic lasers; an examination is made of the state of research on spectral detection of intramolecular and intermolecular interactions and the effect of the laser emission field in the shortwave band.

The collection is intended for specialists on laser probing of the atmosphere, and also for all those interested in the use of laser technology.

UDC 551.510.42

PROCEDURAL PROBLEMS OF LASER PROBING OF A MOLECULAR AND AEROSOLIC ATMOSPHERE

[Abstract of article by G. M. Krekov]

[Text] The paper gives a survey and comparative analysis of effectiveness of current methods of multiple-frequency probing of an aerosolic and molecular atmosphere, including previous research by the author. Some new modifications are suggested that improve precision and informativeness of algorithms for numerical processing of backscattered signals on two and three probing frequencies. The conclusions are illustrated by numerical computer experiments for optical models of the atmosphere corresponding to typical ranges of laser probing waves. Some recommendations are made on optimum planning of experiments. Figures 9, references 98.

UDC 551.510.42:551.521.3

INCORRECT INVERSE PROBLEMS OF LASER PROBING OF ATMOSPHERIC AEROSOLS

[Abstract of article by I. E. Naats]

[Text] A detailed examination is made of the particulars of solution of inverse problems in the class of both continuous and interrupted aerosol distributions; corresponding methods are given for constructing regularizing algorithms, and procedural problems are discussed that are associated with formulating optical experiments in the atmosphere.

The paper gives the theoretical principles of methods of multiple-frequency monostatic and bistatic probing of the atmosphere, and presents examples of interpretation of experimental data of three-frequency probing of a tropospheric aerosol. Figures 9, references 48.

UDC 621.378:551.501

THE THEORY OF DOUBLE SCATTERING AND ITS APPLICATIONS TO PROBLEMS OF LASER PROBING OF AN AEROSOL

[Abstract of article by I. V. Samokhvalov]

[Text] An equation is derived that relates the optical characteristics of the medium and the parameters of the probing beam and transceiver to components of the Stokes vector parameter of doubly scattered radiation as applied to problems of lidar probing of the atmosphere. An investigation is made of the limits of applicability of the equation, and it is shown that doubly scattered radiation is more effective than singly scattered with respect to information yielded on the microstructure of the investigated aerosol. Figures 14, references 43.

UDC 535.33/34

LASER SPECTROSCOPY OF ATMOSPHERIC GASES IN THE SHORTWAVE REGION OF THE SPECTRUM

[Abstract of article by V. P. Lopasov]

[Text] The paper gives a survey and comparative analysis of the results of research (including by the author) on the absorption spectrum of atmospheric gases registered with simultaneous action of different intramolecular and intermolecular perturbations of the states of molecules, and also under the effect of a field of laser emission. It is concluded that under these conditions it is possible to find new spectroscopic effects, and as a result there should be fundamental changes in propagation of laser radiation in a molecular medium. Figures 6, references 74.

[75-6610]

6610
CSO: 1862

NUCLEAR PHYSICS

UDC 539.1.074:621.387.4:539.1.075:532.546

EXPERIMENTAL METHODS OF NUCLEAR PHYSICS

Moscow EKSPERIMENTAL'NYYE METODY YADERNOY FIZIKI in Russian No 5, 1979 (signed to press 30 Jul 79) pp 2, 186-188

[Annotation and table of contents from book "Experimental Methods of Nuclear Physics", edited by V. M. Kolobashkin, Atomizdat, 500 copies, 188 pages]

[Text] The collection includes materials of scientific research completed in June of 1979. The book contains 21 articles dealing with different aspects of experimental methods of nuclear physics: time-of-flight systems for gathering information for gamma telescopes; developments in the field of radiation detection; the nuclear-physics characteristics and processes of transport of fission products in fuel compositions; methods of collecting and measuring samples of rare radionuclides; problems of processing and optimizing physics experiments.

The collection is intended for experimental physicists, and also for undergraduate and graduate students majoring in the area of developing experimental methods of nuclear physics.

Figures 76, tables 5, references 127.

Contents:

[90-6610]

6610
CSO: 1862

UDC 533.9

PHYSICS OF HIGH-CURRENT RELATIVISTIC ELECTRON BEAMS

Moscow FIZIKA SIL'NOTOCHNYKH RELYATIVISTSKIKH ELEKTRONNYKH PUCHKOV in Russian 1980 (signed to press 17 Dec 79) pp 2-4, 164-165

[Annotation, preface and table of contents from book "Physics of High-Current Relativistic Electron Beams", by Anri Amvrosiyevich Rukhadze, Larisa Semenovna Bogdankevich, Stanislav Yefimovich Rosinskiy and Vladislav Georgiyevich Rukhlin, Atomizdat, 1400 copies, 168 pages]

[Text] The book systematically outlines the principles of physics of pulsed high-current electron beams and their interaction with plasma. A detailed examination is made of various equilibrium configurations, shaping and stability of such beams. Some applied problems of high-current electronics are discussed, such as the question of neutralizing and focusing electron beams, relativistic microwave electronics, the problem of relaxation of electron beams in a plasma, and heating of a plasma to thermonuclear temperatures.

For specialists working in the field of physics of high-current electron beams. May be of use to graduate students and upperclassmen in the pertinent colleges and universities.

Tables 3, Figures 29, references 112.

Preface

In recent years various areas of science and engineering have been making extensive use of high-current pulsed electron beams with the following characteristic parameters:

Electron energy	10^5-10^7 eV
Beam current	10^3-10^6 A
Pulse duration	10^{-8}-10^{-6} s
Beam energy	10^2-10^6 J
Pulse power	10^8-10^{13} W.

These fields include inertial thermonuclear fusion initiated by a powerful electron beam, relativistic microwave electronics, powerful semiconductor, chemical and gas lasers with electron-beam pumping, new principles of acceleration of heavy charged particles, power transmission over great distances, technology of exceptionally pure materials and so on. With every passing day the literature includes more and

more research devoted to the physics of high-current electron beams and their numerous applications. By now this research has reached the level where it can be termed a new branch of science -- pulsed high-current electronics -- with its own specific experimental techniques and methods of theoretical analysis.

Despite the enormous number of publications -- both original studies and surveys on separate applied problems of high-current electronics -- monographs in this field are still excessively scarce. It is only very recently that the first monograph came out in our nation by A. N. Didenko, V. P. Grigoriyev and Yu. P. Usov: "Moshchnyye elektronnyye puchki i ikh primeneniye" [Powerful Electron Beams and Their Application], Moscow, Atomizdat, 1977.

The book gives a rather detailed account of the technology of producing powerful electron beams, the transportation of beams in vacuum drift systems and systems filled with neutral gas and dense plsama, and also the use of powerful electron storage rings for collective-field acceleration of ions, although other areas of application of powerful electron beams are discussed only briefly. The principal emphasis is given to presentation of experimental results of studies of the physics of high-current electron beams: description of facilities and diagnostic methods, and also discussion of measurement results.

In this sense, our book does the reverse, being mainly theoretical. We present the principles of the physics of pulsed high-current electron beams, analyze various equilibrium configurations of such beams and their stability, discuss questions of using high-current electron beams in microelectronics, and in this connection we present in some detail the methods of calculating electromagnetic fields and currents induced when high-current electron beams are injected into a spatially confined plasma and a neutral gas.

The presentation of only the theoretical methods of high-current electronics has enabled us to give a more extensive treatment of the problems of physics of pulsed high-current electron beams, and we leave it to the reader to judge the extent to which we have succeeded.

The first and third chapters of the book were written by A. A. Rukhadze, the second and sixth were written by S. Ye. Rosinskiy, the fourth by V. G. Rukhlin, and the fifth by L. S. Bogdankevich.

Contents

[89-6610]

6610
CSO: 1862

OPTICS AND SPECTROSCOPY

UDC 530.182.551.510.42

NONLINEAR OPTICAL EFFECTS IN AEROSOLS

Novosibirsk NELINEYNYYE OPTICHESKIYE EFFEKTY V AEROZOLYAKH in Russian 1980 (signed to press 1 Aug 80) pp 2-5, 183-184

[Annotation, introduction and table of contents from book "Nonlinear Optical Effects in Aerosols", by Vladimir Yevseyevich Zuyev, Yuriy Dmitriyevich Kopytin and Aleksandr Vitol'dovich Kuzikovskiy, Izdatel'stvo "Nauka", 1500 copies, 184 pages]

[Text] The book examines physical aspects of nonlinear optics of scattering media. Applications of this field of knowledge are principally associated with problems of propagation of intense laser emission through a turbid atmosphere. The physical mechanisms of interaction of radiation with macroscopic particles are described, as well as processes of nonlinear propagation of laser emission caused by its action on an aerosol.

The book has been written for an extensive range of specialists dealing with problems of optical communications and propagation of laser beams in the atmosphere. It may be of interest to graduate and undergraduate students majoring in optics and laser physics.

Introduction

The headlong progress in research and development of powerful laser sources of coherent emission, and their use as a major tool in atmospheric-optics studies and long-range atmospheric probing has brought the physics of nonlinear interaction of laser radiation with natural media, and especially with the atmosphere, into the realm of most urgent research problems.

Propagation of high-intensity laser emission in matter is accompanied by changes in the optical parameters of the medium that go beyond the scope of linear electrodynamics. Nonlinear effects caused by the direct action of a field on polarization of the medium are historically the first, and until now the most extensively studied of such phenomena. Another class of phenomena of nonlinear propagation of light that is quite important from a practical standpoint is effects that arise due to a change in thermodynamic parameters of the medium upon linear absorption of emission. Scattering media of the aerosol atmosphere type, where the microscopic optical parameters are determined by averaging over a number of particles, have besides additional "degrees of freedom" that are subject to the action of the field.

The subject matter of nonlinear optics of scattering media is made up of the corresponding class of optical effects caused by processes of radiative heating,

vaporization, dissociation, fragmentation and ionization of the aerosol component, effects of pondermotive action of radiation, the formation of light-induced thermal and hydrodynamic inhomogeneities in the index of refraction of the medium in the vicinity of particles and within the scales of the beam, the change in boundaries of coexistence of an aggregate state of matter, the transition of substances to various states along given thermodynamic trajectories, as well as a number of other phenomena.

The first chapter of the monograph presents the results of calculations by Mie theory on the spatial structure of light fields inside weakly absorbing spheres that are important for an understanding of low-threshold manifestations of nonlinear optics effects in channels, and studies of the pondermotive action of an intense optical wave on transparent particles, which is expressed in acceleration, coagulation and orientation of particles, and resonant buildup of surface oscillations.

The second chapter gives the principal results of research on the nonlinear action of intense laser pulses on the solid fraction of absorbing particles. An examination is made of questions of the formation of thermohydrodynamic perturbations of the index of refraction of the medium in the vicinity of radiation-absorbing particles, and nonlinearity of light scattering by these perturbations at radiation intensities that do not exceed the threshold values of a change in aggregate state and ionization of the particle material. Major emphasis is given to processes of self-stress in a laser beam as it propagates in media with discrete absorbing centers: self-broadening and self-limitation of the intensity of a finite beam upon nonlinear scattering, change in the statistics of the radiation and of the medium, the acoustic mechanism of self-focusing of the light.

Two sections of the second chapter deal with the results of analysis of processes of vaporization, dissociation and ionization of the aerosol material in intense optical fields. The last section illustrates the possibility of photostimulation of processes of heterogeneous condensation on seed nuclei by the behavior of coexistence curves of phase equilibrium in intense optical fields.

The third chapter gives the results of studies of the kinetics of vaporization of a radiation-heated droplet that is a typical element of an aerosol atmosphere; a self-consistent picture is presented of processes of heat and mass transfer from the surface of the droplet, formation of the internal temperature field, change of vaporization mode as a function of the conditions of action, motion of nonuniformly heated droplets. The theoretical conclusions that are compared with the results of experimental studies of the kinetics of vaporization of a droplet under the action of laser emission form the basic input data required for understanding and describing processes of propagation of intense infrared radiation in clouds, fog and precipitation.

The fourth chapter deals with thermal interaction of laser beams and water aerosols. This nonlinear effect is obviously most important in the applied aspect, since it could be the basis for a practical method of dispersing water aerosols. The chapter presents the results of research aimed at developing scientific principles of the method and including analysis of the formation and motion of dissipation waves, configurational and optical properties of the dispersal channel, secondary effects of recondensation and distortions of the optical wave. Data are also given from experiments on dispersal of model media that confirm the correctness of the

theoretical principles, and lead us to hope that the level of knowledge attained in this field will enable proper evaluation of both the outlook and limitations of the method of dispersing water aerosols by laser radiation.

The analysis of nonlinear interaction of laser radiation with water aerosols is limited to regular modes of droplet vaporization, and is based mainly on results found by the authors. This book does not deal with the problem of rapid dispersal of aerosol media; the solution of this problem involves investigation of explosive modes of particle vaporization. Research on thermodynamic and gasdynamic analysis of processes of explosion, and on determining the optical consequences of pulse action on an aerosol has only just begun, but the timeliness of this research leads us to hope for a speedy solution of the problem. The authors also expect rapid progress in the study of nonlinear propagation of light in the presence of fluctuation distortions since the conditions of the actual atmosphere require combined consideration of regular and stochastic self-stressing effects. The observed rise in the number of papers on nonlinear optics of scattering media is evidence of formation of this field as an independent area of atmospheric optics.

Some of the results and conclusions presented in the monograph are published here for the first time. The first and second chapters were written by V. Ye. Zuyev and Yu. D. Kopytin, the third and fourth chapters were written by V. Ye. Zuyev and A. V. Kuzikovskiy.

Contents

6610
CSO: 1862

OPTOELECTRONICS

UDC 621.393

NEW BOOK ON MICROWAVE RADIOHOLOGRAPHY AND OPTICAL DATA PROCESSING

Leningrad RADIOGOLOGRAFIYA I OPTICHESKAYA OBRABOTKA INFORMATSII V MIKROVOLNOVOY TEKHNIKE in Russian 1980 (signed to press 24 Oct 80) pp 2-4, 179-180

[Annotation, foreword and table of contents from the book "Radioholography and Optical Data Processing in Microwave Engineering", edited by USSR Academy of Sciences Corresponding Member L. D. Bakhrakh and Candidate of Engineering Sciences A. P. Kurochkin, Izdatel'stvo "Nauka", 2150 copies, 180 pages]

[Text] Questions of the application of holography and optical data processing in microwave engineering are treated in the collection: techniques and equipment for the visualization of microwave fields and producing images of objects; the holographic method of determining the near field parameters of antennas; questions of the design and specific operational features of acoustical-optical radio signal processing devices; and the study of the correlated optical recognition of images received from space.

Foreword

The papers presented in this collection encompass the following topics: holographic methods and equipment for visualizing microwave and accoustical fields, as well as obtaining images of objects irradiated by microwaves; various aspects of the holographic technique of determining the near field parameters of microwave antennas; optical processing of the signals of antenna arrays; questions of the design of acoustical-optical radiosignal processors.

The papers of A.V. Avrorin and his coauthors as well as L.D. Bayda and coauthors are devoted to the questions of the design of high speed equipment complexes intended for the generation of microwave and acoustical holograms and images.

A new type of display for millimeter and submillimeter holograms, films of various liquids, is studied in the paper of A.S. Klyuchnikov and P.D. Kukharchik.

The paper by O.V. Bazarskiy and Ya.L. Khlyavich is devoted to an analysis of a generalized criterion for the estimation of the resolving power of radioholograms.

The results of experimental studies of the correlation optical recognition of images from space are given in the paper by A.I. Balabanov and coauthor.

The papers of A.G. Buday and his coauthors as well as Yu.V. Sysoyev are devoted to the development of a holographic technique for the determination of near field antenna parameters.

The next group of papers encompasses various questions of optical signal processing for antenna arrays and radio emission sources. The two theoretical papers of A.Yu. Grinev and his coauthors are devoted to an analysis of algorithms for signal processing and estimating the parameters of radio-optical antenna systems of various configurations.

A hybrid optical-digital system for processing the signals received from pulsars is preposed and studied by N.A. Yesepkina and her coauthors.

The collection concludes with the papers by Ye.T. Aksenov and his coauthors as well as S.V. Kulakov, which are devoted to acoustical-optical data processors based on nonlinear acoustical interaction and a study of the influence of elastic wave attenuation and the nonlinearity of light modulators on the parameters of accoustical-optical correlators.

The editors hope that the papers found in this collection will attract the attention of specialists and will facilitate the further refinement and more widescale practical application of the techniques of holography and optical data processing in microwave engineering.

Table of Contents

[98-8225]

8225
CSO: 1862

PLASMA PHYSICS

UDC 537.562

ELECTRON ENERGY DISTRIBUTION FUNCTION AND THREE-BODY STICKING RATE FOR OXYGEN WHEN A GAS IS EXPOSED TO AN IONIZATION SOURCE

Moscow TEPLOFIZIKA VYSOKIKH TEMPERATUR in Russian Vol 19, No 1, Jan-Feb 81 pp 16-21

[Article by E. Ye. Son, Moscow Physicotechnical Institute]

[Text] An examination is made of the problem of the energy spectrum of electrons of an air plasma produced by an external ionizer in the energy region beneath the threshold of vibrational excitation of nitrogen molecules. The resultant spectrum is used to calculate the correction to the three-body sticking rate due to the presence of an external ionizer. This correction is considerable at temperatures below 200 K. The author discusses various effects that may be appreciable in experimental verification of the three-body sticking rate in a nonequilibrium plasma.

Various methods of producing a nonequilibrium plasma under the action of an external ionizer have recently come into extensive use. An examination has been made in the literature of the possibilities of making a nitrogen laser with electron-beam pumping [Ref. 1], a laser with pumping by products of nuclear fission [Ref. 2], and also by preliminary photoionization of gas [Ref. 3]. The ionospheric plasma is also a product of ionization of air by relativistic particles and photoionization. The energy distribution of secondary electrons in this case is strongly non-Maxwellian [Ref. 4], and therefore the rates of elementary processes differ from the values that correspond to Maxwellian energy distribution of electrons. In the region of energies that exceed the threshold of vibrational excitation of nitrogen, such calculations for air were done previously [Ref. 5] with consideration of the processes of electron excitation, ionization and vibrational excitation of molecules. The region below the threshold of vibrational excitation of nitrogen (~0.3 eV) is not considered. In the present paper, the electron energy distribution function is found in this sub-threshold region, and the electron capture rate is calculated for an oxygen molecule with the formation of the vibrationally excited state of the ion $O_2^-\pi_g$ in accordance with the Bloch-Bradbury mechanism [Ref. 6]. The possible mechanism of sticking with formation of dimers O_4 is not taken up in this paper.

Let us consider the process of formation of the energy spectrum of electrons under the action of an external source of ionization on a gas. For the sake of definiteness, we will consider ionization by a beam of monoenergetic electrons with energy $U_n > 1$ keV. In the process of deceleration of the primary electron, electrons are

multiplied in collisions with ionization and excitation of electronic and (at lower energies) vibrational levels of molecules. The energy spectrum of electron flux is one-sided -- electron energy decreases. In the energy region below the vibrational excitation threshold, elastic collisions take place between electrons and gas molecules, molecules are rotationally excited, and at low energies there are Coulomb collisions. These types of collisions lead to an electron flux upward in the spectrum, which is due to accumulation of energy by an electron in collisions of the second kind, mainly with quenching of rotationally excited molecules. On the whole, the spectral electron flux in this energy region is diffusional.

According to the Bloch-Bradbury mechanism [Ref. 6], three-body electron sticking takes place in two stages. On the first stage, an electron is captured with formation of a negative oxygen ion into the vibrational level $O_2^-\pi_g$ ($v = 4, 5, \ldots$), and then in collisions with particles M, the negative ion is either destroyed or is stabilized into the ground vibrational state

$$\begin{gathered} e+O_2 \underset{\tau}{\overset{k_{cap}}{\rightleftharpoons}} O_2^- (v \geqslant 4), \\ O_2^- (v \geqslant 4) + M \begin{cases} \xrightarrow{k_{des}} O_2 + e + M \\ \xrightarrow{k_T} O_2^- + M. \end{cases} \end{gathered} \tag{1}$$

The lifetime of the vibrationally excited state of the negative ion $\tau \sim \hbar/\Gamma$, where the half-width $\Gamma \approx 10^{-5}$ eV [Ref. 7]. The constant of quenching by molecules of oxygen and nitrogen is $k_T(O_2) = 8.9 \cdot 10^{-10} cm^3/s$ [Ref. 8] and $k_T(N_2) = 3.2 \cdot 10^{-11}$ cm^3/s [Ref. 9]. The three-body sticking rate constant corresponding to the Bloch-Bradbury mechanism is

$$k_a = \frac{k_{cap} k_\tau}{\tau^{-1} + [M](k_{des} + k_\tau)}. \tag{2}$$

In this paper, principal attention is given to calculation of k_{cap} in the case of a non-Maxwellian spectrum determined by the action of a source of external ionization. Three-body electron sticking exceeds dissociative sticking at pressures above ~0.1 kPa if the electron spectrum is not too enriched in the high-energy part since dissociative sticking takes place at $\varepsilon \approx 5$ eV [Ref. 8]. In the ionosphere the mechanism of three-body sticking of electrons determines their concentration on altitudes below 100 km; in this region the electron temperature is equal to the gas temperature of ~200-250 K [Ref. 10]. The second stage of reaction (1) is not considered. Therefore the specific partial composition of the gas is unimportant. Further calculations are done for air, which is a mixture of nitrogen and oxygen (78:22), varying insignificantly with altitude [Ref. 10].

Let us consider the problem of finding the electron spectrum in the energy region where three-body sticking occurs. The excitation cross section of level O_2^- is resonant with half-width $\Gamma \approx 10^{-5}$ eV (Fig. 1) and with the first peak at energy $\varepsilon_a = 0.09$ eV corresponding to energy difference between $O_2^-\pi_g$ ($v = 4$) and $O_2^- X^3\Sigma_g^-$ ($v = 0$) with the subsequent peaks at energies corresponding to values of the energies of the $O_2^-\pi_g$ ion ($v > 4$). Upon deceleration the electron passes through these regions and has a certain sticking probability. We will show that such sticking processes can be disrgarded in finding the energy spectrum of electrons, although it is this sticking that determines the electron concentration in the plasma. In the region

of energies near ε_a, losses of electron energy are due to elastic collisions and rotational excitation of molecules. At temperatures ~100-300 K rotational levels with $j \simeq 5$-7 have the greatest probatility of population. The most probable loss of energy is

$$U_R = E_{j+2} - E_j = B_e[(j+2)(j+3) - j(j+1)] = (4j+6)B_e,$$

where E_j is the energy of rotational state j; the rotational constant $B_e = 1.998$ cm^{-1} (N_2), $B_e = 1.446$ cm^{-1} (O_2), which corresponds to $U_R \simeq 3 \cdot 10^{-3}$ eV.

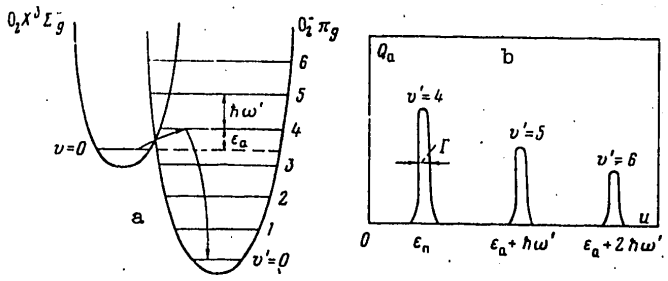

Fig. 1. Diagram of the Bloch-Bradbury mechanism of three-body sticking of electrons to oxygen molecules (a) and typical appearance of cross sections of electron capture by the oxygen molecule as functions of electron energy (b)

Let us evaluate the probability of energy loss in elastic collisions as compared with the rotational values

$$\frac{2m}{M} UQ_m / U_R Q_R \simeq 10^{-3} \ll 1,$$

where Q_m, Q_R are the cross sections of elastic scattering and rotational excitation of molecules by electron impact [Ref. 11]. Estimates show that in this energy region it is sufficient to account for only the rotational excitation of molecules. The time of electron diffusion along the energy axis through the sticking energy region is $\tau_{dif} \sim \Gamma^2/D_R$, where the diffusion coefficient due to rotational excitation is $D_R \simeq \nu_R U_R^2 = \nu_m p_R U_R^2$ (ν_m, ν_R are frequencies of elastic collisions and rotational excitation, p_R is the probability of rotational excitation of a molecule in one collision of an electron and molecule). Comparing τ_{dif} with sticking time $\tau_a^{-1} = [O_2][M]k_a$, we get

$$\frac{\tau_{dif}}{\tau_a} \sim \frac{\Gamma^2 [O_2][M] k_a}{\nu_m p_R U_R^2} \ll 1,$$

and hence the sticking probability is low due to the fact that the electron quickly loses or gains energy in collisional and rotational excitation of molecules, "leaving" the sticking region. At low energies with boundary dependent on the degree of gas ionization, electron-electron collisions become important. The ratio of probabilities of energy losses in electron-electron collisions and with rotational excitation is

$$\frac{UQ_e n_e}{U_n Q_n N} \simeq \frac{1{,}5\cdot 10^7 \alpha}{U},$$

where $\alpha = n_e/N$ is the degree of ionization, U is the electron energy in eV. We will now consider methods of accounting for electron-electron collisions in the low energy region.

To solve the problem of the non-Maxwellian electron spectrum and the influence of this factor on the three-body electron sticking rate for oxygen, let us consider the kinetic equation for the electron energy distribution function in the region $U < U_V$, considering among elastic processes only discrete rotational transitions of the first and second kind

$$\sum_j \{f(U-U_j)(U-U_j)N_{j+2}Q_{j+2,j}(U-U_j) - f(U)UN_jQ_{j,j+2} + \\ + f(U+U_j)N_j(U+U_j)Q_{j,j+2} - f(U)N_{j+2}UQ_{j+2,j}\} = Nf(U+U_v)(U+U_v)Q_v(U+U_v), \quad (3)$$

where N_j is the population of rotational state j, N is the concentration of molecules. The second member accounts for electron transition from the region above the threshold to the sub-threshold region upon vibrational excitation of molecules by electron impact; Q_V is the corresponding cross section of the process. The cross sections of impacts of the first and second kinds satisfy the principle of detailed balance

$$\frac{UQ_{j,j+2}(U)}{(U-U_j)Q_{j+2,j}} = \frac{g_{j+2}}{g_j}, \quad (4)$$

and the populations of rotational states of the molecules are taken as Boltzmannian with temperature T

$$\frac{N_j}{N_{j+2}} = \frac{g_j}{g_{j+2}} \exp\left(-\frac{U_j}{T}\right). \quad (5)$$

With consideration of (4), (5), we get the equation

$$\sum_j N_j UQ_{j,j+2}(U)[-f(U) + e^{-U_j/T} f(U-U_j)] = Nf(U+U_v)(U+U_v)Q_v(U+U_v). \quad (6)$$

We assume that the second member in (1) and (4) is known from solution of the problem of the degradation spectrum of electrons [Ref. 5] in the energy region above the threshold of vibrational excitation of nitrogen $U > U_V$.

In the absence of pumping, when the second member of (3) is equal to zero, the homogeneous difference equation has the solution

$$f(U) = C \exp(-U/T).$$

Let us consider conditions where the magnitude of a rotational quantum is small compared with the gas temperature $U_j \ll T \ll U_V$; then in (4) we can go from the difference form to the differential form

$$\frac{df}{dt}+\frac{f}{T}=\frac{f(U+U_v)(U+U_v)Q_v(U+U_v)}{U\sum_j \delta_j U_j Q_{j,j+2}(U)}=q(U). \tag{7}$$

Here $\delta_j = N_j/N$. Equation (6) has the solution

$$f(U)=\left(C+\int_0^U q(U')e^{U'/T}dU'\right)e^{-U/T}, \tag{8}$$

where the constant C is determined from the normalization condition

$$\int_0^\infty f(U)U^{1/2}dU=1. \tag{9}$$

Estimates show that a source of fast electrons leads to deviation of the distribution function in the region $U \lesssim U_V$, and makes a small contribution to normalization.

We use the resultant distribution function to calculate the capture constant of reaction (1)

$$k_{cap}=\left(\frac{2}{m}\right)^{1/2}\int_0^\infty Uf(U)Q_a(U)dU. \tag{10}$$

The capture cross section has the form of a narrow Breit-Wigner peak with half-width Γ

$$Q_a(U)=\frac{\pi\hbar^2}{2U}\frac{\Gamma^2}{(U-U_a)^2+\Gamma^2/4}. \tag{11}$$

For state $0_2^-\pi_g$ (v = 4), $\Gamma = 10^{-5}$ eV, $U_a = 0.09$ eV,

$$k_{cap}^{(1)}=\frac{2^{1/2}\pi^2\hbar^3}{m^{1/2}}f(U_a)\frac{g_j}{g_e g_M}\Gamma, \tag{12}$$

where the g_j are the statistical weights of the particles.

Upon electron-beam pumping there is an increase in the fraction of electrons in the "tail" of the distribution function, which leads to a correction in the three-body sticking rate $\Delta k_a = k_a - k_a^{(0)}$, where $k_a^{(0)}$ is the rate constant of capture in the case of Maxwellian energy distribution of electrons with temperature T_e

$$\frac{\Delta k_a}{k_a^{(0)}}=\frac{\sqrt{\pi}}{4}\int_0^{\varepsilon_a} T_e^{1/2}f(U+U_v)\frac{(U+U_v)Q_v(U+U_v)}{U\sum_j \delta_j U_j Q_{j,j+2}(U)}. \tag{13}$$

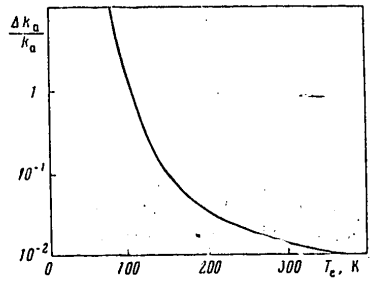

Fig. 2. Relative correction to the sticking constant as a function of electron temperature

The excitation cross sections in this case are resonant both for vibrational and rotational excitation [Ref. 11, 12].

Using the results of calculation of the distribution function for electrons formed by a fast electron beam [Ref. 5], we get the behavior of the three-body sticking rate shown in Fig. 2. At the low electron temperatures typical of the ionosphere, this correction is considerable, the sticking frequency rises sharply, which may lead to a reduction in the concentration of electrons formed by an external ionizer.

Let us discuss some additional factors that can be easily taken into consideration in the given problem. In solving the problem, consideration was taken of sticking that occurs only through one level of the O_2^- ion; accounting for excitation through the other levels is analogous, but taking them into consideration has little effect on the result since the next level v = 5 lies at energies where the distribution function falls off sharply. In solving the kinetic equation, only two-quantum rotational transitions were considered. There are no difficulties involved in accounting for four-level rotational transitions.

Let us consider electron-electron collisions, which are usually difficult to account for because of the nonlinear form of the corresponding collision integral. Under conditions of gas excitation by an external ionizer there is a slight increase in electron temperature (see estimate above), and therefore the sticking threshold considerably exceeds the average electron energy, and in the region of the threshold, electron-electron collisions become important between the threshold electrons and the electrons that have energy T_e. Under these conditions, the integral of electron-electron collisions is linear [Ref. 13], equation (6) is insignificantly complicated, and an analytical solution can be found. For more exact consideration of electron-electron collisions throughout the energy region, the approximation of [14] can be used, but this does not change the results to any extent.

Let us estimate the differential of electron temperature from gas temperature that arises upon degradation of the electron beam in the gas. The kinetic equation for the electron distribution function in the τ-approximation has the form

$$\partial f/\partial t = -\nu(f-f_0)+NS\delta(U-U_n), \tag{14}$$

where S is the number of primary electrons with energy U_n that show up in a unit of time in a unit of volume. Multiplying (14) by $U = mu^2/2$ and integrating by velocities, we get the electron energy balance

$$\frac{d}{dt}(n_eT_e) = -n_e\nu(T_e-T)+SU_n, \tag{15}$$

and after integration of (14) with consideration of losses of the number of electrons in three-body sticking we get the balance of the number of electrons

$$\frac{dn_e}{dt}=\frac{SU_n}{U_0}-\frac{n_e}{\tau_a}. \tag{16}$$

Here $U_0 \approx 35$ eV is the energy expended by the primary electron in forming an electron-ion pair (the pair cost). In the steady state we get from (15), (16) the differentiation of the electron temperature from the gas temperature

$$T_e-T=U_0/\nu\tau_a. \tag{17}$$

In comparing (12) with the results of experiments associated with transmission of an electron beam in a gas, consideration should be taken of the possible arisal of an electric field in the gas due to neutralization of the electron beam. From the expression for Ohm's law

$$j=\sigma[(E+1/e\nabla\mu_e)-\alpha\nabla T] \tag{18}$$

(μ_e is the chemical potential of electrons, α is termoelectromotive force) in a gas surrounded by dielectric walls, we get an estimate for the electric field that arises as a result of inhomogeneity of the distribution of electron concentration of size L, $E_{inh} \sim T_e\nabla n_e/en_e \sim T_e/eL$. In such an electric field, there is additional heating of electrons by an amount $\Delta T_e \sim eE_{inh}\lambda\delta^{-1/2} \sim \lambda T_e/L\delta^{1/2}$, where $\delta = 2m/M$ in weak electric fields, where there is no excitation of rotational states of molecules, while $\delta = \delta_R = \Sigma\delta_j U_j Q_j$, $_{j+2}/\Sigma U_j Q_j$ when this excitation is appreciable. This effect of arisal of a heating field can be disregarded when the inequality

$$\frac{\Delta T_e}{T_e} \sim \frac{\lambda}{L\delta^{1/2}} \ll 1$$

is met. Otherwise heating of electrons in the electric field must be taken into consideration in kinetic equation (1).

The author thanks N. D. Aleksandrov for discussing the work

REFERENCES

1. S. K. Searles, APPL. PHYS. LETT., Vol 25, 1974, p 735.

2. V. M. Andriyakhin, V. V. Vasil'tsov, S. S. Krasil'nikov, V. D. Pis'mennyy, ZHURNAL EKSPERIMENTAL'NOY I TEORETICHESKOY FIZIKI Vol 63, 1972, p 1635.

3. N. G. Basov, E. M. Belenov, V. A. Danilychev, A. F. Suchkov, USPEKHI FIZICHESKIKH NAUK, Vol 111, 1974, p 213.

4. D. R. Suhre, J. T. Verdeyen, J. APPL. PHYS. Vol 47, 1976, p 4484.

5. V. P. Konovalov, E. Ye. Son, ZHURNAL TEKHNICHESKOY FIZIKI Vol 50, No 2, 1980, p 300.

6. F. Bloch, N. E. Bradbury, PHYS. REV. Vol 48, 1935, p 689.

7. G. Parlant, F. Fiquet-Fayard, J. PHYS. B, Vol 9, 1976, p 1617.

8. B. M. Smirnov, "Otritsatel'nyye iony" [Negative Ions], Atomizdat, 1978.

9. N. L. Aleksandrov, TEPLOFIZIKA VYSOKIKH TEMPERATUR, Vol 16, 1978, p 231.

10. P. M. Banks, G. Kockarts, "Aeronomy", N. Y., 1973.

11. Yu. D. Oksyuk, ZHURNAL EKSPERIMENTAL'NOY I TEORETICHESKOY FIZIKI Vol 49, 1965, p 1264.

12. G. J. Schultz, REV. MOD. PHYS., Vol 45, 1973, p 423.

13. B. M. Smirnov, "Fizika slaboionizirovannogo gaza" [Physics of Weakly Ionized Gas], Nauka, 1978, p 131.

14. Yu. B. Golubovskiy, Yu. M. Kagan, R. I. Lyagushchenko, ZHURNAL EKSPERIMENTAL'NOY I TEORETICHESKOY FIZIKI Vol 57, 1969, p 2222.

[8344/0881-6610]

6610
CSO: 8344/0881

UDC 533.9.082.76

DETECTOR PROPERTIES OF A GAS-DISCHARGE PLASMA

Moscow DETEKTORNYYE SVOYSTVA GAZORAZRYADNOY PLAZMY in Russian 1980 (signed to press 3 Mar 80) pp 2, 129

[Annotation and table of contents from book "Detector Properties of a Gas-Discharge Plasma", by Konstantin Ivanovich Kononenko, Atomizdat, 1800 copies, 128 pages]

[Text] The book presents one of the most effective techniques for plasma diagnosis: the method of detector characteristics. An examination is made of the theory of two kinds of detectors: the probe type and the noncontact type (external r-f probe).

The proposed methods are applicable to investigation of a wide variety of plasma phenomena: ionic and electronic resonances, parametric excitation of waves, propagation of ionic-acoustic waves, mechanisms of electron scattering, inelastic collisions of electrons with molecules and ions, recombination of electrons and ions, and much more.

An analysis is made of cases of linear and nonlinear interaction of an electric field with a plasma. An outline is given of certain problems of nonlinear interaction of electromagnetic waves with a plasma.

For scientists and engineers studying the properties of plasma, working with gas-discharge devices, in radio engineering or electronics.

Figures 53, tables 4, references 172.

Contents

6610
CSO: 1862

STRESS, STRAIN AND DEFORMATION

UDC 621.039.517.5

STRESSES ACCOMPANYING TEMPERATURE FLUCTUATIONS

Moscow TEKHNIKA YADERNYKH REAKTOROV: NAPRYAZHENIYA PRI PUL'SATSIYAKH TEMPERATUR in Russian 1980 (signed to press 28 Mar 80) pp 2, 4, 64

[Annotation, introduction and table of contents from book "Nuclear Reactor Engineering: Stresses Accompanying Temperature Fluctuations", by Aleksandr Veniaminovich Sudakov and Anatoliy Sergeyevich Trofimov, Atomizdat, 1100 copies, 64 pages]

[Text] Experimental and theoretical techniques are presented for studying temperature fields and thermal stresses that accompany random fluctuations of temperature in the components of power equipment in atomic electric plants. Results are given from experimental measurements of temperature fluctuations in straight-flow steam generators in the zone of transition to impaired heat exchange. Examples of application of the proposed methods are given.

For specialists dealing with thermal and strength calculations and experimental studies of processes in power equipment.

Figures 37, tables 4, references 61.

Introduction

Processes of heat exchange in various elements of heat engineering equipment in power plants are accompanied by temperature fluctuations. When they are of considerable intensity, they may have an effect on the service life of the equipment.

As of now, no unified approach has been formulated to analysis of temperature fluctuations and evaluation of their influence on the life of equipment. Publications are available in the form of separate articles, reports giving the results of investigation of individual special problems. Of greatest interest from both the theoretical and experimental standpoints is research done at the Physical Power Engineering Institute, Moscow Power Institute and at the Central Boiler and Turbine Institute. However, there is no systematic presentation in the literature of the major problems and solutions.

In this pamphlet the authors attempt to generalize the results of various research works in order to explain fairly simple engineering methods of calculating the main parameters that characterize the fluctuation process. An examination is also made of methods of experimental research, and examples are given to demonstrate the feasibility of using these methods for practical calculations.

Pulsation research should not be considered complete; because of the timeliness of this problem, further elaboration of studies is needed. In this connection it is very important to choose the proper direction of research. If this book will be of assistance here, the authors will feel that they have done their job.

In conclusion the authors thank B. F. Gromov for help and for support in the work, and also D. M. Kalachev, Ye. D. Fedorovich, A. V. Shchedrin who participated directly in experimental research done at the Central Boiler and Turbine Institute

Contents

[84-6610]

6610
CSO: 1862

THERMAL PHYSICS OF LOW-TEMPERATURE SUBLIMATION COOLING

Kiev TEPLOFIZIKA NIZKOTEMPERATURNOGO SUBLIMATSIONNOGO OKHLAZHDENIYA in Russian (signed to press 10 Sep 80) pp 2-4, 231-232

[Annotation, foreword and table of contents from book "Thermal Physics of Low-temperature Sublimation Cooling", by Boris Iyerimiyevich Verkin, Vladimir Fedorovich Getmanets and Rem Sergeyevich Mikhal'chenko, Physicotechnical Institute of Low Temperatures, Ukrainian SSR Academy of Sciences, Izdatel'stvo "Naukova dumka", 1,000 copies, 232 pages]

[Text] The thermophysical properties which determine the kinetics and intensity of sublimation of cryogenic materials in a vacuum are considered in the book, the main principles of external and internal heat and mass transfer during sublimation of porous solidified gases and during solification and self-freezing of them are outlined, analytical relations are presented for calculating steady and transient thermal processes in devices based on solified gases and recommendations are given on optimum management of low-temperature sublimation cooling. The methods are considered and the results are presented of experimental investigation of heat and mass transfer processes in the viscous mode in the capillary-porous structure of porous solidified gases and on their boundary upon heat transfer through the gas interlayers by the contact method. Many of the indicated results are published for the first time.

The book is intended for scientific workers and engineers who develop and operate low-temperature cooling equipment, graduate students and students of the corresponding specialties and may be useful to specialists related to heat and mass transfer processes during sublimation in a vacuum.

Foreword

The great success achieved in the field of physics and low-temperature engineering is related to a significant degree to development and improvement of the methods and technology of using cooling agents. Cryogenic materials in liquid and gaseous states emerged in the role of these agents until quite recently if one does not consider "dry ice," which has long been used in the food, chemical, pharmaceutical and perfume industry, in infrared and vacuum equipment, medicine, machine building, meteorology, agriculture and so on.

Judging by the number of publications and patents [1-28], interest in solid-state cooling agents has recently increased considerably. This is related to the fact

that solidified gases as cooling agents have a clear advantage in temperature level compared to cryogenic liquids (for example, temperature can be reduced from 77 to 30-50 K in solid nitrogen and from 20 to 5-10 K in solid hydrogen) and in the higher values of density and specific heat of vapor phase transition. Moreover, the conversion to solidified gases under reduced gravity conditions makes it possible to eliminate the complex problem of separating the vapor-liquid mixture. Utilizing these advantages and the results of many years of investigations carried out at the Physicotechnical Institute of Low Temperatures, Ukrainian SSR Academy of Sciences, in the field of heat and mass transfer in solidified gases and in more effective shield-vacuum thermal insulation, it was possible to develop new promising sources of cold--sublimation storage devices with operating life up to a year or more [232, 233, 236, 240, 245]. The fundamentals of the thermophysics of processes occurring both in sublimation cold storage devices and in various other installations and devices in which solidified gases are used are outlined in the proposed monograph.

Problems of the kinetics of sublimation and heat and mass transfer during flow of gases in the viscous mode are considered since it is these conditions that occur when solidified gases with saturated vapor pressure from 760 to 0.1 mm Hg are used. The problem of investigating heat and mass transfer during sublimation of solidified gases in the molecular mode is not as timely and is therefore not considered.

The monograph consists of the introduction and five chapters. General data on the thermophysical properties of solidified gases and the kinetics and mechanism of heat and mass transfer during sublimation of solids in a vacuum are presented in the introduction. Chapter 1 is devoted to processes of sublimation and heat transfer during self-freezing of cryogenic liquids in a vacuum. The characteristics of heat and mass transfer along the surface and in the mass of porous solidified gases crystallized under conditions of evacuating vapors above the liquid phase are considered in Chapters 2, 3 and 4.

Chapter 5 contains the results of applying the principles found in the paper to calculation of problems occurring during operation of vessels with solidified gases. The most significant of them are problems of filling geometrically complex vessels with solidified gases and providing effective heat dissipation from the objects to be cooled and thermostatting the latter with sufficient degree of accuracy. These problems stimulated the appearance of a large number of mainly experimental investigations of heat and mass transfer during sublimation of solidified gases. The results of the investigations were published in numerous journals and other publications; they were mainly contradictory and interpreted on the basis of various theoretical prerequisites.

An attempt was made in the given monograph to evaluate the experimental results on heat and mass transfer during sublimation of solidified gases (using available data for other molecular crystals as well) from a unified viewpoint and to supplement them with an analytical description of the main processes specific to devices based on solidified gases.

The outline of the materials is based mainly on the results of the authors' investigations. With regard to the newness of the problem, the given results are obviously far from complete and sometimes are discussion types in nature; therefore, the authors will be grateful to readers for critical comments and advice which they request be sent to the address: 310164, Khar'kov, Prospekt Lenina, 47, FTINT, AN USSR.

Contents

[119-6521]

6521
CSO: 1862

- END -